

Energy-Efficient Routing Protocols for Heterogeneous Wireless Sensor Networks with Smart Buildings Evacuation



Nadia Ali Qassim Al-Aboody

Supervisor: Professor Hamed Al-Raweshidy

Department of Electronic and Computer Engineering
Brunel University London

A Thesis Submitted in Fulfilment of the Requirements for the degree of
Doctor of Philosophy

August 2017

To

The Great Woman who taught me to follow my dreams, My Mother ...

The First Man I Loved, My Father ...

My Lovely Husband and My three beautiful sons ...

My sisters ...

Thank you for your Inspiration, Love and Support

Declaration

I hereby declare that except where specific reference is made to the work of others, the contents of this thesis are original and have not been submitted in whole or in part for consideration for any other degree or qualification in this, or any other university. This thesis is my own work and contains nothing which is the outcome of work done in collaboration with others, except as specified in the text and Acknowledgements.

Nadia Ali Qassim Al-Aboody
August 2017

Acknowledgements

"إِنَّهُ مَنْ يَتَّقِ وَيَصْبِرْ فَإِنَّ اللَّهَ لَا يُضِيعُ أَجْرَ الْمُحْسِنِينَ"

سورة يوسف الآية 90

First of all, I am infinitely thankful to Allah for continuously blesses me and for providing me with strength and perseverance to achieve this work. Secondly, I would like to express my appreciation and gratefulness to the Ministry of Higher Education-Iraq for funding my Ph.D. study.

It is difficult to put in words my gratitude to my supervisor Professor Hamed Al-Raweshidy. His enthusiasm, care and motivation have helped to make my Ph.D. experience much more interesting and productive. He has provided me with encouragement, inspiration, friendship and support. Professor Hamed, I am in debt to you and your kindness will not be forgotten.

I am also thankful to my second supervisor Dr. Maysam Abbod for his time and advice during my research. And, would like to show appreciation to my colleagues at the Wireless Networks and Communications Centre (WNCC), my friends at Brunel University and my gratitude to all the staff at Brunel University as well.

Mostly, I am deeply grateful to my parents who raised me with a love of science and supported me at all times. To my sisters for their continues support and encouragement, and to my children Ali, Mohammed and Hassan; I can not turn back time but I will try to make up for the times that I have missed spending with you. Finally, I wish to thank my loving, supportive, encouraging, and patient husband, whose faithful support during my studies is so appreciated.

Abstract

The number of devices connected to the Internet will increase exponentially by 2020, which is smoothly migrating the Internet from an Internet of people towards an Internet of Things (IoT). These devices can communicate with each other and exchange information forming a wide Wireless Sensor Network (WSN). WSNs are composed mainly of a large number of small devices that run on batteries, which makes the energy limited. Therefore, it is essential to use an energy efficient routing protocol for WSNs that are scalable and robust in terms of energy consumption and lifetime. Using routing protocols that are based on clustering can be used to solve energy problems. Cluster-based routing protocols provide an efficient approach to reduce the energy consumption of sensor nodes and maximize the network lifetime of WSNs.

In this thesis, a single hop cluster-based network layer routing protocol, referred to as **HRHP**, is designed. It applies centralized and deterministic approaches for the selection of cluster heads, in relation to offer an improved network lifetime for large-scaled and dense WSN deployments. The deterministic approach for selecting CHs is based on the positive selection mechanism in the human thymus cells (T-cells). HRHP was tested over six different scenarios with BS position outer the sensing area, it achieved a maximum average of 78% in terms of life time.

To further reduce energy consumption in WSN, a multi-hop algorithm, referred to as **MLHP**, is proposed for prolonging the lifetime of WSN. In this algorithm, the sensing area is divided into three levels to reduce the communication cost by reducing the transmission distances for both inter-cluster and intra-cluster communication. MLHP was tested over fourteen cases with different heterogeneity factors and area sizes and achieved a maximum of 80% improvement in terms of life time.

Finally, a real-time and autonomous emergency evacuation approach is proposed, referred to as **ARTC-WSN**, which integrates cloud computing with WSN in order to improve evacuation accuracy and efficiency for smart buildings. The approach is designed to perform localized, autonomous navigation by calculating the best evacuation paths in a distributed manner using two types of sensor nodes (SNs), a sensing node and a decision node. ARTC-WSN was tested in five scenarios with different hazard intensity, occupation ratio and exit availability over three different areas of evacuation and achieved an average of 98% survival ratio for different cases.

Table of contents

List of figures	xii
List of tables	xvi
Abbreviations	xix
1 Introduction	1
1.1 Wireless Sensor Networks	2
1.1.1 Smart Sensors	4
1.1.2 Path-loss model	5
1.1.3 Data Aggregation	7
1.2 Taxonomy of Network Design Strategies in WSNs	8
1.2.1 Single-level clustering structure	9
1.2.2 Multi-level clustering structure	10
1.3 WSNs Applications	11
1.3.1 Smart Homes and Intelligent Buildings	11
1.3.2 Human Health Monitoring	13
1.3.3 Intelligent Water Systems	14
1.3.4 Other Applications	14
1.4 Limitations and Challenges in WSNs	14

1.4.1	Technical challenges in WSNs	15
1.4.2	Routing challenges in WSNs	16
1.5	Thesis Motivation	17
1.6	Research Aim and Objectives	18
1.7	Contributions	19
1.8	Thesis Scope	20
1.9	Thesis Outline	21
2	Literature Review	23
2.1	Introduction	23
2.2	Heuristic Approaches	26
2.2.1	Low Energy-Adaptive Clustering Hierarchical Protocol (LEACH)	26
2.2.2	Stable Election Protocol (SEP)	28
2.2.3	Distributed Energy-Efficient Clustering Protocol (DEEC)	29
2.2.4	Energy Efficient Heterogeneous Clustered (EEHC)	30
2.2.5	Enhanced Heterogeneous LEACH Protocol for Lifetime Enhance- ment (EHE-LEACH)	32
2.2.6	Gateway-based Energy-Aware Multi-hop Routing protocol for WSNs (M-GEAR)	34
2.2.7	Tree Based Clustering (TBC)	35
2.3	Meta-heuristic Approaches	36
2.3.1	LEACH-Centralized (LEACH-C)	37
2.3.2	A Genetic Algorithm in LEACH-C Routing Protocol for Sensor Networks (GA-C)	38
2.3.3	A Evolutionary Approach for Load Balanced Clustering Problem for WSN (GA-LBC)	39
2.3.4	Energy-aware Clustering for WSNs using PSO Algorithm (PSO-C)	40
2.3.5	Energy-aware Evolutionary Routing Protocol for Dynamic Clus- tering of WSNs (EAERP)	41
2.3.6	Energy Balanced Unequal Clustering Protocol (EBUC)	42
2.4	Supplementary Remarks	44

2.5	Summary	45
3	HRHP: Hybrid T Cell Based CH-Selection for Prolonging Network Life Time in Large-Scale WSN	47
3.1	Introduction	47
3.2	Human T-Cell Positive Selection Mechanism	48
3.3	The proposed HRHP Settings	50
3.3.1	Network Model	50
3.3.2	Energy Model	52
3.3.3	Cluster Formation	54
3.4	Performance Evaluation	59
3.4.1	Scenario 1	61
3.4.2	Scenario 2	64
3.4.3	Scenario 3	67
3.4.4	Scenario 4	70
3.4.5	Scenario 5	73
3.4.6	Scenario 6	76
3.5	Summary	79
4	Multi Layer Hierarchical Routing Protocol (MLHP)	80
4.1	Introduction	81
4.1.1	Grey Wolf Optimizer (GWO)	81
4.2	MLHP Initialization	85
4.2.1	Network Model in MLHP	85
4.2.2	Energy Model	87
4.3	Cluster Number Calculation	87
4.3.1	Optimal number of CHs (k_1) for Level One	88
4.3.2	Optimal number of CHs (k_2) for the rest of the network	89
4.4	Cluster Heads Selection	89
4.4.1	Centralized selection of CHs for Level One	90

4.4.2	Probabilistic GWO-based selection of CHs in Level Two	91
4.4.3	Distributed selection of CHs in Level Three	92
4.5	Performance Evaluation	95
4.6	Simulation Parameters and Settings	98
4.6.1	Simulation Parameters	99
4.6.2	Simulation Settings	99
4.7	Simulation Results	102
4.7.1	Network Stability and Operational Time	102
4.7.2	Heterogeneity over Small-Scaled Networks	106
4.7.3	Heterogeneity over Large-Scaled Networks	115
4.8	Summary	124
5	Adaptive Real-time Clouded Sensor Network-based Approach for Emergency Navigation (ARTC-WSN)	125
5.1	Introduction	126
5.2	Related Work	129
5.3	Proposed Approach	131
5.3.1	Modeling the Area of Evacuation	131
5.3.2	ARTC-WSN Conceptual Model	132
5.3.3	Cloudification Phase	135
5.4	Simulation Setup and Results	136
5.4.1	Simulation Design and Setup	136
5.4.2	Results: Evacuation Area and Hazard Intensity	138
5.4.3	Results: The Number of Evacuees	144
5.4.4	Results: The Number of Available Exits	146
5.5	Summary	148
6	Conclusions and Future Research Directions	150
6.1	Conclusions	150
6.2	Future Research Directions	155

Table of contents	xii
-------------------	-----

Bibliography	157
---------------------	------------

List of figures

1.1	Generalized view of WSN.	3
1.2	A block diagram of a smart sensor.	4
1.3	Potential growth in worldwide IoT sensor deployments, millions.	5
1.4	Friis Free Space Equation.	6
1.5	Data aggregation strategies in wireless sensor networks	8
1.6	Single-level network design.	10
1.7	Multi-level network design.	11
1.8	The measured electricity use for ten nearly identical homes, showing considerable variations in energy use.	12
1.9	Thesis scope.	20
1.10	Thesis Outline.	22
2.1	(a) Typical flat structured network. (b) Typical hierarchical structured network. (c) Tree-based structured network	25
2.2	The network model of EHE-LEACH.	33
2.3	The network model of M-GEAR.	35
2.4	Tree level construction in TBC.	36
3.1	Overall scheme of T-cell development in the thymus.	49
3.2	HRHP Network Model.	51

3.3	Energy Dissipation model.	52
3.4	Example of cluster formation challenge.	54
3.5	Format of <i>Gather</i> and <i>REPLY</i> packets: (a) <i>Gather</i> , (b) <i>REPLY</i>	55
3.6	Format of <i>Identify</i> packet.	55
3.7	Process of cluster formation in the proposed algorithm.	58
3.8	Average residual network energy levels for scenario 1, $Area = 200 \times 200$	63
3.9	Average residual network energy levels for scenario 2, $Area = 300 \times 300$	66
3.10	Average residual network energy levels scenario 3, $Area = 500 \times 500$. .	69
3.11	Average residual network energy levels scenario 4, $Area = 200 \times 200$. .	72
3.12	Average residual network energy levels scenario 5, $Area = 300 \times 300$. .	75
3.13	Average residual network energy levels scenario 6, $Area = 500 \times 500$. .	78
4.1	Grey wolf social hierarchy.	82
4.2	Grey Wolf Optimizer Flowchart.	83
4.3	Network Model.	86
4.4	Centralized Selection in Level One.	91
4.5	<i>HELLO_Msg</i>	92
4.6	Total network remaining energy for $100 \times 100 m^2$ area and $N = 100$. .	96
4.7	Total network remaining energy for $100 \times 100 m^2$ area and $N = 200$. .	96
4.8	Total network remaining energy for $200 \times 200 m^2$ area and $N = 100$. .	97
4.9	Total network remaining energy for $200 \times 200 m^2$ area and $N = 200$. .	98
4.10	Network lifetime for small-scale network, $N = 100$, $\alpha = 1$, $\beta = 0.5$	107
4.11	Network lifetime for small-scale network, $N = 100$, $\alpha = 2$, $\beta = 1$	108
4.12	Network lifetime for small-scale network, $N = 200$, $\alpha = 1$, $\beta = 0.5$	110
4.13	Network lifetime for small-scale network, $N = 200$, $\alpha = 2$, $\beta = 1$	111
4.14	Case1: Total residual energy, $N = 100$, $\alpha = 1$, $\beta = 0.5$	112
4.15	Case2: Total residual energy, $N = 100$, $\alpha = 2$, $\beta = 1$	112
4.16	Case3: Total residual energy, $N = 200$, $\alpha = 1$, $\beta = 0.5$	113
4.17	Case4: Total residual energy, $N = 200$, $\alpha = 2$, $\beta = 1$	113

4.18	The total number of packets sent to the BS for small-scale area with heterogeneity: (a) ($\alpha = 1$ and $\beta = 0.5$) for 100 nodes. (b) ($\alpha = 2$ and $\beta = 1$) for 100 nodes. (c) ($\alpha = 1$ and $\beta = 0.5$) for 200 nodes. (d) ($\alpha = 2$ and $\beta = 1$) for 200 nodes.	114
4.19	Network lifetime for large-scale network, $N = 100$, $\alpha = 1$, $\beta = 0.5$	116
4.20	Network lifetime for large-scale network, $N = 100$, $\alpha = 2$, $\beta = 1$	117
4.21	Network lifetime for large-scale network, $N = 200$, $\alpha = 1$, $\beta = 0.5$	118
4.22	Network lifetime for large-scale network, $N = 200$, $\alpha = 2$, $\beta = 1$	119
4.23	Total residual energy, $N = 100$, $\alpha = 1$, $\beta = 0.5$	121
4.24	Total residual energy, $N = 100$, $\alpha = 1$, $\beta = 2$	121
4.25	Total residual energy, $N = 200$, $\alpha = 1$, $\beta = 0.5$	122
4.26	Total residual energy, $N = 200$, $\alpha = 1$, $\beta = 2$	122
4.27	The total number packets sent to the BS for large-scale area with heterogeneity: (a)($\alpha = 1$ and $\beta = 0.5$) for 100 nodes. (b) ($\alpha = 2$ and $\beta = 1$) for 100 nodes. (c) ($\alpha = 1$ and $\beta = 0.5$) for 200 nodes. (d) ($\alpha = 2$ and $\beta = 1$) for 200 nodes.	123
5.1	A typical architecture of integrated WSNs and CC for emergency and evacuation management.	128
5.2	Graph representation of the building.	133
5.3	The conceptual model of ARTC-WSN.	134
5.4	Comparison of the average evacuation time for evacuation area of $100 \times 100 m^2$	139
5.5	Comparison of the average evacuation time for evacuation area of $200 \times 200 m^2$	140
5.6	Comparison of the average evacuation time for evacuation area of $300 \times 300 m^2$	142
5.7	Comparisons of total death ratio for small-scale evacuation areas.	143
5.8	Comparison of total death ratio for moderate-scale evacuation areas.	143
5.9	Comparisons of total death ratio for large-scale evacuation area. simulation runs for 300 evacuees.	144

5.10 Comparison of the evacuation time when number of evacuees ranges between 100 and 500.	145
5.11 Comparison of the number of dead for different occupation rates for experiment 4.	145
5.12 Comparison of the percentage of death percentage for different exits availability.	147
5.13 Comparison of evacuation time for different exits availability for experiment 5.	148

List of tables

1.1	Biosensors and Biosignals	13
2.1	Comparison of clustering protocols with respect to clustering attributes.	46
3.1	Simulation Parameters	61
3.2	Network life time results obtained from scenario 1	61
3.3	Network life time results obtained from scenario 2 with BS location (150,310)	64
3.4	Network life time results obtained from scenario 3 with BS location (250,510)	67
3.5	Network life time results obtained from scenario 4 with BS location (210,210)	70
3.6	Network life time results obtained from scenario 5 with BS location (310,310)	73
3.7	Network life time results obtained from scenario 6 with BS location (510,510)	76
4.1	CH_Neighbour_Table	93
4.2	Case1: Network life time, Area= $100 \times 100 m^2$	95
4.3	Case2: Network life time, Area= $200 \times 200 m^2$	97
4.4	Simulation Parameters	100

4.5	Scenario-I Settings: Network Stability and Operational Time	101
4.6	Scenario-II Settings: Heterogeneity over Small-Scale Network)	101
4.7	Scenario-III Settings: Heterogeneity over Large-Scale Network	101
4.8	Network Stability: Average number of communication rounds at which the first node in the network dies for small-scale and large-scale networks with different node density.	105
4.9	Network Operational Time: Average number of communication rounds at which half of nodes in the network dies for small-scale and large-scale networks with different node density.	105
4.10	Average life time percentage improvement over other protocols for small- scale network ($N = 100, \alpha = 1, \beta = 0.5$)	107
4.11	Average life time percentage improvement over other protocols for small- scale network ($N = 100, \alpha = 2, \beta = 1$)	108
4.12	Average life time percentage improvement over other protocols for small- scale network ($N = 200, \alpha = 1, \beta = 0.5$)	109
4.13	Average life time percentage improvement over other protocols for small- scale network ($N = 200, \alpha = 2, \beta = 1$)	111
4.14	Average life time percentage improvement over other protocols for large- scale network ($N = 100, \alpha = 1, \beta = 0.5$)	115
4.15	Average life time percentage improvement over other protocols for large- scale network ($N = 100, \alpha = 2, \beta = 1$)	117
4.16	Average life time percentage improvement over other protocols for large- scale network ($N = 200, \alpha = 1, \beta = 0.5$)	118
4.17	Average life time percentage improvement over other protocols for large- scale network ($N = 200, \alpha = 2, \beta = 1$)	120
5.1	A classification scheme of evacuation based on two dimensions: the timing and duration of evacuation.	127
5.2	The percentage of survivals for area of evacuation $100 \times 100 m^2$	140
5.3	The percentage of survivals for area of evacuation $200 \times 200 m^2$	141
5.4	The percentage of survivals for area of evacuation $300 \times 300 m^2$	141

5.5	The average percentage of survivals when number of evacuees ranges between 100 and 500.	144
5.6	The average percentage of survivals for different number of exits	146

Abbreviations

ACO	Ant Colony Optimization
ABC	Artificial Bee Colony Optimization
ARTC-RR	Adaptive Real-Time Clouded-Reverse Rout
ARTC-WSN	ARTC based WSN protocol
BS	Base Station
CC	Cloud Computing
CD4	Cluster of Differentiation 4
CH	Cluster Head
CM	Cluster Member
CPN	Cognitive Packet Network
DE	Differential Equation
D_N	Double Negative
DN	Decision Node
DNA	DeoxyriboNucleic Acid
DP	Double Positive
DSP	Dijkstra Shortest Path algorithm
DEEC	Distributed Energy-Efficient Clustering Protocol
EAERP	Energy-Aware Evolutionary Routing Protocol
EBUC	Energy Balanced Unequal Clustering Protocol
EEHC	Energy Efficient Heterogeneous Clustered
EHE-LEACH	Enhanced Heterogeneous LEACH protocol for lifetime Enhancement
EM	Emergency Management
EN	Emergency Navigation

FND	F irst N ode D ead
GA	G enetic A lgorithm
GA-C	GA -based C lustering protocol
GA-LBC	GA based L oad B alanced C lustering Protocol
GPS	G lobal P ositioning S ystem
GWO	G rey W olf O ptimizer
HND	H alf N ode D ead
HRHP	H ybrid R outing P rotocol for H eterogeneous W SN
ID	I dentification
ICT	I nformation and C ommunication T echnology
IoT	I nternet of T hings
LCD	L iquid C rystal D isplay
LEACH	L ow E nergy A daptive C lustering H ierarchy
LEACH-C	LEACH - C entralized
LND	L ast N ode D ead
MAC	M edium A ccess C ontrol
M-GEAR	G ateway-based E nergy-Aware M ulti-hop R outing protocol for WSNs
M2M	M achine to M achine
MHC	H istocompatibility C omplex C lass
MLHP	M ulti L ayer H ierarchical routing P rotocol
MTE	M inimum T ransmission E nergy
OCP	O ptimal C overage P rotocol
OS	O perating S ystem
PSO	P article S warm O ptimization
PSO-C	PSO - based Energy-aware C lustering protocol
QoS	Q uality of S ervice
RHMS	R emote H ealth M onitoring S ystems
RSSI	R eceived S ignal S trength I ndicator
SA	S imulated A nnealing
SEP	S table E lection P rotocol
SN	S ensor N ode
T-cell	T hymus C ell
TCR	T -cell R eceptor
TBC	T ree B ased C lustering
TDMA	T ime D ivision M ultiple A ccess
WBSN	W ireless B ody S ensor N etwork
WSN	W ireless S ensor N etworks

Chapter 1

Introduction

THE Internet is migrating from Internet of people to the Internet of Things (IoT), it is estimated by 2020 the number of connected devices will reach 50 billion [1]. These devices will largely vary in terms of characteristics including their functionality and processing capabilities, they can communicate and exchange information without the interference of human through a Machine-To-Machine (M2M) paradigm [2]. M2M communications are strongly application-oriented, Wireless sensor networks (WSNs) can boost the adoption of M2M and thus enabling IoT. WSNs have attracted the attention in research and in businesses schemes due to their potential applications in several areas such as simple monitoring systems, smart homes [3], agriculture (temperature, pressure, humidity, etc.), smart surfaces, vehicles, location services for humans, and e-health [4]. However, energy limitation is still one of the most demanding problems for many real-world deployments of WSNs. Sensor nodes are battery-powered; therefore energy optimization has been one of the main objectives for a robust protocol design.

Therefore, it is essential to use an energy efficient routing protocol for WSNs that are scalable and robust in terms of energy consumption and lifetime. Using flat sensor network architecture poses serious issues on the performance of the network, the unattended low-powered sensor nodes (SNs) can deplete their energy quickly resulting in a short network lifetime. However, using routing protocols that are based on clustering can be used to solve these problems. Cluster-based routing protocols

provide an efficient approach to reduce the energy consumption of SNs and maximize the network lifetime and scalability of WSNs.

This chapter discusses WSNs and smart sensors in section 1.1. Some of applications for WSNs are described in section 1.3. The main limitations and challenges facing WSNs are provided in section 1.4, this thesis motivation is shown in section 1.5. The research aim and objectives are illustrated in section 1.6, the contributions of this work are presented in section 1.7. Finally, the thesis outline is displayed in section 1.9.

1.1 Wireless Sensor Networks

A typical WSN involves tens to thousands of small low-power, low-cost and intelligent sensor nodes (SN) and one or more base stations (BS) [5]. Usually SNs are statically deployed over the sensing area, but they can also be mobile and able to communicate with the environment. The objective of WSN is to monitor one or more characteristics of a particular area called “Area of interest” or “The sensing area” [6].

SNs work in a collaborative way to sense and gather the monitoring parameters, but also they can work autonomously. They are generally equipped with non-rechargeable batteries once deployed in the area of interest they keep operating until they consume their power. SNs can implement different functions including sensing the environment, communicating with neighbouring nodes, and in many cases performing basic computations on the data being collected [7], [8] which make WSNs excellent choice for many applications [6],[9].

WSNs suffer from limited communication range, scalability, and energy efficiency is a major constraints of WSNs [10]; SNs can spend their energy in several situations, data transmission is one of the most energy wasting source and therefore, routing is a key technique to be considered. Finding and maintaining routes in WSNs is important due to the energy restrictions and transmission range restrictions. Design of energy efficient routing protocol for WSN is of great challenge to prolong the network’s lifespan [11].

Clustering has been considered to be one of the strategies to overcome the energy problems in WSN’s. It partitions the sensing area into multiple clusters and in each cluster, a certain node will perform the task of a leader node, called a cluster head (CH). CH’s role is to communicate with the cluster members (CM), collect the data from CMs, aggregate the data, and send it to a central BS using a hierarchical routing

protocol [12] [8]. Thereby, clustering helps avoiding internal collisions by enabling SNs to communicate their data with their respective CH only, they do not have to share the communication channel with the nodes in other clusters [13]. The aggregation of data at CHs greatly reduces the energy consumption in the network by minimizing the total data messages to be transmitted to the BS. Fig. 1.1 shows the generalized view of WSNs, which consists of a BS, CHs and SNs deployed in a geographical region [14].

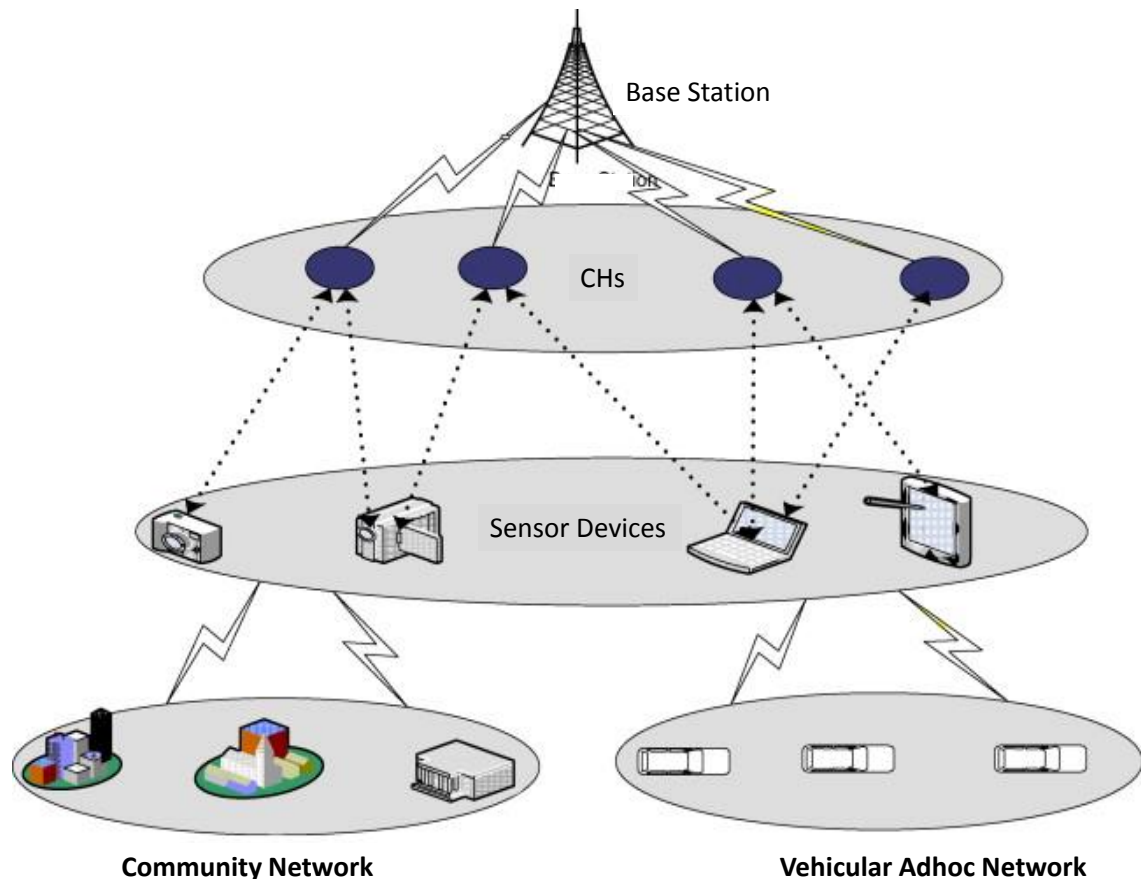


Fig. 1.1 Generalized view of WSN.

Once the clusters established, the communication between the nodes can be either intra-cluster or inter-cluster. Intra-cluster communication comprises the data exchanges between the CMs nodes and their respective CH. Inter-cluster communication includes transmission of the data between the CHs and the BS. Inter-cluster communication is an important aspect and essential feature of WSNs, a simple approach to communicate is a single hop-based approach, in which each CH sends data directly to the BS. Another method is a multi-hop based approach, in which intermediate nodes participate in data packets forwarding between the CH and the BS [7].

1.1.1 Smart Sensors

The significant improvements in instruments and instrumentation systems are due to the integration of micro-sensors, nano-sensors, and smart sensors in measurement systems [15]. A conventional sensor requires extensive external signal processing circuits an component to measure different parameters such as physical, chemical, or biological and renovate them into electrical signal. The term (Smart Sensors) was first used in the mid 1980's to differentiate a new class of sensors from conventional ones, smart sensors have the ability to perform functions to increase the quality of the information gathered rather than passing only raw signals [15] and they can communicate with other devices. Among these functions: self-identification, self-testing, lookup tables, and calibration curves, all these functions are conducted by the integration of sensors with micro-controllers, microprocessor or logic circuits on the same chip and can be programmed externally. Fig. 1.2 illustrate a general structure of a smart sensor.

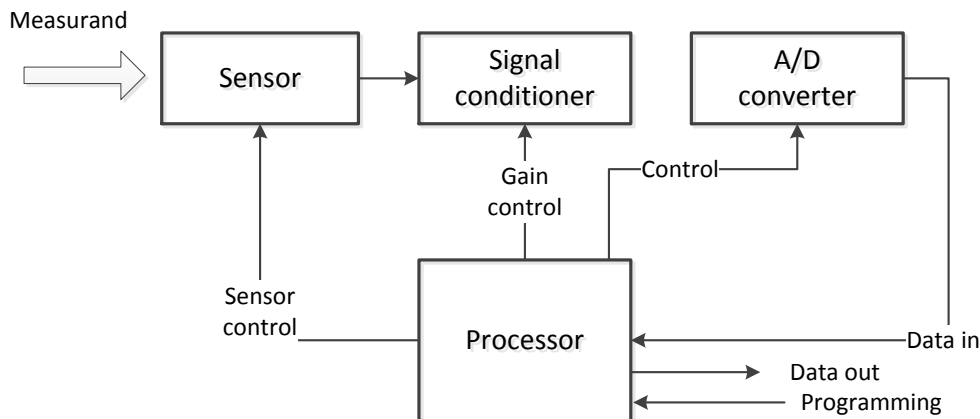


Fig. 1.2 A block diagram of a smart sensor.

The global increasing use of smart sensors, such as in smart buildings [16], [17], smart meters [18], wearable devices [19], [20] and many more systems made the Internet of Things (IoT) become possible [21]. Fig. 1.3 shows the potential growth in millions worldwide for IoT sensor deployment. (Chart analysis performed by the Deloitte Center for Financial Services [22] based on Gartner research [23])

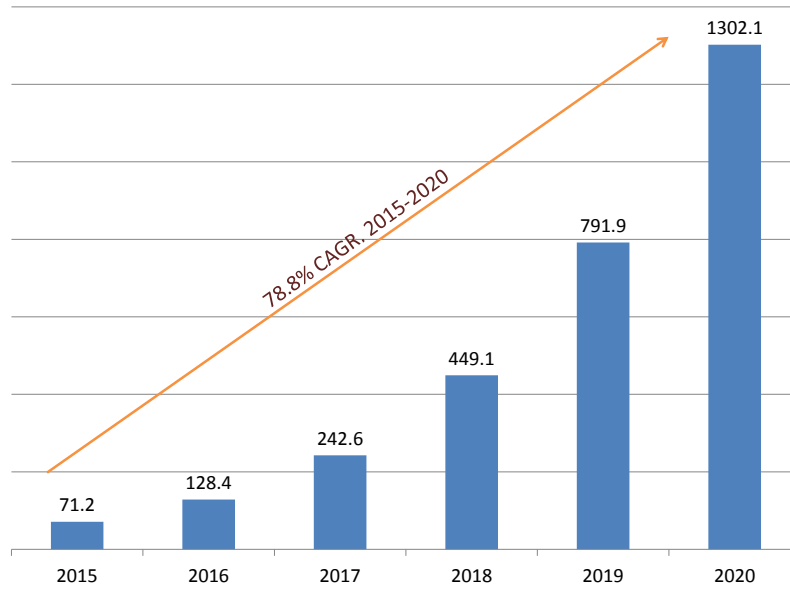


Fig. 1.3 Potential growth in worldwide IoT sensor deployments, millions.

1.1.2 Path-loss model

Unlike wired channels that is predictable and stationary, wireless channels are random and suffer from propagation that depends on the transmission path between the receiver and the transmitter [24]. The path-loss estimation is based on the circuitry characteristics in the field of wireless communication networks. When signals are sent from a transmitter to a receiver circuitry, the path-loss is estimated as the function of the propagated signal of the transceiver. This is calculated as the reduction in power density that occurs as a radio wave propagates over a distance, and can be put as [25]:

$$\text{Maximum path lose} = \text{transmit power} - \text{reciever sensitivity} + \text{gain} + \text{losses} \quad (1.1)$$

The transmission path vary from simple line-of-sight to one that is severely obstructed by buildings or even mountains. Propagation is caused by several mechanisms including reflection, diffraction, and scattering, propagation models have focused on predicting the average signal strength received from the transmitter at a given distance, as well as the change of the signal strength in close spatial proximity to particular location. When there is a clear line-of-site between the transmitter and the receiver, they undergo free space propagation. The free space power received by an antenna

which is separated from a radiating antenna by a distance (d) is given by Friis free space equation [24]:

$$P_r(d) = P_t G_t G_r \frac{\lambda^2}{(4\pi d)^2} \quad (1.2)$$

where, G_t and G_r are the transmitter and the receiver antenna gains respectively. λ is the wavelength, d is the distance between the transmitter and the receiver. P_t is the transmitted power and P_r is the received power (Fig. 1.4, [25]).



Fig. 1.4 Friis Free Space Equation.

If the antenna gains not considered, path loss can be expressed as [15]:

$$P_r(d) = \frac{\lambda^2}{(4\pi d)^2} \quad (1.3)$$

With the free space model, the energy loss due to channel transmission is comparative to the square distance separation of the transmitter-receiver circuitry, which is estimated as $\nu = 2$ for a distance d . And for the multi-path model, it estimates this channel transmission loss as $\nu = 4$ for a distance d .

Free space loss and multi-path fading are the models used in previous studies on clustered WSNs and was adapted in this work, the multi-path model is often used to estimate longer transmission range (between CHs and BS), while the Friis free space model is used for shorter transmission (between CMs and their associated CH).. LEACH [26], SEP [27] and MGEAR [28] consider the crossover distance between $\nu = 2$ and $\nu = 4$, when the BS location lies outside the sensing field. The same values are considered in this work as the chosen simulation scenarios assume that the BS has two locations, one in the middle upper far of the sensing field and another location lies in the right corner of the sensing field.

1.1.3 Data Aggregation

Data aggregation objective is to reduce network resource consumption where a node is capable of gathering data from multiple sources and performs simple compression function or use a spatial correlation to reduce the received data into a single packet. There are four common strategies for aggregations [29]: Centralized Approach, In-Network aggregation, Tree-Based Approach, and Cluster-Based Approach (Fig. 1.5).

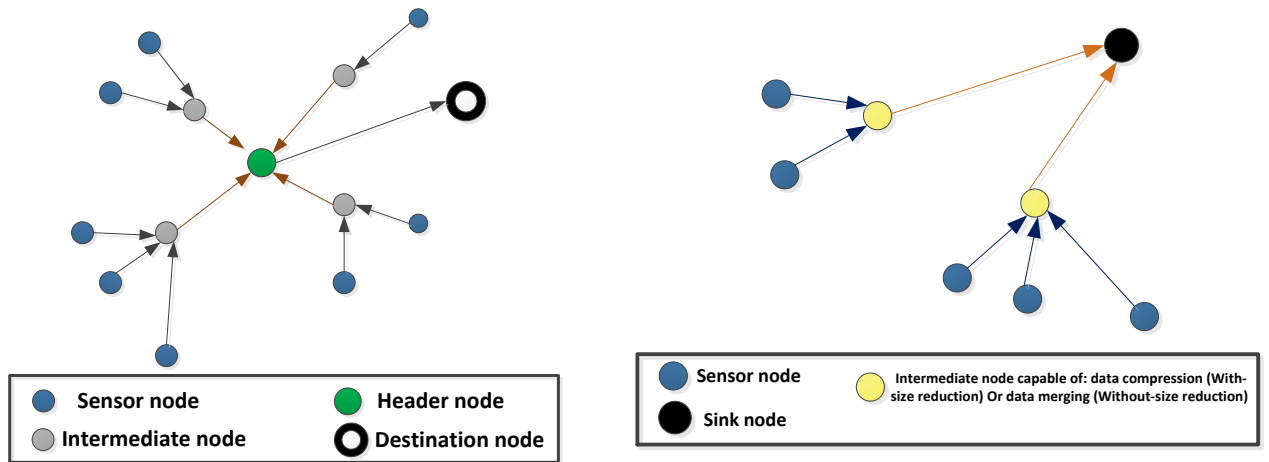
In the **Centralized Approach**, as illustrated in Fig. 1.5a, each node sends data to a central node (leader node that can be queried) through the shortest possible route using a multi-hop wireless protocol. SNs send the data first to intermediate nodes, and then these intermediate nodes send the data to a leader node which is the powerful node. The leader node then aggregates the data and sends it to the sink node. A large number of messages have to be transmitted in this approach for a query, in the best case, equal to the sum of external path lengths for each node.

In-Network Aggregation is the global process of gathering and routing information through a multi-hop network, processing data at intermediate nodes aiming to reduce energy consumption (Fig. 1.5b). In-network aggregation can be in two approaches: *with size reduction* and *without size reduction*. In-network aggregation with size reduction reduces the packet length to be transmitted or forwarded towards the sink by combining & compressing the data packets received by a node from its neighbours. In-network aggregation without size reduction merges the data packets in a single data packet without processing the value of the received data.

Tree-Based Approach, constructs an aggregation tree to perform data aggregation. This tree could be a minimum spanning tree, rooted at the sink and its leaves are the source nodes as can be seen in Fig. 1.5c. Each node has an intermediate parent node to forward its data and the aggregation done by the parent nodes. The flow of data starts from leaves nodes up to the sink.

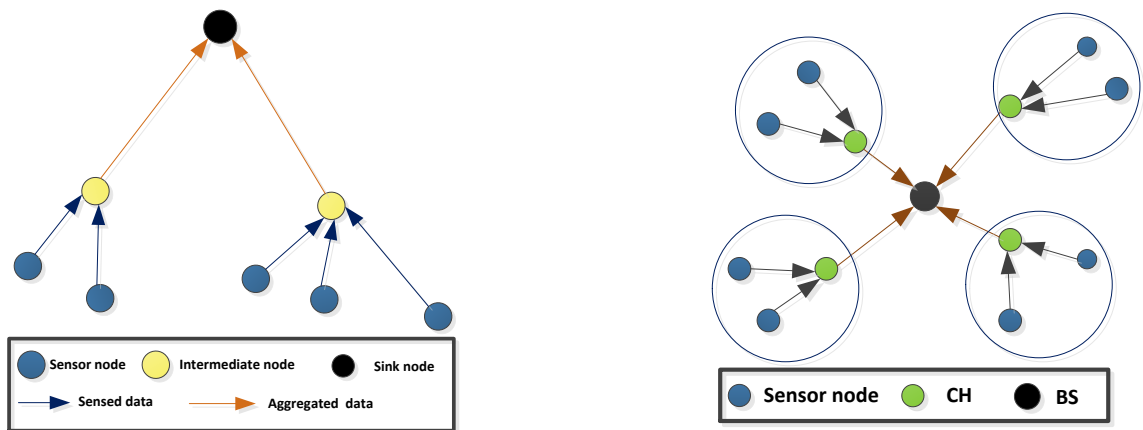
In **Cluster-based approach**, CHs do the role of aggregator which aggregate data received from CMs locally and then transmit the result to the BS. Fig.1.5d

For the purpose of this study, we assume a perfect data aggregation model similar to the one used in a number of previous studies.



(a) Centralized data aggregation.

(b) In-network data aggregation.



(c) Tree-based data aggregation.

(d) Cluster-based data aggregation.

Fig. 1.5 Data aggregation strategies in wireless sensor networks

1.2 Taxonomy of Network Design Strategies in WSNs

WSNs can communicate using routing protocols that utilize a single-level or a hierarchical (multi-level) communication mode to send their data to the BS. In a single-level cluster structure, nodes far away from the BS are likely to die out faster than closer nodes due to the long distance of transmission. On the other hand, in a multi-level

cluster network structure, it is clear that the nodes closer to the BS will die out faster as a result of being over-burdened from relaying packets of other far away nodes.

Designing energy aware protocols for WSNs that meet the requirements of the different communication models was motivated by the shift in communication paradigm from any-to-any in adhoc networks to many-to-one in WSNs. One of the main design objectives of the different communication modes is to reduce the communication cost to further extend the network life time and often decision depends on the network size and the nodes density. A network design of communication hierarchies can produce desirable results if properly implemented. The mentioned communication paradigms with respect to the energy consumptions in the network for a clustered architecture design are discussed next.

1.2.1 Single-level clustering structure

When a direct communication with the BS is established without nodes relaying their packets, it is referred to as single-hop or sometimes as single-level mode. The design of a single-level technique vary depends on the network topologies and the protocol requirements. A protocol design may require cluster formation, where nodes form clusters among themselves such that, cluster members send the data to respective CHs and the CHs perform data aggregation before forwarding the refined data to the BS [30].

On the contrary, a protocol design can completely adopt a layered architecture where the nodes are required to send their data directly to the BS. The downside of a layered design appears in large-scale networks where the BS is located far away from the nodes. Direct transmission, in this case, will require large transmission energy as shown by [26], this method is not so effective for large-scale networks since the node's energy will decay faster which will affect the overall network lifetime of the system. However, if the BS is within the sensing region, the performance could be optimal since the BS is in reachable small distance from the nodes, and it will be the only data reception point which leads to minimizing energy cost function of data aggregation on the total energy of the network system.

Fig. 1.6 represents the single-level communication mode for a clustered WSN with BS located in the middle of the sensing area.

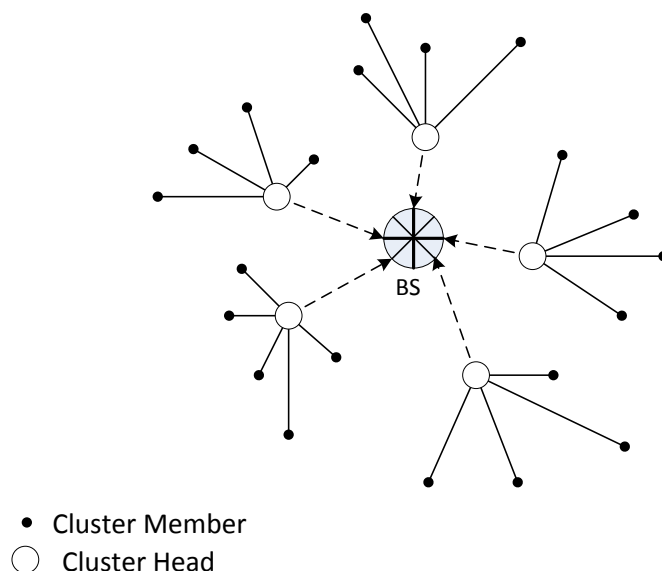


Fig. 1.6 Single-level network design.

1.2.2 Multi-level clustering structure

The concept of multi-level model was built on the idea that nodes further away from the BS can transmit their packets to nodes closer to the BS. One of the earliest works to use this model is the Minimum-Transmission-Energy (MTE) [31], the authors estimated that a packet with a transmission distance more than $(2\rho^{-1})$ should be routed through an intermediate node, and ρ was expressed as the density in the intermediate area. The main goal of their scheme is to use the route with minimum energy consumption. However, data aggregation is another factor that will affect the performance of the network, as for the intermediate nodes they will consume more energy aggregating the packets received from far distanced nodes. Therefore, deploying a multi-level architecture is desirable if the network is large enough to compensate for the aggregation energy of the CHs.

Fig. 1.7 illustrates the multi-level communication mode for a clustered WSN with BS located in the middle of the sensing area.

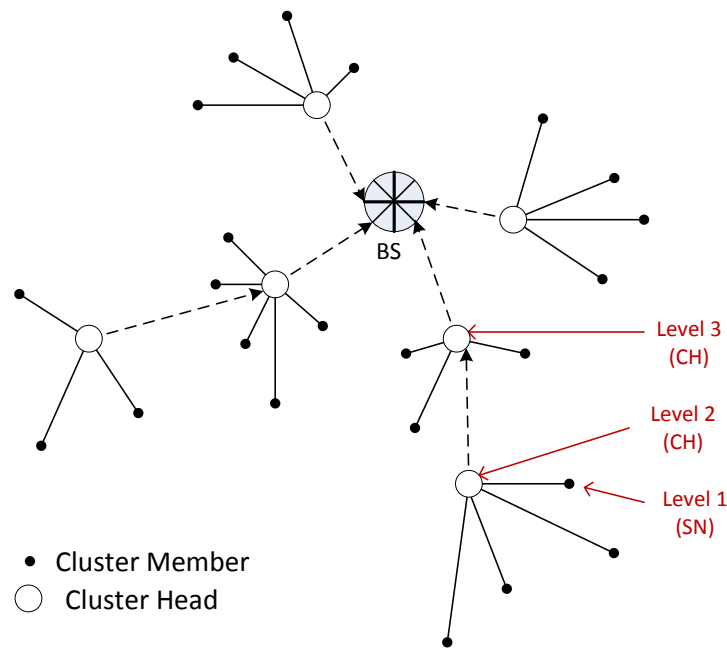


Fig. 1.7 Multi-level network design.

1.3 WSNs Applications

WSNs are currently employed in different infrastructure systems ranging from human body monitoring and early warning systems to smart homes and smart buildings [32]. Some WSNs applications are briefly introduced in this section.

1.3.1 Smart Homes and Intelligent Buildings

With the growing conception and the rising costs of energy, as well as the insufficiency of fossil fuels, a need has been arisen to adapt new strategies for making intelligent buildings. For example in Europe, the energy consumption of buildings (residential and tertiary) represents 40% of the total energy consumption, industry is 30% and transportation is 30% [32]. A study by Danny Parker of Florida Solar Energy Centre [33] showed that the total energy use of 10 identical homes varied by a factor of three, even though they had the same floor area ($102m^2$), were on the same street, built in the same year and with similar efficiencies. This variation is even larger at the energy

end use level (e.g. up to 10.6 times in space heating energy use) [34]. As illustrated in Fig. 1.8.

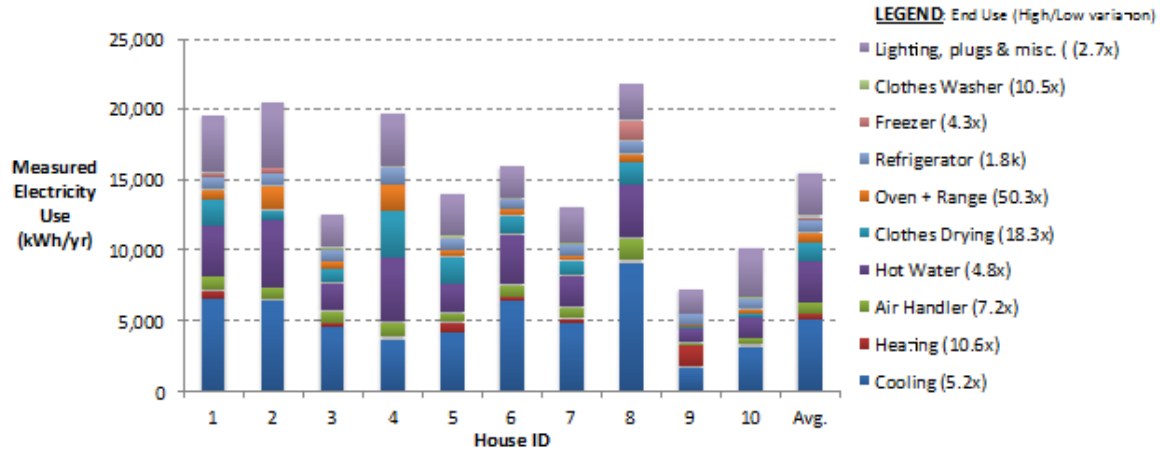


Fig. 1.8 The measured electricity use for ten nearly identical homes, showing considerable variations in energy use.

WSNs was adapted in automated control and monitoring systems for intelligent building, as an example, in 2008, collaborative programme named HOMES has been launched by Schneider Electric in France [35]. Intelligent buildings can optimize their energy consumption, reduce operating expenses and improve safety and security by using smart SNs [17].

Several management systems for smart buildings using WSNs have been proposed in the literature [36–38]. The WSNs used in these systems consist of different types of SNs measuring parameters such as temperature, humidity, light, and asphyxiating smoke, they may also include actuators, gateways, servers, and communication and application software on different levels and home appliances [38].

In order to cover the entire building, the management systems used in intelligent buildings require the use of multihop communication. Specific data-centric or hierarchical protocols can be used to realize this requirement [37]. Besides, network's energy efficiency is another important requirement for such systems [38].

The protocols proposed in this thesis are suitable for large-area monitoring systems and for smart buildings emergency control.

1.3.2 Human Health Monitoring

In the past two decades, health monitoring systems have rapidly evolved due to the ageing population increased number, increased in people number who needs continuous health monitoring and health care rising costs [39]. Remote health monitoring systems (RHMS) and Wireless Body Sensor Networks (WBSNs) have great potential to enable smart real-time assisting e-health applications [40].

RHMS have the potential to change the way health care is currently delivered for older adults, such as in age related diseases [41]. Human body monitoring is performed using small and intelligent medical sensors that can be worn or implanted in the human body called wearable devices or biosensors [42], [43] [44]. Several sensing technologies can be integrated as part of a wearable health-monitoring system, some of them are depicted in Table 1.1 along with their corresponding measured physiological signals [39].

Table 1.1 Biosensors and Biosignals

Type of Bio-signal	Type of Sensor	Description of measured data
Electrocardiogram (ECG)	Skin/Chest electrodes	Electrical activity of the heart (continuous waveform showing the contraction and relaxation phases of the cardiac cycles)
Blood pressure (systolic & Diastolic)	Arm cuff-based monitor	Refers to the force exerted by circulating blood on the walls of blood vessels, especially the arteries
Respiration rate	Piezoelectric/ piezoresistive sensor	Number of movement indicative of inspiration and expiration per unit time (breathing rate)
Body and/or skin temperature	Temperature probe or skin patch	A measure of the body's ability to generate and get rid of heat
Heart rate	Pulse Oximeter/ skin electrodes	Frequency of the cardiac cycle

Health monitoring applications are related to human health and life, therefore they demand high reliability [45] [46] and also to be energy efficient to ensure long time operation of the system [44], [47].

1.3.3 Intelligent Water Systems

Intelligent water systems have been an important part of WSN applications. Clean water availability is one of today's planet's limited resources, water consumption is 300% of what it was in 1950 due to strong growth of the world's population [32]. Water pollution and human activities against estuaries, call for environment monitoring systems. During the last five decades, the Guadalquivir estuary, located in the Southwestern Iberian Peninsula, has experienced profound modifications in relation to its original morphology and natural dynamics [48].

Water sensors allow the monitoring of water parameters that affect water quality in reservoirs. They integrated with a wireless communication facility to efficiently send the collected information when deployed in remote places like rivers, lakes or the sea [49]. Monitored sites in such applications can reach several tens of hectares, therefore the key requirements in designing routing protocols for those systems are energy efficiency, scalability and coverage [9].

1.3.4 Other Applications

There are many other WSNs related applications. For example, WSNs can be applied to monitor the traffic on the motor way or provide traffic control to improve transportation quality. Food chain and fast delivery companies can manage the workflow of their cargos via WSNs [50]. WSNs can be also used for smart parking or in cars to avoid car collision and it also can be used to monitor vehicle speed to reduce fuel consumption [51]. In short, WSNs are still in the early development stage and many applications can be proposed for the use of human or for protecting plant earth.

1.4 Limitations and Challenges in WSNs

WSNs are ideal for inaccessible areas hence they are able to operate unattended, and they are equipped to handle complex functions such as in-network processing (data aggregation), information fusion and computation, and transmission activities. However, WSNs are resource constrained [52]. SNs are generally equipped with non-rechargeable batteries, and once deployed in the area of interest they keep operating until they run out of power. Therefore, SNs are required to use their resources (including energy)

efficiently in order to extend their effective network lifetime [53]. Several challenges are encountered in designing WSNs such as technical and routing challenges.

1.4.1 Technical challenges in WSNs

Major issues that affect the design and performance of a WSN are as follows:

- **Operating System:** Operating Systems (OSs) for WSNs should have an easy programming paradigm and be less complex than the general operating systems. The application logic for WSNs OS is more important than the low level hardware issues like scheduling, preempting and networking which should be considered by application developer. Various OSs developed for SNs such as TinyOS [54], Mantis Operating System [55] and Nano-Qplus [55].
- **Hardware and Software:** WSNs consist of a large number of sensors, sensors should be cost effective. Sensor network hardware platforms have Micro Electro-Mechanical Systems (MEMS) sensor technology, digital circuit design, FPGAs (field programmable gate arrays), system integration for low power consumption and a low-power sophisticated radio frequency (RF). Deployment of FPGA to reduce power consumption is a great challenge. Microcontrollers should have cycle states (active, sleep, and idle) for power saving. Software in WSN should be hardware independent and energy efficient. Algorithms and protocols should be designed in such a way that they should be less complex and be helpful in reducing energy consumption [56], [57], [58].
- **Deployment:** deployment in WSNs vary from wired networks [59], [60]. In real world locations that are hard to reach, sensors are dropped from helicopter; and in some locations, sensors are placed according to some topology. It is very difficult and cumbersome activity depends on the demographic location of the application that how network will be deployed. Deployment of SNs may results in network congestion due to many concurrent transmission attempts made by several SNs or because of nodes locations on the sensing area.
- **Limited Memory and Storage Space:** A sensor is a tiny device with a small amount of memory and storage space. For example, MICA mote [61] measuring 1.0 by 0.25 inches (2.5 x .64 centimetres) and uses Atmel ATmega 128L processor running at 4 megahertz. The 128L is an 8-bit microcontroller that has 128

kilobytes of on-board flash memory to store the mote's program. Therefore, it is a challenge to limit the code size of the routing algorithm

1.4.2 Routing challenges in WSNs

Routing is a key element for sensor networks, a detailed description is provided in this section for the challenges facing routing in WSNs. Assurance data transmission to the BS should be considered in routing design but at the same time nodes' limited resources is another important factor to be considered in designing routing protocols.

Network heterogeneity [62] is one of the main challenges in designing routing protocols for WSNs. WSNs can be classified into homogeneous sensor networks and heterogeneous sensor networks [8]. In a homogeneous network, SNs have identical capacities and functionality with respect to sensing, communication, and resource constraints [63]. SNs in a heterogeneous WSN in the other hand consist have different hardware design, and may not execute the same code, or perform the same functions. In particular, they vary in their maximum battery capacity. Therefore, prolonging the lifetime of a heterogeneous WSN requires the network routing protocol to consider the heterogeneity of the motes. Since communication is the dominant process for energy consumption in motes [64], the upper bound on the lifetime of WSNs is constrained by the communication costs and battery capacity.

Other design metrics can determine the performance of a sensor network, including:

- **Energy efficiency:** in WSNs, energy [65] is consumed in data collection, data processing, and data communication. SNs have to rely on a limited supply of energy (e.g., batteries). Usually SNs monitors harsh and dangerous environments such as forest and building fire, volcanic mountain and underwater. Battery replacement or recharging is not practicable in such environments. It is wise to manage energy to extend the lifetime of the network [9]. Design, develop and implement energy efficient protocols is the most crucial research challenge in WSNs [52], [58].
- **Quality of Service (QoS):** Quality of service (QoS) [66], [67] is the level of services provided by the sensor networks to its users. It is mandatory for WSNs to provide good QoS as they are being used in various real time and critical applications [68]. Network topology in WSNs is application related, therefore it may change constantly and the available state information for routing is inherently

imprecise, which make assuring good QoS difficult. QoS mechanisms should be designed for an unbalanced QoS constrained traffic; since the data is aggregated from many SNs to a BS which leads to unbalanced traffic in sensor network.

- **Scalability:** routing algorithms should operate efficiently in a wide range networks, which contains thousands or hundreds of thousands of nodes. Network performance must not significantly degrade as the network size or node density increases. Design of such routing protocols is very important to the future of sensor networks in IoT [21] [69]. Scalability can be measured in terms of the number of un-clustered nodes. The higher number of un-clustered nodes the lower performance of the protocol in terms of scalability.

1.5 Thesis Motivation

WSNs differ from the traditional wireless ad hoc networks in several aspects. First, SNs are usually densely deployed, the number of SNs in a WSN can be several orders of magnitude higher than the nodes in an ad hoc network. Second, SNs are disposed to hardware failures due exposure to environmental aspects. Third, the topology of a sensor network changes very frequently. Forth, since a large number of SNs are densely deployed, neighbor nodes may be very close to each other [9][70]. Hence, SNs mainly use broadcast communication paradigm, whereas most ad hoc networks are based on point-to-point communications. Thus, energy efficiency, data delivery reliability and scalability are key requirements in WSNs.

Topology control is one of the earliest and most important research topics in the literature of WSNs. The primary role of topology control is to maintain network connectivity and to optimize network lifetime and throughput [71][72]. Generally, there are two topology control approaches in WSNs, the transmission range control, and the hierarchical topology control. In most of the transmission range control approaches, the geometrical position information is used for designing power-efficient network topologies in WSNs. In the hierarchal architecture, the network is divided into smaller clusters and the nodes perform different tasks. One of the efficient topology control methods is clustering SNs to prolong the network's energy efficiency, data delivery reliability and scalability [73] [74].

In order to have an efficient clustering and routing protocol, low energy consumption during clustering and routing should be considered to enhance the network energy

efficiency. Meanwhile, owing to dynamic process environments and the inherent limitation of various hardware and software resources, no single topology will always be best for all applications.

Heterogeneity of the network, redundancy of transmitted data, and the large number of nodes are also challenges to be added for the design of routing protocols in sensor networks.

To optimise energy consumption of routing protocols in WSNs, different techniques were employed in routing and proposed in the literature including data aggregation and in-network processing, clustering technology, genetic algorithms and ant colony algorithms. Such techniques offer various possibilities for routing optimisation but also limited by challenges related to network size, heterogeneity and the size of nodes deployed.

Our motivation for this work is to be able to reduce the energy consumption and prolong the network life time through designing routing protocols that can better manage node heterogeneity and large network size. As a secondary goal, we aim to design a real-time autonomous emergency evacuation approach to increase the survival ratio for smart buildings. MaTlab simulations with complete comparison in terms of energy consumption and network life time are used for the preliminary validation and testing of the proposed algorithms.

1.6 Research Aim and Objectives

The overall aim for the study is to develop routing protocols that could balance the energy consumption in heterogeneous WSNs together with prolonging the network life time in large area networks, as well to develop an emergency navigation algorithm in smart buildings. The research aim is addressed through the following objectives:

1. Review the available literature aimed at improving the energy consumption in WSNs.
2. Develop a selection mechanism that guarantees selecting the best candidate nodes in the network to perform as cluster heads.
3. Merge hierarchal and tree techniques to reduce the intra transmission distance between the cluster heads and the base station.

4. Design a hierarchal routing protocol for large scale networks that can equally and efficiently distribute the energy consumption across all nodes and still achieve an extended network lifetime compared with the state-of-the-art designs architecture in the literature.
5. Design a multi-layer routing protocol for heterogeneous WSN that can equally and efficiently distribute the energy consumption across all nodes and still achieve an extended network lifetime compared with the state-of-the-art designs architecture in the literature.
6. Develop and implement a real-time autonomous emergency evacuation approach for smart buildings that ensures a better survival ratio for different scenarios and hazard intensity ratio.
7. Validate empirically the simulation scenario results.

1.7 Contributions

The main contributions of this thesis include:

1. Comprehensive taxonomy of the significant efforts aimed at improving energy consumption in routing protocols for WSNs.
2. Design and implementation a clustering routing protocol that adapts a centralized approach as well a distributed approach based on human T-Cell positive selection to select the CHs in the network, for the purpose of prolonging the network life time and to balance energy within the network.
3. Design and implementation of a multi-layer energy-efficient clustering protocol that adapt hierarchal techniques based on the Grey Wolf Optimizer (GWO) that define a multi-objective fitness function for CH selection, and also perform tree solution based on a cost function to minimize the transmission distances between the CHs and the BS.
4. Design and implementation of a distributed intelligent emergency evacuation approach based on cloudified WSN for smart building that provides real-time navigation to the evacuees. The main purpose of the approach is to maximize the safety of the obtained paths by adapting to the characteristics of the hazard,

evacuees behaviour and environment condition. It also employs an on-demand cloudification algorithm which improves the evacuation accuracy and efficiency for critical cases.

1.8 Thesis Scope

This thesis proposes a paradigm to prolong the network lifetime of WSNs by reducing and balancing energy consumption during routing process, this involves applying several techniques including clustering, tree formation and distributed and centralized control for the minimization of transmission distances in large-scaled networks. Also, proposing an emergency navigation routing for smart building for different network scales. Therefore, it was essential to outline a clear scope to successfully achieve the objectives in the given time frame. Fig. 1.9 summarize the thesis scope.

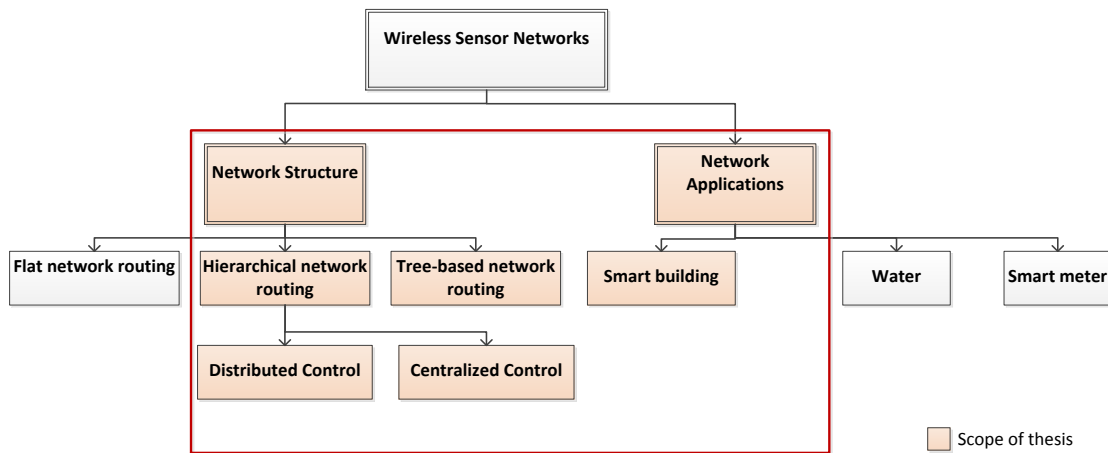


Fig. 1.9 Thesis scope.

The taxonomy of routing techniques in WSNs structure is detailed in [75]. Based on network structure, routing protocols or algorithms in WSNs can be classified into three classes, namely flat-based, hierarchical-based, and tree-based routing protocols. Hierarchical routing use deterministic or centralized control [76]. In this thesis, we combine hierarchical and tree-based routing protocols with deterministic and centralized control and propose two routing protocols for the enhancement of the performance of the network in terms of energy consumption. Then we propose an emergency evacuation system for smart buildings to enhance the survival rate of evacuees in crowded areas with different scaled network size.

1.9 Thesis Outline

This thesis is organized into six chapters as illustrated in Fig. 1.10. Each chapter will start with a brief introduction providing an overview and highlighting the main contributions of the chapter and the end of each chapter a brief summary is presented.

Chapter 2: This chapter presents an overview on the state-of-the-art techniques of clustering protocols in WSNs. It first presents the taxonomy of energy optimization strategies, and then describes the routing protocols based on heuristic and meta-heuristic approaches.

Chapter 3: This chapter gives a detailed description of the proposed single hop hierarchical clustering routing algorithm (called HRHP) for the heterogeneous environment. In HRHP, cluster-heads are selected based on the positive T-cell selection mechanism in the thymus. The selection guarantees only the best nodes to be selected for the purpose of prolonging the network life time and to save network energy.

Chapter 4: This chapter presents an energy-efficient clustering routing algorithm (called MLHP) to further optimize the WSNs energy consumption by combining two key strategies: hierarchical and tree data transition techniques to reduce the intra transmission distance between the cluster head and the base station. In the deterministic part, a cluster head selection is developed based on the GWO. And for the tree transmission, a cost function is adapted for further energy stabilizing.

Chapter 5: This chapter gives the detailed description of two proposed real-time autonomous emergency evacuation approaches that integrate cloud computing to wireless sensor networks in order to improve evacuation accuracy for smart buildings. These approaches provide a distributed path finding for evacuees. Also, SNs identify the occurrences of a common evacuation problem which happens when evacuees are directed to safe dead-end areas of the building. Safe dead-end areas are characterized to be safe at the start of the evacuation process since they are far from the incident but the downside is that they are also far from the exit. When such situation is identified, the proposed approach employs cloudification to efficiently and carefully handle this problem.

Chapter 6: This chapter concludes the thesis and explores suggestions for future research.

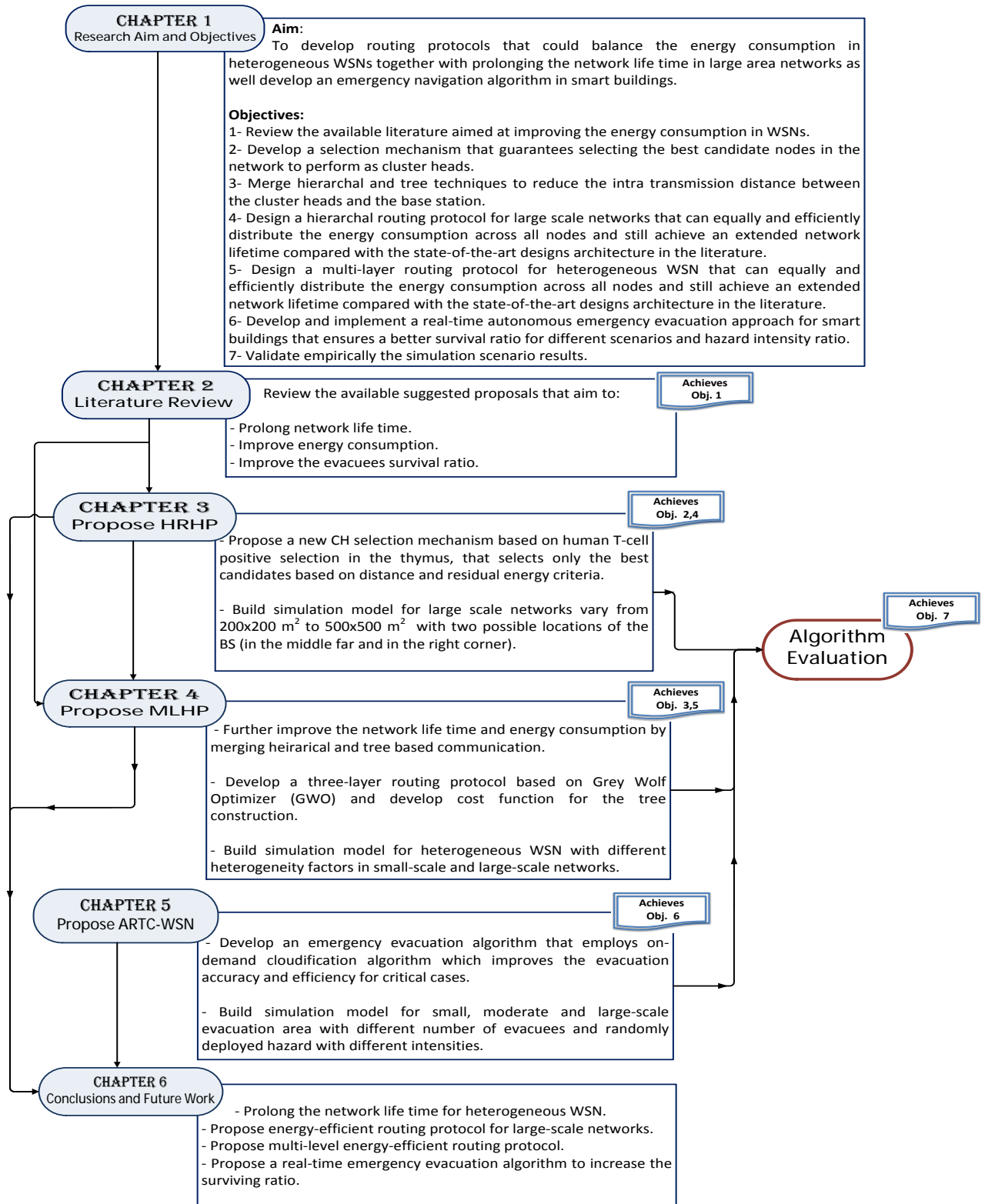


Fig. 1.10 Thesis Outline.

Chapter 2

Literature Review

2.1 Introduction

As mentioned in the previous chapter, mostly, the main challenge of wireless sensor networks (WSNs) deployment is with the energy management, as sensor nodes (SNs) will mainly have limited source of energy. In order to achieve a robust result for data communication, it is important to allow SNs to work in a collaborative manner so as to achieve a collective objective.

Sensor networks can be classified into homogeneous and heterogeneous networks [77] based on the nodes characteristics. In a homogeneous network, SNs have identical characteristics with respect to the various aspects of sensing, communication, and resource constraints [78]. A heterogeneous network consists of nodes with different hardware capacities including battery functionality and different topologies are used which makes the network a very complex network. Since the dominant energy consuming process in a mote is communication, network lifetime is constrained by the communication costs and battery capacity. Therefore, prolonging the lifetime of a heterogeneous WSN requires the network routing protocol to consider the heterogeneity of the motes [79].

Routing protocols for WSNs mainly classified into flat, hierarchical and tree-based routing based on the underlying network structure [8]. Nodes have the same functionality in flat routing and they collaborate together to perform the sensing task.

Flat routing protocols were introduced to overcome the shortage within the direct transmission [78] which is energy constrains. In direct transmission, all nodes send the data directly to the BS which make far away nodes die faster than nodes nearer to BS. Flat networks are multi-hop networks where nodes transmit the sensed data to the nearest node until reaching the BS. This approach helped far away nodes remain alive longer with respect to the nodes nearer to BS, however, since the number of nodes is large in such networks, it is not feasible to assign a global identifier to each node. This has led to data-centric routing, where the BS sends inquiries to certain regions and waits for data from the sensors located in the selected regions. Moreover, flat-routing protocols did not solve the problem of energy and network life time. Fig. 2.1a shows a typical flat structured network.

Originally, hierarchical (also called a clustered-based) routing methods was proposed in wireline networks, which offer well-known techniques with special advantages related to scalability and efficient communication. The concept of hierarchical routing is utilized to solve the problem of energy consumption in WSNs by achieving energy-efficient routing, where nodes play different roles [78] to effectively distribute the energy load among the nodes in the network. Nodes with higher-energy levels can play the role of a cluster head (CH) to process and send the information, while low-energy nodes can be the cluster members (CMs) to perform the sensing in the proximity of the target. The creation of clusters and rotating the role of CH, hierarchical routing reduces energy consumption within a cluster and thus contributes to the whole network scalability and lifetime. Performing data aggregation and fusion in order to decrease the number of transmitted messages to the BS is an efficient way to lower energy consumption within a cluster. Fig. 2.1b hierarchical structured network.

In tree-based routing, tree is constructed by all SNs in a network, data transmitted from leaf nodes to their parent nodes. Parent nodes then send the received data to their parent nodes, this process continues up to the BS. This structure balances the energy consumption between the nodes and extends the network lifetime to some extent [80]. However, the main drawback of this structure is that if used for large-scaled areas it will contain too many levels from root to leaf nodes which consume more memory for data transmission. Fig. 2.1c shows a tree-bases structured network.

Balanced clusters within the network can further increase the performance of the network [81], this is achieved by a centralized control from the BS. Nodes send their energy level to the BS in the setup state, members to be declared as CHs are only those

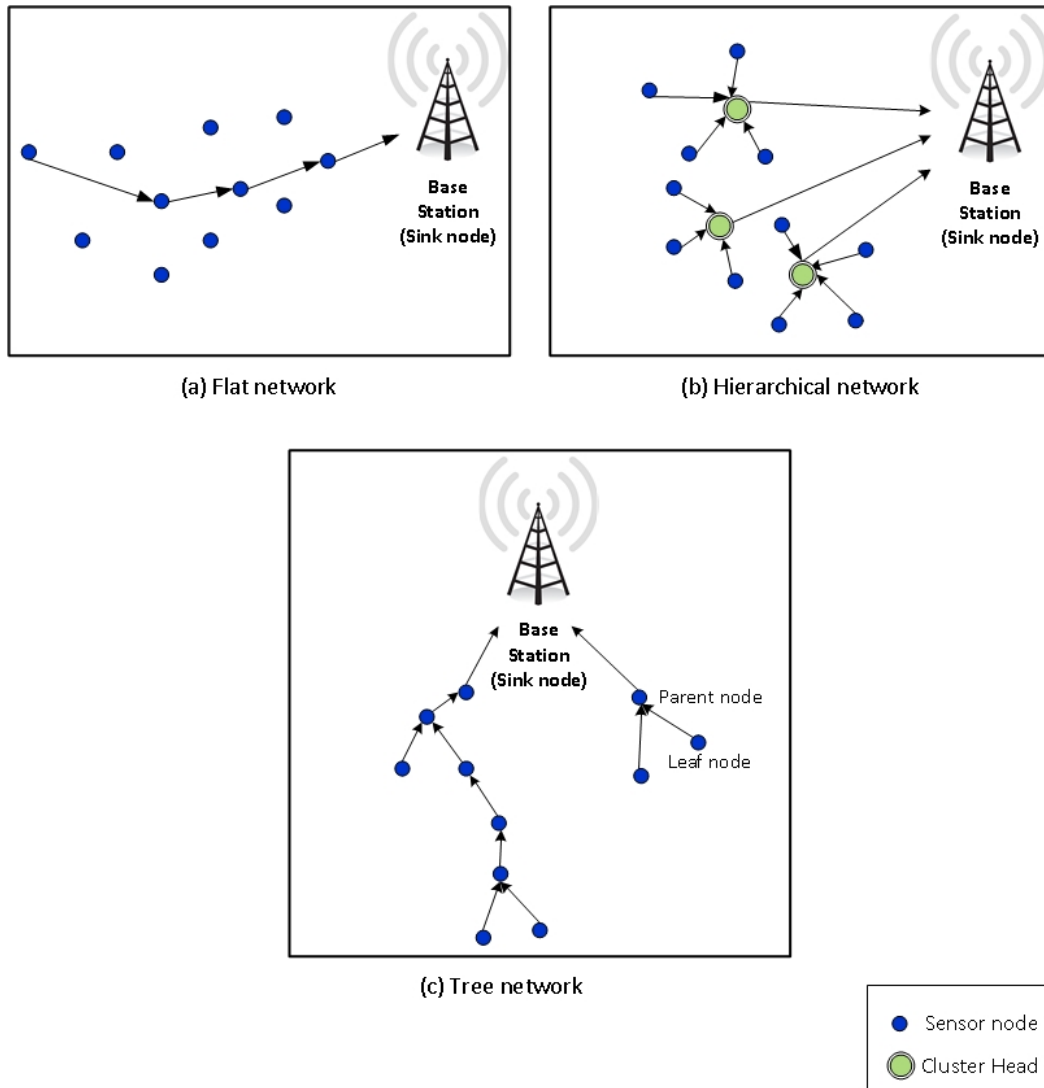


Fig. 2.1 (a) Typical flat structured network. (b) Typical hierarchical structured network. (c) Tree-based structured network

having energy above a fixed threshold, and after BS announces the cluster information to members, the steady state phase starts. However, this technique is not sufficient with large number of nodes and over large areas where the communication distances huge leading to more energy wasted over communication. A distributed control in this case is more efficient, the decision to select a CH is taken by the nodes in the network [26]. Each node will assign a probability factor and the heights will be announced as a CH. However, the frequently the CHs rotate is a factor needs to be considered. If the selection is rotate frequently, it will cause the node more energy loss as it needs to communicate with other nodes and to re construct the cluster.

Development of WSN will continue to receive attention for the reasons that they are powerful for any monitoring application ranging from military to smart homes and cities emerging to the Internet of Things (IoT) [82][83] [84]. Various state-of-the-art techniques have been applied to optimize energy consumption in WSNs, clustering techniques have been studied extensively to improve the performance of WSNs and especially energy efficiency and network life time [8],[52],[85],[86]. The first two contributions in this thesis, which are described in Chapter3 and Chapter4, has been informed and influenced by a variety of other research efforts, which will be described in this chapter. The review will highlight the state-of-the-art methods as applied to routing protocols in WSNs.

The discussion in this chapter presents a review of energy optimization clustering techniques based on heuristic approaches in section 2.2 and metaheuristic approaches in section 2.3.

2.2 Heuristic Approaches

Heuristic algorithms usually find a solution close to the best one among the possible available solutions in acceptable time, but they do not guarantee that the best solution will be found, therefore they may be considered as approximately and not accurate algorithms [87]. These algorithms sometimes treated as accurate when the obtained solution is proven to be the best. The method used from a heuristic algorithm is one of the known methods, such as greediness; however, these algorithms need to be easy and fast, therefore they ignores or even suppresses some of the problem's demands. This section describes some of the routing algorithms that fall into the heuristic definition.

2.2.1 Low Energy-Adaptive Clustering Hierarchical Protocol (LEACH)

One of the first and most common cluster-based routing protocols [85] in WSNs is LEACH [26], it was designed for homogeneous networks and succeed to prolong the network's lifetime to some extend compared to the flat-based routing protocols. LEACH does not require global information of the network; hence, it is completely distributed approach. Nodes in LEACH arrange themselves into single-level clustering structure (as explained previously in sec. 1.2.1, Fig. 1.6), each cluster has one cluster head (CH)

that collects the data from the cluster members (CMs), aggregate the received data, and send it to the base station (BS).

LEACH divides the operation time into rounds, each round is divided into two phases, namely the set-up phase and the steady-state phase which is always longer than the set-up phase to minimize the overhead. In the set-up phase, clusters are organized, while in the steady-state phase, data is delivered to the BS.

During the *set-up phase*, when a node announces itself as a CH, it broadcasts an advertisement message to the other nodes with its location and waiting for joint request from members. Other nodes decide which cluster to join for this round based on the Received Signal Strength Indicator (RSSI) of the advertisement and send a joint request to its CH. In order to equalize the energy load distribution among the CHs, SNs compete among themselves to be declared as CHs, the decision is based on the suggested percentage of CHs for the network and the number of times the node has been a CH so far. In each round, SNs choose a random number between 0 and 1, a successful candidate to become a CH in the current round is the node with random number less than the following threshold:

$$T(n) = \begin{cases} \frac{P}{1 - P \times (r \bmod 1/P)}, & \text{if } n \in G \\ 0, & \text{Otherwise} \end{cases} \quad (2.1)$$

where P is the percentage of CHs (e.g. $P=0.05$ which is equivalent to 5%), r is the current round and G is the set of nodes which have not been elected as a CH in the last $(1/P)$ rounds, for calculation purposes, $\frac{1}{P}$ is rounded to the nearest integer. During the first round, $r = 0$ and each node has a probability P of becoming a CH. Nodes that are currently CHs in the first round cannot be CHs for the next $\frac{1}{P}$ rounds. After $\frac{1}{P} - 1$ rounds, $T = 1$ for any nodes that have not yet been CHs, and after $\frac{1}{P}$ rounds, all nodes are once again eligible to become CHs.

During the *steady-state phase*, SNs sense and transmit data to the CHs which then compress the received data and send the aggregated packet to the BS directly. LEACH uses Time Division Multiple Access (TDMA) to avoid inter-cluster and intra-cluster collisions. After a determined round-length time, the network return into the set-up phase and enters another round of CH election.

LEACH can achieve better reduction in energy consumption compared to direct communication by not allowing nodes to serve as a CH in the next round. However,

LEACH has a number of shortcomings. First, LEACH assumes that all nodes can transmit with enough power to reach the BS if needed and it uses single-hop routing which makes it not feasible in large scale WSNs due to the limited energy resource of sensors. Second, CHs are randomly chosen without any consideration to the limited resources of a sensor including its residual energy and its distance from the CH and the BS. Thus, the distribution of CH number is quite uneven, which cause more energy consumption. Finally, according to the LEACH authors, the rotation of CHs also leads to a dynamically changing cluster sizes which in a way is a source of fault tolerance.

2.2.2 Stable Election Protocol (SEP)

Smaragdakis et al. [27] was the first to investigate the possibility and the impact of energy-heterogeneity, which results from nodes consuming different amount of energy over time. Sources of energy-heterogeneity could be recognized by: 1) Nodes position from the BS, nodes nearer to the BS consumes less energy when communicating with the BS; 2) The number of times a node selected as a CH, which reflects the amount of energy consumed for data aggregation; 3) Nodes could fail during transmission as a result of the deployment environment or an obstacle; 4) New fully charged nodes might installed to recharge the network and 5) Some nodes can be powered with energy harvesting sources such as solar or wind. Based on this investigation, an energy heterogeneous-aware protocol called Stable Election Protocol (SEP) was proposed.

CHs selection in SEP is based on weighted probabilities of each node. The researchers used a two node energy classification to illustrate the energy-heterogeneity of the network. Nodes with lower energy levels were labelled as ‘normal nodes’ and other nodes with higher level of energy were labelled as ‘advanced nodes’. Each type of node elect itself as a CH based on new sets of threshold indication function given below:

$$T(n_{nrm}) = \begin{cases} \frac{P_{nrm}}{1 - P_{nrm} \times (r \bmod 1/P_{nrm})}, & \text{if } n \in G' \\ 0, & \text{Otherwise} \end{cases} \quad (2.2)$$

$$T(n_{adv}) = \begin{cases} \frac{P_{adv}}{1 - P_{adv} \times (r \bmod 1/P_{adv})}, & \text{if } n \in G'' \\ 0, & \text{Otherwise} \end{cases} \quad (2.3)$$

The probability to become a CH (P) in LEACH is replaced with P_{nrm} and P_{adv} indicating the weighted probabilities, which translates into thresholds $T(n_{nrm})$ and $T(n_{adv})$ of election for both the normal and advanced nodes respectively. The values for P_{nrm} and P_{adv} are calculated as:

$$\begin{aligned} P_{nrm} &= P/(1 + m\alpha), \\ P_{adv} &= P(1 + \alpha)/(1 + m\alpha) \end{aligned} \quad (2.4)$$

where m is the proportion of the advanced nodes with α times more energy than the normal nodes. With the above governing equations the SEP protocol improved significantly the network lifetime of WSNs compared with the LEACH protocol. However, the drawback of SEP is that the CHs election among the two types of nodes is not dynamic, which results in nodes that are far away from the powerful nodes will die first.

2.2.3 Distributed Energy-Efficient Clustering Protocol (DEEC)

The Distributed Energy-Efficient Clustering Protocol (DEEC) [88] was also proposed to cope with the network energy-heterogeneity, following the thoughts of SEP [27], DEEC assumed there are nodes deployed with different energies in the network. The process of electing CHs in DEEC is based on the ratio between the residual energy of each node and the average energy of the network. The number of times for a certain node to become a CH differs according to the node initial and the residual energies.

The researchers further estimated the ideal value of the network life time which is used to compute the reference energy that each node should spend during a round. They proposed a set of leading equations to ensure high energy nodes have more chances of being elected as CHs. They choose the probability P_i to become a CH as:

$$\begin{aligned} P_i &= p_{opt} \left[1 - \frac{E(r) - E_i(r)}{E(r)} \right] \\ &= p_{opt} \frac{E_i(r)}{E(r)} \end{aligned} \quad (2.5)$$

where $E_i(r)$ is the residual energy of node i at round r , p_{opt} is the initial probability of a node to become CH in a homogeneous setup as used in LEACH and $E(r)$ is the estimated average energy of the network at round r , which is calculated as:

$$E(r) = \frac{1}{n} E_{total} \left(1 - \frac{r}{R_{max}}\right) \quad (2.6)$$

$$R_{max} = \frac{E_{total}}{E_{round}} \quad (2.7)$$

where R_{max} is the maximum rounds of the network lifetime, n is the nodes number in the network, E_{total} is the total energy of the network at start of deployment, E_{round} is the total energy consumed by all nodes in each round.

DEEC was able to further extend the network lifetime compared with the LEACH and SEP protocols by using this method of estimation. However, advanced nodes always penalize in DEEC, particularly when their residual energy reduced and become in the same range as the normal nodes causing the advanced nodes to die faster than the others nodes.

2.2.4 Energy Efficient Heterogeneous Clustered (EEHC)

The impact of energy heterogeneity of nodes in a clustered network was also studied by [89], where an Energy Efficient Heterogeneous Clustered (EEHC) was proposed. EEHC assumes that nodes are distributed uniformly over the sensing area, and a percentage of the deployed SNs are equipped with more energy resources than the other SNs. Three types of SNs were proposed that equipped with different energy levels, where nodes under first level are known as ‘normal nodes’, second level nodes are the ‘advanced nodes’, and third level nodes are the ‘super nodes’. Super nodes have the highest energy among the three types; hence they have the highest chances of selection as a CH.

EEHC calculates the optimal number of CH (K_{opt}) based on the size of the sensing area M and the total number of nodes n in the network. Two cases were considered in calculating K_{opt} , the first one is when the BS is located in the centre of the sensing area and that the distance between a node and its CH or the BS is less than or equal to a pre-determined distance threshold d_0 . K_{opt} in this case is calculated as below (full equation derivative can be found in [89]):

$$K_{opt} = 0.765 \times \frac{M}{2} \quad (2.8)$$

If there is a significant percentage of nodes with distance to the BS is greater than d_0 , and given the average distance between a CH and the BS d_{BS} , then k_{opt} is calculated as:

$$K_{opt} = \sqrt{\frac{n}{2\pi}} \sqrt{\frac{\epsilon_{fs}}{\epsilon_{mp}}} \frac{M}{d_{BS}^2} \quad (2.9)$$

where ϵ_{fs} is the path-loss in a free space attenuation, and ϵ_{mp} is the path loss in a multipath fading.

The optimal probability of a node to become a CH, p_{opt} , can be determine as follows:

$$p_{opt} = \frac{K_{opt}}{n} \quad (2.10)$$

Let m be the fraction of advanced and super nodes from the total number of nodes n in the network, and m_0 is the percentage of super nodes that are equipped with α times more energy than the normal nodes. The rest $n \times m \times (1 - m_0)$ are the advanced nodes that are equipped with β times more energy than the normal nodes and the remaining $n \times (1 - m)$ are normal nodes. Then the weighted probabilities for normal, advanced and super nodes are, respectively:

$$p_n = \frac{p_{opt}}{1 + m \times (\beta + m_0 \times \alpha)} \quad (2.11)$$

$$p_a = \frac{p_{opt}}{1 + m \times (\beta + m_0 \times \alpha)} \times (1 + \beta) \quad (2.12)$$

$$p_s = \frac{p_{opt}}{1 + m \times (\beta + m_0 \times \alpha)} \times (1 + \alpha) \quad (2.13)$$

The threshold $T(sn)$ used to elect the CH in each round for the normal, advanced and super nodes is calculated as follows, respectively:

$$T(sn) = \begin{cases} \frac{P_n}{1 - P_n \times (r \bmod 1/P_n)}, & \text{if } sn \in G \\ 0, & \text{Otherwise} \end{cases} \quad (2.14)$$

$$T(sa) = \begin{cases} \frac{P_a}{1 - P_a \times (r \bmod 1/P_a)}, & \text{if } sa \in G' \\ 0, & \text{Otherwise} \end{cases} \quad (2.15)$$

$$T(ss) = \begin{cases} \frac{P_s}{1 - P_s \times (r \bmod 1/P_s)}, & \text{if } ss \in G'' \\ 0, & \text{Otherwise} \end{cases} \quad (2.16)$$

Where r is the current round, G is the set of normal nodes, G' is the set of advanced nodes and G'' is the set of super nodes that have not become CHs within the last $1/P$ rounds. When CHs are elected, similar to LEACH, the other nodes in the network choose the best suitable cluster to join according to the RSSI value of the advertisement packet. Then CHs take the responsibility to transmit the data packets with a single-hop to the BS.

EEHC provides a way to calculate the optimal number of CHs based on the network's density and it is applicable for both homogeneous and heterogeneous WSNs, and it. However, if the BS located far from the SNs, calculating k_{opt} usually results in a large number of CHs more than the expected which will affect the network's energy efficiency.

2.2.5 Enhanced Heterogeneous LEACH Protocol for Lifetime Enhancement (EHE-LEACH)

Tyagi et al. [90] proposed a distance based routing protocol called Enhanced Heterogeneous LEACH (EHE-LEACH), to overcome the instability of SEP protocol. In their research they focused on enhancing the life span of the network by proposing a planned distance based threshold which divides the network field into two portions. They proven their assumption on the following:

If the distance between BS and sensor node is sufficiently small then consumption of energy is small for direct communication in comparison to cluster based.

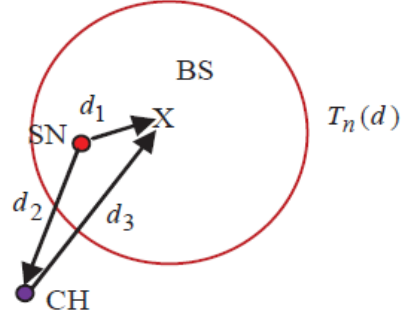


Fig. 2.2 The network model of EHE-LEACH.

Where, d_1 is the distance between BS and SN, d_2 is the distance between SN and CH, d_3 is the distance between CH and BS and $T_n(d)$ is a fixed distance based threshold which is used for the bifurcation of direct and cluster based communication in the planned scheme. SNs near to the BS use direct communication and those which are distant from the BS use group based communication.

Similar to EEHC, nodes in EHE-LEACH are uniformly distributed over the sensing area with a difference that EHE-LEACH uses two levels of node heterogeneity only, normal and advanced nodes that have more initial energy in comparison to the normal nodes. CHs are selected on the same basis of weighted probabilities proposed by [89], for the normal nodes as in Eq. 2.11 and advanced nodes as in Eq. 2.12. And the same threshold will apply as the following for both normal and advanced nodes respectively:

$$T(S_{nrm}) = \begin{cases} \frac{P_{nrm}}{1 - P_{nrm} \times (r \bmod 1/P_{nrm})}, & \text{if } sn \in G \\ 0, & \text{Otherwise} \end{cases} \quad (2.17)$$

$$T(S_{adv}) = \begin{cases} \frac{P_{adv}}{1 - P_{adv} \times (r \bmod 1/P_{adv})}, & \text{if } sa \in G' \\ 0, & \text{Otherwise} \end{cases} \quad (2.18)$$

EHE-LEACH was evaluated on different network scenarios, with BS located at one of the corners of network field and secondly at the centre of network field. To assess the act of EHE-LEACH, two key parameters known as: Half Nodes Alive (HNA) and Last Node Alive (LNA) were selected. The distance based selection of threshold with the

ratio of 1:9 between direct and cluster based communication. It has been observed that EHE-LEACH has better network lifetime with respect to various parameters in comparison to the other well-known proposals such as LEACH and SEP. However, the researches tested their protocol for small-scaled network with the size of $(100 \times 100 m^2)$ with a total of 100 nodes. The performance of EHE-LEACH is compromised when used for large-scaled networks with small number of node deployment where the distances between the nodes will become large. Another major drawback of EHE-LEACH is that it does not consider the network coverage. Moreover, each node in EHE-LEACH requires additional global knowledge about the number of normal nodes, advanced nodes, and their initial energy.

2.2.6 Gateway-based Energy-Aware Multi-hop Routing protocol for WSNs (M-GEAR)

The authors of [28] emphasizes on the transmission distance impact on the performance of the WSN, they proposed a gateway based energy-aware multi-hop routing protocol (M-GEAR) which divides the sensor nodes into four regions based on the nodes location with the BS positioned out of sensing area. They also placed a special node termed as Gateway at the centre of the sensing area. Region one is near the BS, region four is near the gateway, and the other two regions, which are far from the BS, are divided into equal halves as illustrated in Fig.2.3.

Region one and four are termed as non-clustered regions, nodes in these regions use direct communication to send packets directly to BS or gateway respectively because nodes are located to small distances from the BS or the gateway. The other two regions are termed as clustered regions where nodes in these regions take part in the CHs formation exactly the same way as of LEACH; SNs transmit their data to the gateway node through their CHs and the gateway node aggregate the received data and send it to the BS.

M-GEAR performs better than LEACH in terms of residual energy, throughput and lifetime; however, it has some limitations. In M-GEAR, the nodes have to decide whether to take part in clustering or in direct communication at every round which increases overheads. Furthermore, implementing gateway is expensive in terms of energy and it is not practical in WSNs. Moreover, when the sensing area increase with

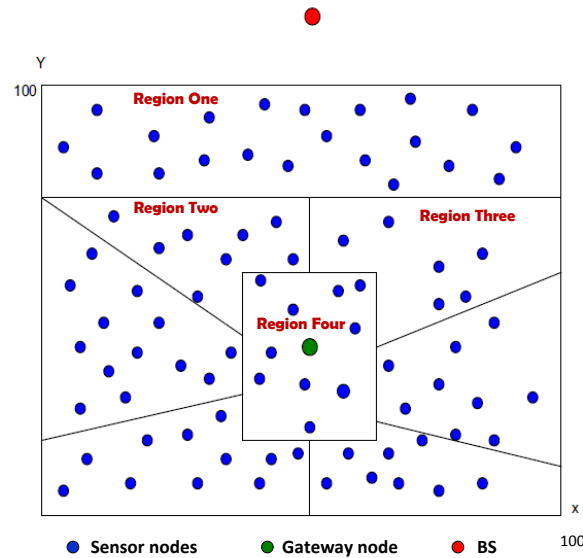


Fig. 2.3 The network model of M-GEAR.

small number of sensors deployed, the distances between the nodes and the BS will increase which will result in nodes consuming their energy faster.

2.2.7 Tree Based Clustering (TBC)

Tree based clustering (TBC) [91] is an improved version of LEACH protocol, it constructs clusters with random selection of CHs same as LEACH but also constructs a tree inside the cluster. TBC function in three phases, the first phase for cluster formation and the other two for the formation and construction of the tree.

In the first phase, clusters are formed but with only 5% of nodes performing as CHs. Each cluster constructs a tree with the member nodes where the CH becomes the root. During the second phase, tree formation is completed and the tree level for each member node in the cluster is decided. While the third phase is a tree construction phase, the CH makes decision and chooses a parent for its CMs to send their data to the assigned parents based on the TDMA scheduling that CH had broadcast to all the CMs.

TBC assumes that nodes in the network are homogeneous, location aware and can estimate the distance from the root to the node. The basis for determining the levels in the cluster is based on the distance of a node to the root and calculated as follows,

$$d_{\alpha} = \frac{d_{max}}{\alpha} \quad (2.19)$$

Where, d_{α} is the average data transmission distance between two adjacent levels of the tree, d_{max} is the distance of the farthest node from the CH and α is the number of levels decided according to the size of the network. Fig. 2.4 shows an example of level formation with $\alpha = 4$. The CH is located at level 0, nodes in higher levels selects a parent from the lower level which is nearest to itself. For a node in level $L(i)$, it will choose the node in $L(i) - 1$ that is nearest to itself as its parent node.

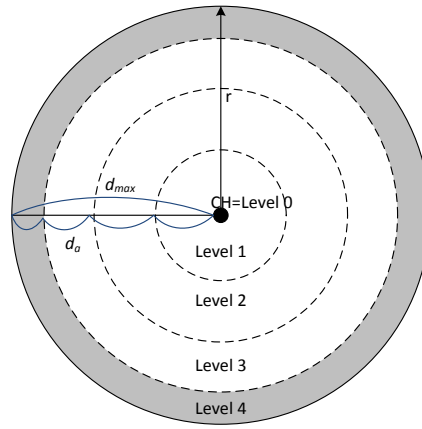


Fig. 2.4 Tree level construction in TBC.

TBC has several advantages over LEACH, it balances energy among the nodes, nodes in TBC maintain their neighbour's information, and constructing the routing tree is deterministic. However, TBC suffers from the similar limitation like LEACH. Moreover, with small number of levels, the transmission distance becomes too long and more energy is consumed for the data transmission. In a contrast, when the number of levels is high, excessive packet forwarding is required and energy is wasted which make TBC not suitable for large-scaled networks.

2.3 Meta-heuristic Approaches

As discussed in section 2.2, heuristic means to find or to discover the solution by trial and error. In modern applications, as always, money, resources and time are always limited therefore an optimal utility of these available resources is crucially important. Based on these needs, optimization or nature-inspired algorithms were developed for

the period of 1980s and 1990s [92]. These algorithms are referred to as *metaheuristics* [93][94], Meta- means beyond or higher level which generally perform better than simple heuristics algorithms in finding solutions. They can also be considered as a [95]

Master strategy that guides and modifies other heuristics to produce solutions beyond those that are normally generated in a quest for local optimality

Metaheuristics algorithms can find the quality solutions in a reasonable amount of time, however, one of the difficulties with these algorithms is that there is no guarantee that optimal solutions can be reached. Therefore, adjusting these protocols to be used with WSNs routing is a key factor in the protocol success.

2.3.1 LEACH-Centralized (LEACH-C)

LEACH-centralized (LEACH-C) [81] is a centralized version of the LEACH protocol. The BS in LEACH-C controls the CHs selection and cluster formations, unlike LEACH, where nodes are self-configured into clusters. The steady-state of LEACH-C is identical to that of LEACH [26], however, the set-up phase in LEACH-C is different. During the set-up phase, each node sends its location and the remaining energy level to the BS, which then uses this information to find a predetermined number of CHs by implementing a Simulated Annealing (SA) approach and configure the network into clusters.

CHs selection is made on the basis of location information and remaining energy level of all the SNs. The BS calculates an average energy level, nodes considered in the selection of CHs are those nodes with remaining energy level above the average energy level, and those nodes with energy level below the average energy level are considered not eligible to become CHs to ensure even distribution of load among the SNs.

BS chose the clusters to minimize the amount of energy for the CMs nodes to transmit their data to the CH, through minimizing the total sum of squared distances between all the CMs and the closest CH which is given by:

$$Total_{Dist} = \sum_{n=1}^N dist(n, CH_n)^2 \quad (2.20)$$

Where N is the total number of nodes in the network and $dist(n, CH_n)$ is the distance from that node to its respective CH.

The BS in LEACH-C produces better clusters that require less energy for data transmission by utilizing its global knowledge of the network. BS also choses a fixed number of CHs in each round that equals to a predetermined optimal value. However, LEACH-C requires Global Positioning System (GPS) or other location tracking methods for SNs to know the location. Moreover, it obligates the nodes to perform a direct communication with the BS in every round at the setup-phase for information forwarding, in order for the BS to have a global view of the WSN at all times which will result in more energy consumption and overhead.

2.3.2 A Genetic Algorithm in LEACH-C Routing Protocol for Sensor Networks (GA-C)

A genetic algorithm (GA)-based clustering protocol (GA-C) was proposed in [96] to minimize the total network distance by finding the optimal set of CHs.

GA-C follows the trail of LEACH-C in forcing centralized control for selecting the CHs. Same as LEACH-C, in the set-up phase, all SNs send information about their residual energy status and locations to the BS. BS then uses GA and defines a fitness function to find the best clusters. GA-C ensures that CHs are only selected from those nodes with sufficient energy. To ensure that, GA-C randomly initializes each chromosome of its population with the *IDs* of the nodes that have an above average energy level. And that each CH can send its data directly to the BS.

The fitness function is defined as the minimization of the distance from the CHs to the BS plus the total distance from CMs to their respective CHs. The fitness function used to evaluate any chromosome C_j is defined as follows:

$$Fitness(C_j) = \sum_{k=1}^K \sum_{\forall n_i \in C_{j,k}} d(n_i, CH_{n_i})^2 + d(CH_{C_{j,k}}, BS)^2 \quad (2.21)$$

Where K is the CHs number and $CH_{C_{j,k}}$ is CH number k in chromosome C_j .

In GA-C, the BS utilizes its global knowledge of the network to produce better clusters that require less energy for data transmission. However, GA-C suffer from the same drawbacks as LEACH-C and CHs selection happen in every round which yield to more energy consumption when re-structuring the clusters.

2.3.3 A Evolutionary Approach for Load Balanced Clustering Problem for WSN (GA-LBC)

GA-LBC [97] is a centralized GA-based protocol designed to solve the load balancing problem of the CHs. In this protocol, the CHs are determined a priori and cluster formation is decided in a way that the maximum load of each CH is minimized by finding the optimal assignments of non-CHs nodes to CHs.

The fitness function of GA-LBC is assembled on the basis of the standard deviation (σ) of the CH load that gives an even distribution of the load per cluster. If m CHs and n sensor nodes, the standard deviation of a CH load is given by:

$$\sigma = \sqrt{\frac{\sum_{j=1}^m (\mu_{S_j} - W_j)^2}{m}} \quad (2.22)$$

$$\mu = \frac{\sum_{i=1}^n d_i}{m} \quad (2.23)$$

Where, μ is the average load, d_i is the load of the SN S_j and W_j is the overall load of CH. Smaller standard deviation values produce higher fitness values.

Therefore, the fitness function to evaluate chromosome C_j is given by:

$$Fitness(C_j) = \frac{1}{\sigma_{C_j}} \quad (2.24)$$

GA-LBC was compared to the results of applying both GA and Differential Equation (DE) algorithms on the formulated problem. The authors of GA-LBC proved that the GA-based approach achieved faster convergence than the DE-based approach.

Although GA-LBC objective is to create load-balanced clusters, it ignores how the CHs are selected and hence it ignores other network factors like the energy efficiency and the inter-cluster communication cost.

2.3.4 Energy-aware Clustering for WSNs using PSO Algorithm (PSO-C)

PSO-C [98] is a centralized particle swarm optimization (PSO)-based clustering protocol that is implemented at the BS. PSO-C considers the node's remaining energy and its physical distance from the CMs when selecting the CHs. According to the authors' assumption, PSO-C can produce clusters that are evenly positioned throughout the whole network's field.

At the beginning of each set-up phase, all nodes send information about their current energy status and locations to the BS. The BS then calculates the average energy level of all nodes and only selects nodes to act as a CH candidate with an above average energy level. Next, the BS executes the PSO algorithm to decide the best CHs that can minimize the fitness function. This function tries to minimize both the maximum average Euclidean distance of nodes to their associated CHs and the ratio of the total initial energy of all nodes to the total energy of the CH. The fitness function used in PSO-C to evaluate any particle P_j is given by:

$$Fitness(P_j) = w_1 \times F_1(P_j) + (1 - w_1) \times F_2(P_j), w_1 > 0 \quad (2.25)$$

$$F_1(P_j) = \max_{k=1,2,\dots,K} \sum_{\forall n_i \in C_{P_j,k}} \frac{d(n_i, CH_{P_j,k})}{|C_{P_j,k}|} \quad (2.26)$$

$$F_2(P_j) = \frac{\sum_{i=1}^N E(n_i)}{\sum_{k=1}^K E(CH_{P_j,k})} \quad (2.27)$$

Where $F_1(P_j)$ is the maximum average Euclidean distance of the SNs to their respective CH, $|C_{P_j,k}|$ is the number of nodes that belong to the cluster C_k of particle P_j and $F_2(P_j)$ is the ratio of total initial energy of all the SNs in the network with the total current energy of the CHs candidates in the current round. While, w_1 is a user defined weight used to weight the contribution of each sub-objective and K is the number of total clusters.

The fitness function, $Fitness(P_j)$, was formulated as a minimization function with the responsibility of concurrently minimizing the intra-cluster distance between nodes

and their CHs, as quantified by $F_1(P_j)$, and of optimizing the energy efficiency of the network as quantified by $F_2(P_j)$.

PSO-C takes into consideration the cost of both the inter-cluster communication and the network's energy efficiency, the authors of [99] showed that PSO-C outperforms GA and K-means-based clustering protocols in terms of convergence time, network energy efficiency and data delivery. However, PSO-C calculates the fitness function repeatedly and to do so, in every round nodes need to directly communicate their information with the BS causing more energy consumption for larger areas of monitoring.

2.3.5 Energy-aware Evolutionary Routing Protocol for Dynamic Clustering of WSNs (EAERP)

EAERP [100] is a single-hop centralized clustering protocol where the selection of CHs is controlled by the BS. During the election phase, the BS runs an evolutionary based protocol to optimize the CH selection for cluster formation, an initial population of individuals is generated and each individual is evaluated using a fitness function. Each individual of the EAERP population is represented such that it implicitly facilitates the formation of a dynamic number of CHs during the single and throughout the entire rounds of the routing protocol. These individuals will go through evolutionary operators – selection, recombination and mutation – with pre-determined probabilities to improve the quality of the individuals, this loop will continue until the termination criteria are satisfied.

EAERP uses the same energy consumption model defined by LEACH [26] to compute the energy dissipated during the data transmission process. Cluster formation is based on nodes satisfying a fitness function to be selected as CHs. Which is defined as the minimization of the total dissipated energy in the network and measured as the sum of the total energy dissipated from the CMs to send data signals to their CHs plus the total energy spent by CH nodes to aggregate the data signals and send the aggregated data to the BS.

A complete clustered route solution is regarded as an individual, I . Formally, the fitness function used to evaluate an individual I_k is defined below:

$$Fitness(I_k) = \left(\sum_{i=1}^{nc} \sum_{s \in C_i} E_{TX_{s,CH_i}} + E_{RX} + E_{DA} \right) + \sum_{i=1}^{nc} E_{TX_{CH_i,BS}} \quad (2.28)$$

where nc is the total number of CHs, $s \in C_i$ is a CM associated to the i_{th} CH node, $E_{TX_{node1,node2}}$ is the energy dissipated for transmitting data from $node1$ to $node2$. The energy dissipated during the process of transmitting (E_{TX}) and receiving information (E_{RX}) is computed using the first order radio model [26] and E_{DA} is the energy dissipated during data aggregation process in the i_{th} CH.

After finding the optimal set of CHs, each CM determines the cluster to which it belongs by selecting the CH that requires the minimum energy consumption for communicating, which is the closest CH.

EAERP uses a centralized method that leads to better performance since the BS utilizes its global knowledge of the network to produce better clusters that require less energy for data transmission. However, the fitness function in EAERP is repeatedly calculated in every round, which force nodes to directly communicate their information with the BS causing more energy consumption for larger areas of monitoring.

2.3.6 Energy Balanced Unequal Clustering Protocol (EBUC)

EBUC [101] is a centralized clustering protocol, similar to PSO-C, it uses PSO at the BS to find the optimal set of CHs and their associated clusters. EBUC partitions the sensing area into clusters of unequal sizes, where the clusters are created such that the ones near the BS have a fewer number of nodes, and thus increases the number of clusters around the BS. The CHs of these clusters can preserve more energy for inter-cluster communication.

In the first set-up phase, all the SNs send information about their initial energy status and location to the BS. The BS can estimate the energy level of all nodes in the set-up phase of the following rounds considering the nodes' information sent from the first round and by computing the energy dissipation of the SNs in the last round. Similar to LEACH-C and PSO-C, only the nodes with an above average energy level are eligible to be CH candidates for the current round.

The BS uses PSO and defines a fitness function to find the optimal clusters, this function takes into consideration minimizing the intra-cluster distance, balancing the energy consumption between the CHs and producing clusters with uneven sizes to balance the energy consumption among the CHs. The fitness function used to evaluate any particle P_j is defined as follows:

$$Fitness(P_j) = w_1 \times F_1(P_j) + w_2 \times F_2(P_j) + w_3 \times F_3(P_j) \quad (2.29)$$

$$F_1(P_j) = \max_{k=1,2,\dots,K} \sum_{\forall n_i \in C_{P_j,k}} \frac{d(n_i, CH_{P_j,k})}{|C_{P_j,k}|} \quad (2.30)$$

$$F_2(P_j) = \frac{\sum_{i=1}^N E(n_i)}{\sum_{k=1}^K E(CH_{P_j,k})} \quad (2.31)$$

$$F_3(P_j) = \frac{\sum_{i=1}^K d(BS, CH_{P_j,k})}{K \times d(BS, NC)} \quad (2.32)$$

Where, function $F_1(P_j)$ is the maximum average Euclidean distance between the SNs and their respective CHs and $|C_{P_j,k}|$ is the number of nodes that belong to the cluster C_k of particle P_j . Function $F_2(P_j)$ is the ratio of the total initial energy of all the SNs in the network with the total current energy of the CH candidates in the current round. Function $F_3(P_j)$ is the ratio of the average Euclidean distance of the CHs to the BS with the Euclidean distance of the network centre (NC) to the BS. w_1 , w_2 and w_3 are user-defined weights used to weight the contribution of each of the sub-objectives, $w_1 + w_2 + w_3 = 1$.

The fitness function $Fitness(P_j)$ was formulated as a minimization function that has three main objectives: to simultaneously minimizing the intra-cluster distance between nodes and their CHs, as quantified by $F_1(P_j)$, optimizing the energy efficiency of the network as quantified by $F_2(P_j)$, and also of producing clusters with different sizes, as quantified by $F_3(P_j)$. According to the authors of [101], a small value of $F_1(P_j)$ and $F_2(P_j)$ suggests sufficient clusters with optimum set of nodes that have sufficient energy to perform the CH tasks. And a small value of $F_3(P_j)$ means that there are more CHs in the area closer to the BS.

For the inter-cluster communication, EBUC adopts a greedy algorithm to choose a relay node for each CH. Each CH, s_i chooses its relay node rn_i based on the node's residual energy and distance to the BS by using a greedy approach. The node rn_i has the least value of the cost function among all the CHs located between node s_i and the BS. The cost function is defined as:

$$\text{cost}(s_i, s_j) = \frac{d^2(s_i, s_j) + d^2(s_j, BS)}{E(s_j)} \quad (2.33)$$

Where $d(s_i, s_j)$ is the distance from node s_i to node s_j , $d(s_j, BS)$ is the distance between node s_j and the BS, and $E(s_j)$ is the residual energy of node s_j .

EBUC provides a method to construct the inter-cluster communication tree and it takes into consideration the cost of both inter-cluster communication and intra-cluster communication as well as the network's energy efficiency. However, it only applicable for situations where the BS is located outside the sensing area.

2.4 Supplementary Remarks

Table 2.1, provides an overview of the described protocols. Two broad strategies types can be classified based on the algorithms described in this chapter, namely globalised strategies (centralized control by BS) and localised strategies (deterministic control by nodes). If using a globalised strategy, the protocol makes routing decisions based on the global state of the system. In localised routing algorithms, the nodes mostly make routing decisions on the basis of the location of their neighbours and the destination.

Global routing algorithms can exploit the state information available to them in order to maximise network lifetime. However, it requires continuous communication between the nodes for global energy information of all nodes in the network which is necessary in order to gather this state information; a global addressing scheme is thus required and the overhead of identification (ID) maintenance rises rapidly with the number of nodes. It is impractical to deploy such algorithms in networks containing a large number of sensor nodes.

Localised routing algorithms have better scaling properties, but it requires direct communication with the BS for transmitting relevant information which seriously degrades network lifetime performance when the base station is far away from the nodes. Hence, it is impracticable to deploy such algorithms in large scaled network where direct communication will cause enormous energy consumption. Clustering methods were used to improve the network lifetime performance and other protocols considered the residual energy in each node in deciding the probabilities of each node to become a CH. Energy consumption was reduced when using clustering methods by using CHs to aggregate data before sending received data to the BS.

The goal of maximising network lifetime in large-scale sensor networks is further complicated in resource-constrained heterogeneous WSNs where traditional homogeneous routing techniques are inefficient. New techniques are needed to effectively exploit the hardware capabilities of the multiple types of mote present in such networks.

2.5 Summary

This chapter reviewed some of the routing techniques used in WSNs. The chapter enveloped and presented the state of the art for routing techniques as heuristic (traditional) and meta- heuristic (optimization), which aimed to reduce energy consumption in WSNs. One approach to extend the network lifetime in heterogeneous WSNs is by considering the advantages of both global and localized approaches to be implemented in a way where centralized control is forced for regions near the BS and by selecting only those nodes with higher capabilities to act as a CH, a proposed HRHP protocol uses this technique and will be explained in details in chapter 3. Another approach is by using topology control to keep the transmission distance low, therefore MLHP protocol was proposed and will be discussed in details in chapter 4.

Table 2.1 Comparison of clustering protocols with respect to clustering attributes.

Clustering Protocol	Clustering Method	Clustering Approach	No. of CHs	Connectivity to BS	Network Type	Protocol's objectives	
						EE ^b	Large-scaled Network
LEACH	Distributed	Prob. ^a /Random	Variable	One-hop	Homogeneous	✓	✗
SEP	Distributed	Prob.	Variable	One-hop	Heterogeneous	✓	✓
DEEC	Distributed	Prob.	Variable	One-hop	Heterogeneous	✓	✗
EEHC	Distributed	Prob./Energy	Fixed (Depends on the network density)	One-hope	Homogeneous/Heterogeneous	✓	✗
EHE-LEACH	Distributed	Prob./Energy	Fixed (Depends on the network density)	One-hope	Homogeneous/Heterogeneous	✓	✗
M-GEAR	Distributed/Gateway	Prob.	Variable	Multi-hop	Homogeneous	✓	✗
TBC	Distributed/Tree	Prob.	Fixed (5% of the network size)	Multi-hop	Homogeneous	✓	✗
LEACH-C	Centralized	SA	Fixed (5% of the network size)	One-hop	Homogeneous	✓	✗
GA-C	Centralized	GA	Fixed (5% of the network size)	One-hop	Homogeneous	✓	✓
GA-LBC	Centralized	GA	Variable	One-hop	Homogeneous	✓	✓
PSO-C	Centralized	PSO	Fixed (5% of the network size)	One-hop	Homogeneous	✓	✗
EAERP	Centralized	EA	Variable	One-hop	Homogeneous/Heterogeneous	✓	✗
EBUC	Centralized	PSO	Fixed (5% of the network size)	Multi-hop	Homogeneous	✓	✓

^aProb: Probabilistic^bEE: Energy Efficiency

Chapter 3

HRHP: Hybrid T Cell Based CH-Selection for Prolonging Network Life Time in Large-Scale WSN

3.1 Introduction

For the purpose of improving the lifetime in WSNs, grouping sensor nodes (SNs) in clusters considered to be an efficient topology control approach. The performance of clustering is greatly affected by the selection of Cluster Heads (CHs), which are the leading nodes that create the clusters and control the member nodes. The objective of clustering is to search amongst a group of SNs and find a set of nodes that can act as CHs. The challenge is to find a set of nodes that serve the network in the best form and preserve the network energy.

Several clustering protocols have been proposed in the literature. However, most of these protocols assumed that CHs can send the data directly to a centred base station (BS) regardless the transmission distance. Nodes in WSN have limited communication range, and the BS is usually located far from the sensing area. Therefore, a more realistic clustering approach would consider the location of the nodes as well the location of the BS.

This chapter presents a hybrid routing protocol for heterogeneous WSNs, named HRPH, to prolong the network lifetime in large-scaled wireless sensor networks (WSNs). It introduces a procedure to choose fixed number of CHs during the cluster formation phase, which is based on the positive selection mechanism in the human thymus cells (T-cells). A positive selection is applied first, which is responsible for ensuring that all T-cells that recognize self-protein are selected. Negative selection is then applied to all cells that express harmful or useless antigens, so that they receive an elimination signal and die [102].

The decision to select CHs places importance on the node's distance from other nodes and from the BS (net distance), the residual energy of the nodes, and the density of nodes. Centralized and distributed controls are applied to guarantee self-adaptive routing. Simulation results show an improvement in network lifetime in terms of the Last Nodes Dead (LND), and also a longer stability period in terms of First Node Dead (FND) compared to the existing protocols. The next section provides an overview about the human T-Cell positive selection mechanism. Section 3.3 exhibits the details of the proposed MLHP algorithm, section 3.4 presents the performance results of the proposed algorithm and finally, section 3.5 summarizes this chapter.

3.2 Human T-Cell Positive Selection Mechanism

T (thymus-derived) lymphocytes have vital roles in the immune system [103], and are generated from stem cells. During development in the thymus, T-cells go through a process of selection and testing to ensure that cells expressing harmful or useless antigen receptors do not mature (Fig. 3.1). Before they enter the thymus, stem cells lack antigen receptors, and also lack the proteins CD3, CD4, and CD8 on their surface; they are said to be *double negative* (D_N , or $CD4^- CD8^-$). When they enter the thymus, T-cells generate receptors (TCRs) with different sequences and specificities by rearranging their DeoxyriboNucleic Acid (DNA) [104].

During passage through the thymus, these cells differentiate into T-cells that express both CD4 and CD8 (*double positive* (DP)). A double-positive cell differentiates into either a CD4 or a CD8 positive cell, depending on the molecule engaged. If a TCR engages with a major histocompatibility complex class (MHC) I molecule, that T-cell becomes CD8-positive (i.e. cytotoxic). Likewise, if a TCR engages with an MHC II molecule, that T-cell becomes CD4-positive (i.e. a helper cell).

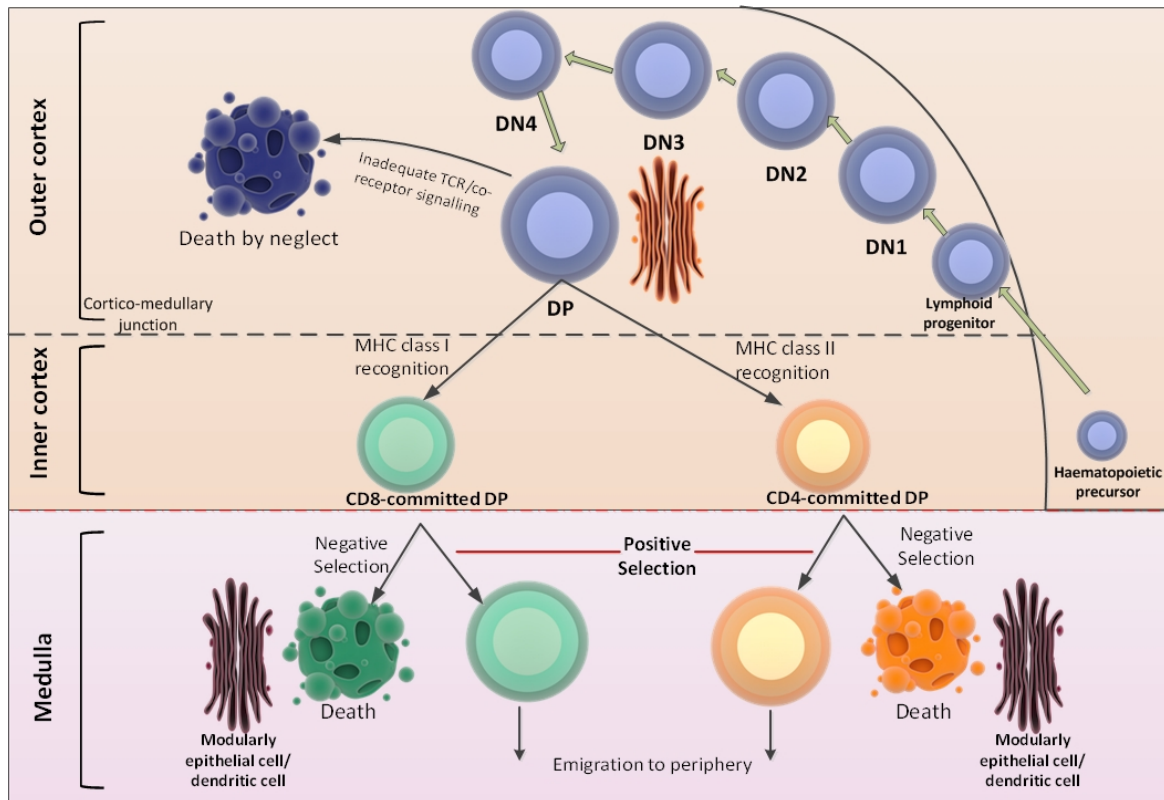


Fig. 3.1 Overall scheme of T-cell development in the thymus.

CD8-positive ($CD8^+$) cells eliminate cells infected with viruses and tumor cells, and are involved in allograft rejection [105]. In contrast, CD4-positive ($CD4^+$) cells help other cells to stimulate immune responses, including antibody responses. Moreover, they help eliminate pathogens that exist inside host cells. For a T-cell to become positively selected and to be allowed to mature, its TCR must have the ability to interact with foreign peptides bound to polymorphic self-MHC molecules, whereas T-cells that express self-reactive antigen receptors are negatively selected and receive a death signal. In other words, those cells which have the required knowledge will be selected and survive. In our proposed algorithm for WSNs, only the nodes with sufficient resources (energy and distance) are selected to become a CH. The selection is based on the residual energy of the node, its location in the sensing area, and the number of adjacent neighbors of the node.

3.3 The proposed HRHP Settings

The proposed algorithm makes use of several different approaches to improve the performance of the network and prolong its lifetime:

- *Network model*: the algorithm uses a network model in which sensor nodes are randomly deployed over the sensing area, which is divided based on a distance threshold into two regions: R1, which is nearer to the base station (BS), and R2, which is the remaining area. The justification for selecting this network model is based on [106], where it was shown that the energy of the nodes can be utilized efficiently when multiple topologies are used while keeping the transmission distance to a minimum.
- *Cluster formation*: nodes are formed into groups (clusters) and positive selection is used to select CHs based on the residual energy, the location of the CH represented by the net distance from nodes and from the BS (Net_d to BS), and the number of adjacent neighbors.

The algorithm also applies two techniques for the CHs selection, centralized control by the BS for R1 and deterministic control by the nodes for R2. When the network field is small, centralized control by the BS may be a better option, rather in large areas a deterministic approach is more efficient. In the first round of the HRHP, the BS determines the number of CHs that are selected, based on their suitability. When the network field is of medium to large size, deterministic control by the nodes is applied. A positive-selection cluster-based approach is used, it improves the network lifetime with less energy consumption.

3.3.1 Network Model

The proposed network model considers three stationary types of nodes in terms of their initial energy and their processing capabilities, namely normal nodes with the lowest energy, m_1 advanced nodes equipped with β times more energy, and m_2 super nodes equipped with α times more energy, to keep the total energy of our network equivalent to other algorithms for reasons of comparison. These nodes are randomly deployed in the network area, can access the BS at any time, and always have data to send as illustrated in Fig. 3.2. Once deployed in the network they keep operating until they consume all their power and die.

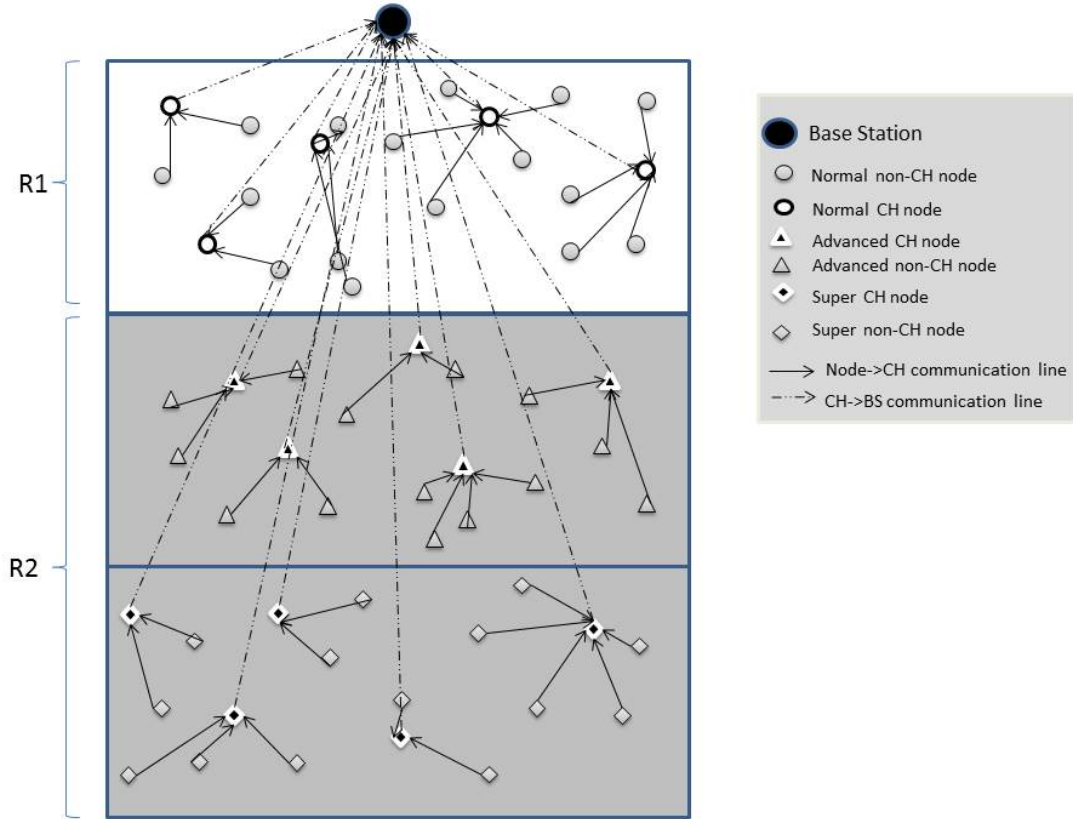


Fig. 3.2 HRHP Network Model.

HRHP divides the network area into two logical areas based on a distant threshold, in which R1 is region one that is closer to the BS and R2 is the second region. Once nodes have been deployed, they continue to operate until they have consumed all their energy, and they then die. The BS is located in the middle of the network and is not energy constrained.

The total number of nodes can be represented as:

$$Total(n) = (1 - (m1 + m2)) \times N + m1 \times N + m2 \times N \quad (3.1)$$

Illustration 3.1: If $N = 100$, $m1 = 0.3$ and $m2 = 0.2$, then the network will contain $((1 - (m1 + m2)) \times N = 50 \text{ nodes})$ which represents number of the normal nodes, $(m1 \times N = 30 \text{ nodes})$ which represents the number of advanced nodes, and $(m2 \times N = 20 \text{ nodes})$ which represents the number of super nodes in the network.

3.3.2 Energy Model

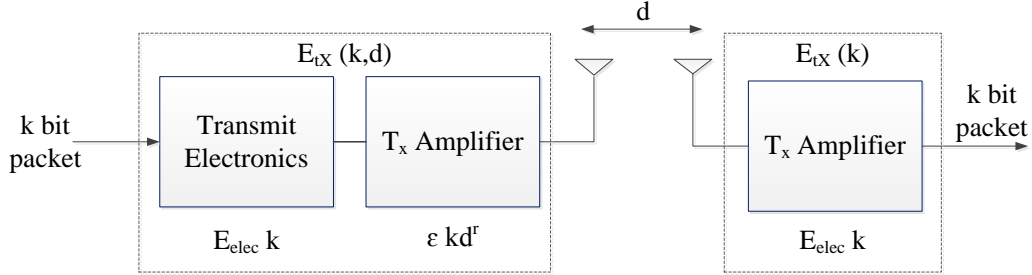


Fig. 3.3 Energy Dissipation model.

In order to achieve an acceptable signal-to-noise ratio, the proposed algorithm considers a common energy model introduced in LEACH [26] by Heinzelman, as illustrated in Fig. 3.3.

The total energy (E_T) of the network is

$$E_T = E_0((1 - (m1 + m2)) \times N + ((1 + \beta)m1 \times N) + ((1 + \alpha)m2 \times N)) \quad (3.2)$$

where E_0 is the initial energy of a node, $m1$ is the percentage of advanced nodes, $m2$ is the percentage of super nodes. N is the total number of nodes. α is the percentage of extra energy level for super nodes and β is the percentage of extra energy levels for super nodes. The free-space (f_s) attenuation channel mode is used to calculate the energy consumption during the process of routing data transmission when the distance between the transceivers is less than a distance threshold d_0 , and the multipath ϵ_{amp} fading channel mode is used when the distance between the transceivers is greater than or equal to d_0 .

The total network energy dissipation, in a clustered network, is expressed as the sum of the energy consumed by the SNs to sense the event and transmit it to their associated CHs or to the BS. If the sending node was the CH then the consumed energy will be the sum of energy: spent by the CH to sense the environment, to receive data from CMs, to perform data aggregation, and to send all the data to the BS. Therefore, the amount of energy dissipated in CH would be higher than the SNs. Energy consumption is also affected by the cluster members in each cluster and the distance from the BS [107]. If the BS located at the centre of a square area, the optimal energy cost function dissipated by a CH can be expressed mathematically as:

$$E_{CH} = kE_{elec}l + kE_{DA}(l + 1) + E_{Tx}(k, d_{toBS}) \quad (3.3)$$

Where, k is the packet size. E_{elec} is the energy dissipated by both the transmitter and receiver circuits, n is the total number of nodes in the network, E_{CH} is the energy consumed by the CH to receive l number of k bits from CMs, and E_{DA} is the energy consumed by the CH to aggregate the data and then transmit with $E_{Tx}(k, d_{toBS})$ energy to the BS. The free space path-loss model is used here since the BS is at the centre of the sensing area. Hence, if the SN is a CM, the energy consumed is given as:

$$E_{non-CH} = kE_{elec} + k\epsilon_{fs}d_{toCH}^2 \quad (3.4)$$

The total energy consumed in a single-level communication network will be the sum of energy depleted by CMs and the CH and can be expressed as:

$$E_{cluster} \approx E_{CH} + \frac{N}{c}E_{non-CH} \quad (3.5)$$

Where, E_{CH} is the CH's energy. E_{non-CH} is the CMs' energy. N is the total number of nodes and c is the total number of clusters. However, to ensure an optimal setup for this type of communication mode, an optimal number of CHs per round needs to be considered along with the battery dimensioning that must guarantee a certain network lifetime.

The energy consumption of the sensor node during the process of sending (k) bit of data over a distance (d) is

$$E_{TX}(k, d) = k \cdot E_{elec} + \epsilon_{amp} \cdot k \cdot d^r \quad (3.6)$$

The energy consumption of the sensor node during the process of receiving 1 kbit of data over a distance d is

$$E_{RX}(k, d) = E_{elec} \cdot k \quad (3.7)$$

In Eq.(3.6) and Eq.(3.7), E_{elec} is the energy consumption of the circuit during the process of sending and receiving data, and ϵ_{amp} is a magnification time of the signal amplifier. The energy consumption of the radio signal transmission is proportional to a power of the distance, d^r . If the transmission distance is short, i.e., $d < d_0$, then $r = 2$; otherwise, if the transmission distance is long, i.e., $d > d_0$, then $r = 4$.

According to the energy dissipation model in Fig. 3.3 and Equations (3.6) and (3.7), the energy consumed for data communication depends highly on the distance of transmission between the sender and the receiver using the free space and multi-path fading channel models. Therefore, reducing the energy consumption can be achieved by keeping the transmission distance low. HRHP can maintain low transmission distance between the CH and the BS using multi-hop.

3.3.3 Cluster Formation

When the clusters are fixed and the CHs are rotated in every round, a member node may consume more power than necessary to communicate with its CH when there is another CH close by (See Fig. 3.4 for an example). When node *A* communicates with its CH (node *B*), it consumes more transmission power than it would if node *C* was the CH. Moreover, if the current operating CH has sufficient energy, greater than or equal to a required threshold, it is not efficient to change that CH, as this then effects the entire cluster and causes more energy loss as a result of the process of rearranging the cluster. Therefore, a hybrid cluster formation method, taking proper account of the location of the nodes and their residual energy is presented in the following sections. Centralized control is implemented for nodes in R1 based on the suitability of those nodes, and distributed control is implemented for nodes in R2, depending on the positivity of those nodes. Hence, self-adaptive control is guaranteed without outside intervention.

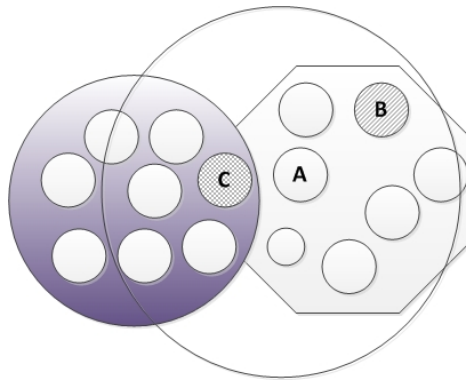


Fig. 3.4 Example of cluster formation challenge.

At the start of cluster formation (in the first round only), the BS broadcasts a *Gather* packet containing its identity (BS_ID). All nodes respond with a *REPLY* packet containing their identification (S_ID), their residual energy (E_r), and their

location coordinates ($X_{\text{node}}, Y_{\text{node}}$). The format of the *Gather* and *REPLY* packets is shown in Fig. 3.5.



Fig. 3.5 Format of *Gather* and *REPLY* packets: (a) *Gather*, (b) *REPLY*.

The BS then (1) categorizes the nodes into Level 1 (nodes in R1) and Level 2 (nodes in R2), (2) performs calculations based on the level of each node to select the CHs, and (3) broadcasts an *Identify* packet to the nodes containing the CH IDs and the altitude of the node (*Altitu*) based on its location. The *Identify* packet is shown in Fig. 3.6.



Fig. 3.6 Format of *Identify* packet.

A detailed description of the initialization stage (the CH selection process) is provided next.

3.3.3.1 CH Selection in R1

When the BS has received the required information from the nodes in R1, it selects a suitable fixed number $K1$ of CHs. The selection of CHs is based on the initial energy E_0 , residual energy E_r , energy consumption ratio ECR , and net distance to the BS $Net_{d \text{ to BS}}$ of the node. $Net_{d \text{ to BS}}$ is calculated first as in Algorithm 1, ECR [108] is calculated as in Eq. 3.8, and the suitability as in Eq. 3.9:

$$ECR(m) = \frac{E_0}{(E_0 - E_r)}, \quad (3.8)$$

$$Suitability(m) = \frac{E_r}{(ECR \times Net_{d \text{ to BS}})}. \quad (3.9)$$

Nodes with the highest suitability are selected as CHs and the BS broadcasts an *Identify* message to the nodes in R1 containing the CH IDs and the altitudes of the nodes. Each node stores altitude values in the neighbor table and chooses the nearest CH as its CH. A setup round will only take place again if a CH broadcasts its

unsuitability to remain as a CH and designates the best existing node in the cluster to become the next CH. The next CHs are selected from within the cluster and thus there is no setup overhead at the beginning of a round.

Algorithm 1 Calculation of $Net_{d \text{ to BS}}$

```

for  $i = 1 : N$  do
  for  $j = 1 : N$  do
    * Distance from node $i$  to other R1 nodes
     $d(i, j) = \sqrt{(X_{\text{node } i} - X_{\text{node } j})^2 + (Y_{\text{node } i} - Y_{\text{node } j})^2}$ ;
     $Dis(i) = Dis(i) + d(i, j)$ ;
  end for
  * Distance from BS to node
   $DBS(i) = \sqrt{(X_{\text{node}} - X_{\text{BS}})^2 + (Y_{\text{node}} - Y_{\text{BS}})^2}$ ;
  * Net distance from BS to node
   $Net_{d \text{ to BS}}(i) = DBS(i) + Dis(i)$ ;
end for

```

While the selection process is running in R1, a distributed CH selection based on T-cell positive selection takes place simultaneously in R2.

3.3.3.2 CH Selection in R2

Once they have been deployed, the nodes in R2 are designated as double negative (D_N). When the BS receives a *REPLY* message from the nodes, it divides R2 into subregions (clusters) using Eq.3.10 below, calculates the Euclidean distances d between the nodes and the BS as in Eq.3.11, and then sends an *Identify* message to the superior (advanced and super) nodes only, changing their status to double positive (DP):

$$ClustersNo. = \frac{Max_{R2 \text{ distance}}}{Transm/2}, \quad (3.10)$$

where $Max_{R2 \text{ distance}}$ is the maximum distance between nodes in R2 and the BS, $Transm$ is the transmission range between a nodes and the BS for a distance d , and

$$d = \sqrt{(X_{\text{BS}} - X_{\text{node}})^2 + (Y_{\text{BS}} - Y_{\text{node}})^2}, \quad (3.11)$$

where $(X_{\text{BS}}, Y_{\text{BS}})$ and $(X_{\text{node}}, Y_{\text{node}})$ are the coordinates of the BS and the sensor node, respectively.

When a CH node receives an *Identify* message, it broadcasts a “*Hello*” message containing the ID and location of the CH, and waits for a join request from a cluster

member (CM) to finalize the cluster. The CM node decides the next hop according to the following equation, where node i has a probability $P(i, j)$ of selecting node j for its next hop:

$$P(i, j) = \begin{cases} \frac{H(i, j)}{\sum_{l \in NT(i) \& H(i, l) > 0} H(i, l)} & \text{if } j \in NT(i) \& H(i, j) > 0, \\ 0 & \text{otherwise,} \end{cases} \quad (3.12)$$

where,

$$H(i, j) = \frac{\text{hopCount}(i, CH) - \text{hopCount}(j, CH)}{d(i, j)} \cdot E_r(j) \quad (3.13)$$

and

$$H(i, l) = \frac{\text{hopCount}(i, BS)}{d(i, BS)} \cdot E_r(i) \quad (3.14)$$

Where $d(i, j)$ is the Euclidean distance between node i and node j , $NT(i)$ is the neighbor table of node i , and E_r is the residual energy of node j .

When a CH node reaches a threshold energy Th , it broadcasts a “*Compete*” message to its associated CMs asking for their energy levels. The CH then hands over to the node with the next highest energy level, broadcasts the new ID and location of the CH to the CMs, and changes its status to D_N . A flowchart of the process of cluster setup in R1 and R2 is presented in Fig. 3.7.

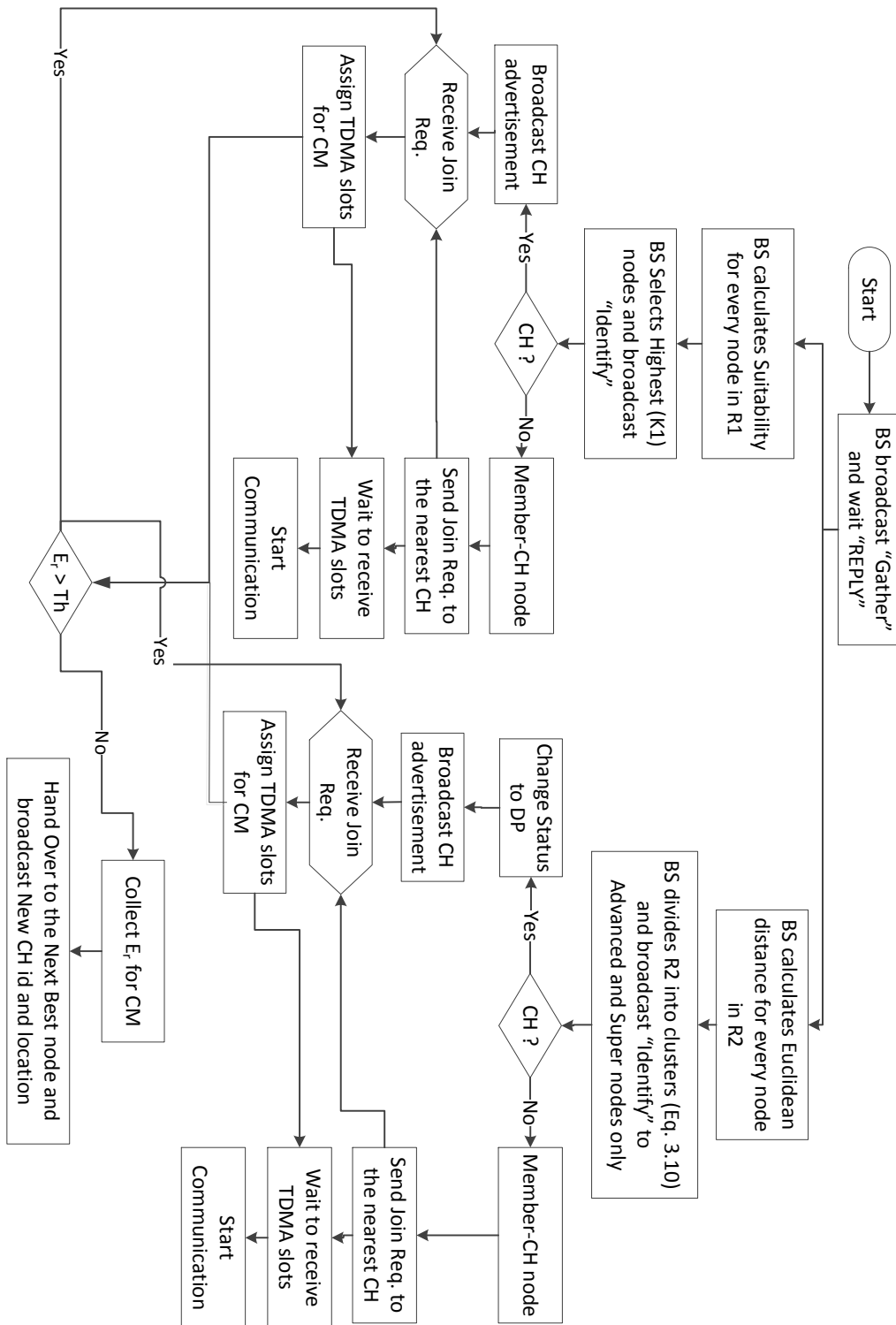


Fig. 3.7 Process of cluster formation in the proposed algorithm.

3.4 Performance Evaluation

In this section, the obtained results and a discussion is provided for the validation of the proposed algorithm (HRHP). To evaluate the performance of the proposed algorithm, a comparison has been done with the existing algorithms, namely LEACH, MGEAR, and SEP, in six different predefined scenarios in which there are two different cases with respect to node deployment which is $N=100$ and $N=200$ nodes. Location of the BS has two varieties in the scenarios: either in the upper middle far of the sensing area or at the right corner. Nodes are randomly distributed over selected areas of (200×200) , (300×300) , and $(500 \times 500) m^2$.

All the reported results are obtained from an average of ten simulation runs and the comparison against other algorithms was in terms of: Stability period, Operational time, Network life time and Energy consumption.

- In **scenario 1**, the BS located in the upper middle far of $(200 \times 200) m^2$ area with two cases of node distribution $N = 100$ nodes and $N = 200$ nodes.
- In **scenario 2**, the BS located in the upper middle far of $(300 \times 300) m^2$ area with two cases of node distribution $N = 100$ nodes and $N = 200$ nodes.
- In **scenario 3**, the BS located in the upper middle far of $(500 \times 500) m^2$ area with two cases of node distribution $N = 100$ nodes and $N = 200$ nodes.
- In **scenario 4**, the BS located in right corner of $(200 \times 200) m^2$ area with two cases of node distribution $N = 100$ nodes and $N = 200$ nodes.
- In **scenario 5**, the BS located in right corner of $(300 \times 300) m^2$ area with two cases of node distribution $N = 100$ nodes and $N = 200$ nodes.
- In **scenario 6**, the BS located in right corner of $(500 \times 500) m^2$ area with two cases of node distribution $N = 100$ nodes and $N = 200$ nodes.

The main reason behind choosing these scenarios is to exploit the effects of BS location, network size and node density among the compared algorithms. The algorithms were tested through simulation using MatLab R2012b, simulation is used as a mean to evaluate the performance of the proposed approaches and test their correctness. Compared to actual system development and other testing methods, simulation is preferred for different reasons: First, simulation is cost-effective since it can be conducted before

any implementation is available. Second, it is time-efficient since it simulates years in minutes of computer time and can operate faster than actual systems. Third, it is helpful to obtain results for complex systems. Forth, simulation is safe. It avoids all kinds of danger. If a system performs very quickly in real life, simulation can be slowed down to study behavior more easily. Therefore, it offers a full control to the developer to carefully examine features of their interest. More importantly, simulation allows comparison of many alternative designs and rules of operation.

The metrics considered commonly to estimate the stability period, operational time, network lifetime, and energy consumption. The definitions of the measures that were used in this work are described bellow as follows:

- ***Stability period***: the time interval from the start of operation of the network until First Node Dead (FND). This metric is important for the cases were the death of a single node is crucial and would effect the complete network function. However, in several applications and cases the death of a single node is not very important and the network can operate successfully after the first node dies.
- ***Operational time***: is defined as the number of rounds for which 50% of the total nodes are active, Half Node Dead (HND). Which is useful when considering the coverage aspect of the network boundaries by WSN.
- ***Network lifetime***: the time interval from the start of network operation until Last Node Dead (LND).
- ***Network residual energy***: is the total remaining energy of nodes at certain time intervals of the total life time.

In the described scenarios, elected CHs and clusters are formed at the beginning of the network setup and only hand over to other CH when the current CH's residual energy reaches a threshold, this will prevent extra energy wasted in selecting CH at each round as most of current algorithms do. Then each CM node sends 4000 bits of data to its CH.

Each elected CH aggregates the received packets with a defined ratio before transmitting to the BS. The aggregation ratio is set to 10% as employed in the protocols discussed in the literature. The rest of initial parameters are shown in Table 3.1.

Table 3.1 Simulation Parameters

Parameter	Value
Initial energy	$E_0 = 0.5$ J
Probability to be CH (P)	0.1
Data aggregation energy cost	$EDA = 50$ nJ/bit
Packet size	4000 bits
Transmitter/receiver electronics, E_{elec}	50 nJ/bit
Transmit amplifier, ϵ_{fs}	10 pJ/bit/m ²
Transmit amplifier, ϵ_{amp}	0.0013 pJ/bit/m ⁴

3.4.1 Scenario 1

In this scenario, the BS is located at the upper middle far of the network boundaries in the location (100 , 210). The nodes are randomly deployed over the area of (200×200 m²) with two node density cases (100 and 200 nodes distribution). HRHP is compared to LEACH, MGEAR, and SEP protocols in terms of protocol stability (FND), operational time (HND), network life time (LND) and the network residual energy.

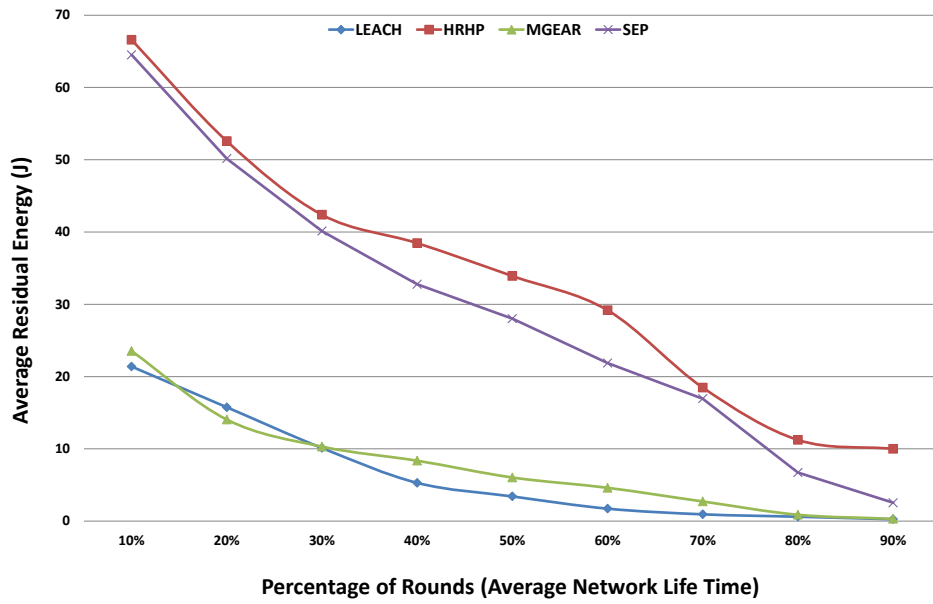
Table 3.2 shows the results obtained for FND, HND and LND from comparing HRHP to other protocols. HRHP has the highest round rate for nodes starting death (FND: at round 490 for 100 nodes) leading to longest stability period, (HND: at round 1281 for 100 nodes) meaning longer operational time and (LND: at round 5800 for 100 nodes) producing the longest life time among the protocols. HRHP stability period in terms of FND is extended compared with that of LEACH by an average of 48%, MGEAR by an average of 53% and SEP by an average of 26% with the different number of deployment. Improvement in operational time value in terms of HND is extended compared with that of LEACH by an average of 39%, MGEAR by an average of 14% and SEP by an average of 2% with the different number of deployment, i.e more balanced energy dissipation for the different number of nodes deployment.

Table 3.2 Network life time results obtained from scenario 1

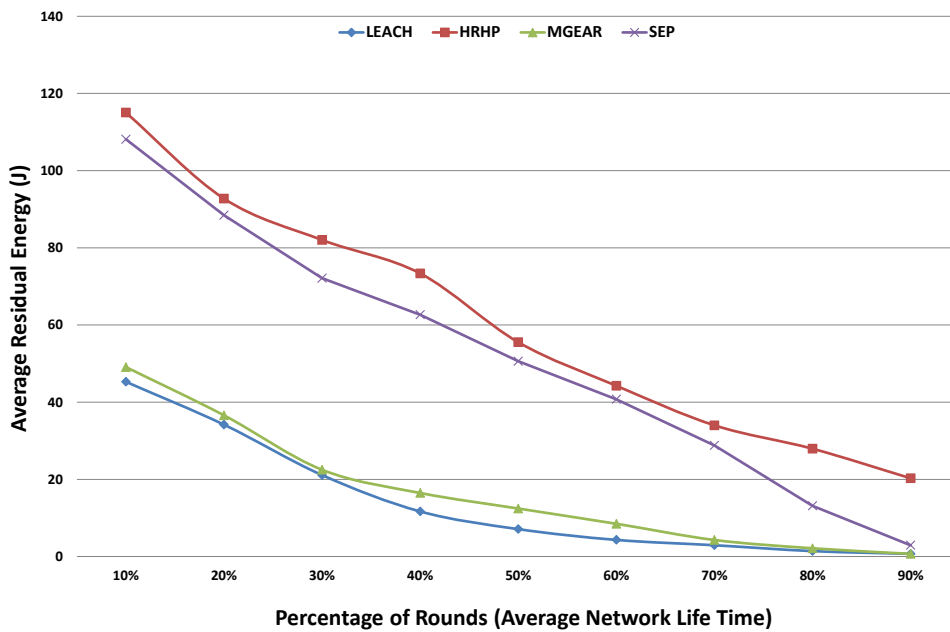
Algorithm	Results obtained for 100 nodes			Results obtained for 200 nodes		
	FND	HND	LND	FND	HND	LND
LEACH	322	830	1142	311	908	1364
HRHP	490	1281	5660	820	1575	5800
MGEAR	329	1154	2423	228	1303	2438
SEP	361	1241	4327	608	1558	5080

When increasing the number of nodes to 200, HRHP performance is increased by a percentage change of 67.35% for FND, which led to longer stability period compared to 100 nodes deployment case. HRHP also extended its operational time by 22.95% and for the network life time, it is increased by 2.47%. Moreover, in comparison with other protocols, HRHP has the longest network life in terms of LND when compared with the other protocols, HRHP network life time is extended compared with that of LEACH by an average of 78%, MGEAR by an average of 58% and SEP by an average of 50% with the different number of deployment. These results indicates that HRHP has better control with node distribution over ($200 \times 200 m^2$) area compared with other protocols.

The network residual energy is an important parameter to measure the performance of the protocols. Fig. 3.8 illustrates the total remaining energy depletion at certain average time percentage of the total network time. In both deployment cases, HRHP maintain the highest residual energy levels for the different times of network life. HRHP outperform other protocols over area ($200 \times 200 m^2$) in energy efficiency due to its suitable choice of cluster size and CHs as observed in Fig 3.8 for node deployment of 100 nodes (Fig. 3.8a) and with 200 nodes (Fig. 3.8b), in this figure the network residual energy is measured accordantly to the percentage of average network life time (represented by rounds).



(a) Average residual network energy levels for $N = 100$.



(b) Average residual network energy levels for $N = 200$.

Fig. 3.8 Average residual network energy levels for scenario 1, $Area = 200 \times 200$

3.4.2 Scenario 2

In this scenario, the sensing area is increased to $(300 \times 300 m^2)$ with two node density cases (100 and 200 nodes distribution). The BS is located in the middle far of the network at (150, 310). Through increasing the sensing area to $(300 \times 300 m^2)$ for 100 nodes, LEACH stability period decreases by a percentage change of 72.67%, MGER decreases by 78.42% and SEP by 39.89%, while HRHP stability period decreases by 42.45% compared to the first scenario. Although SEP scores less degradation in its stability change, its operational time shows a decrease of 46.66% which is higher than HRHP (45.28%). Furthermore, its network life time was only increased by a percentage change of 3.02%. While HRHP network life was increased by a of 12.45%. It is apparent from this that over the time, nodes using HRHP protocol lose its energy slower than other protocols and therefore having the maximum operational and network life time.

Table 3.3 shows the results obtained from comparing HRHP to other protocols. HRHP remains to have the highest indicators compared to other protocols when increasing the area of interest to $300 \times 300 m^2$ for both cases of nodes deployment. HRHP indicators for 100 nodes as follows: (FND: at round 282) leading to longest stability period, (HND: at round 701) meaning longer operational time and (LND: at round 5286) producing the longest life time among the protocols. HRHP performance improved for the same area when the number of nodes increased to 200 nodes, were (FND extended to round 479), (HND extended to round 1059) longer operational time, and (LND extended to round 5944) which is the longest network life time compared to other protocols.

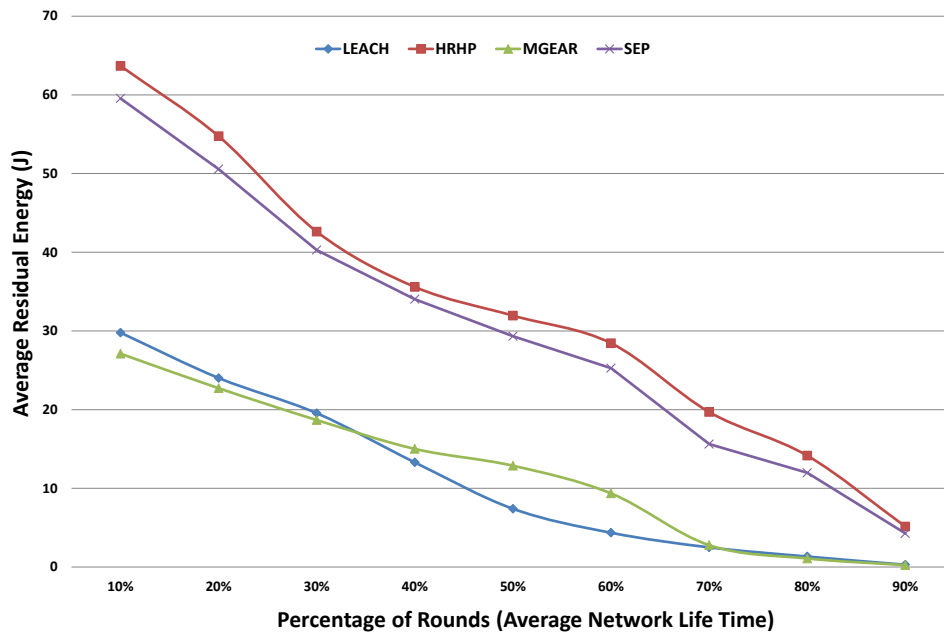
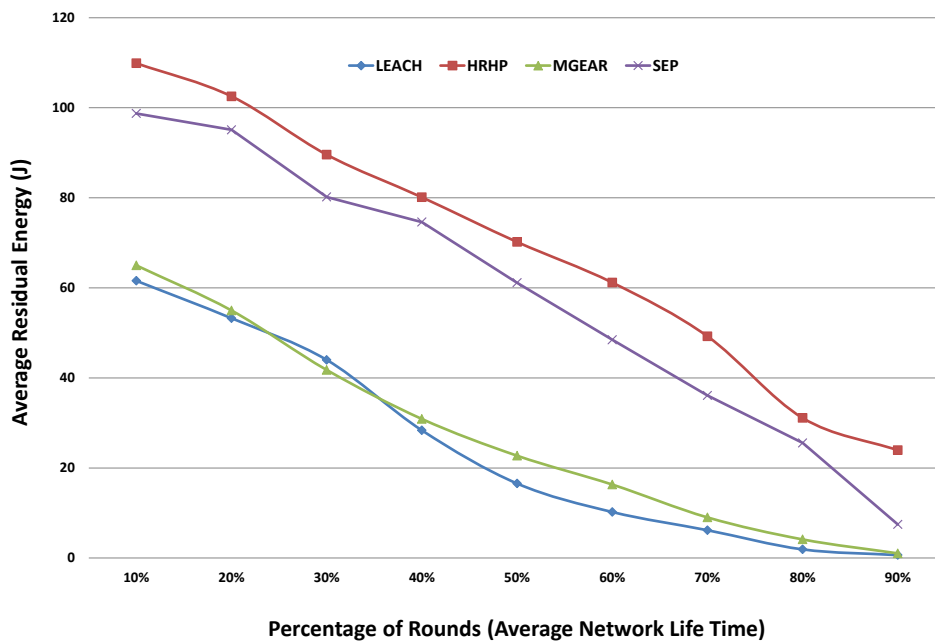
Table 3.3 Network life time results obtained from scenario 2 with BS location (150,310)

Algorithm	Results obtained for 100 nodes			Results obtained for 200 nodes		
	FND	HND	LND	FND	HND	LND
LEACH	88	487	1012	73	512	1300
HRHP	282	701	5286	479	1059	5944
MGEAR	71	588	2488	68	629	3514
SEP	217	662	4741	179	954	4884

Comparing HRHP to other protocols, the stability period time in terms of FND is rapidly extended from LEACH by an average of 77%, MGEAR by an average of 80% and SEP by an average of 43% with the different number of deployment, which higher performance than the area $300 \times 300 m^2$. HRHP also show an improvement in the operational time value in terms of HND compared with that of LEACH by an

average of 41%, MGEAR by an average of 28% and SEP by an average of 8% with the different number of deployment, i.e more balanced energy dissipation for the different number of nodes deployment. Moreover, HRHP has the longest network life in terms of LND when compared with the other protocols. HRHP network life time is extended compared with that of LEACH by an average of 79%, MGEAR by an average of 47% and SEP by an average of 44% with the different number of deployment.

Fig 3.9 illustrates the results obtained for measuring the energy efficiency for the area of deployment with size ($300 \times 300 m^2$). Fig. 3.9a shows the results for 100 nodes deployment and Fig. 3.9b shows the results for 200 nodes. HRHP outperform other protocols in terms of residual energy levels as can be seen from the figures.

(a) Average residual network energy levels for $N = 100$.(b) Average residual network energy levels for $N = 200$.Fig. 3.9 Average residual network energy levels for scenario 2, $Area = 300 \times 300$

3.4.3 Scenario 3

In this scenario, the network is extended to ($500 \times 500 m^2$) with two node density cases (100 and 200 nodes distribution) and the BS is located at the upper middle far of the network boundaries (250, 510). The simulation results for the two cases are given in Table 3.4.

Increasing the area to $500 \times 500 m^2$ increases the communication distances between the nodes and the BS due to the wide scattering of nodes. Therefore, the performance of the protocols decreases for different nodes deployment compared to the previous two scenarios. However, HRHP remains controlling the network having the highest network life time among the protocols as illustrated in Table 3.4.

Table 3.4 Network life time results obtained from scenario 3 with BS location (250,510)

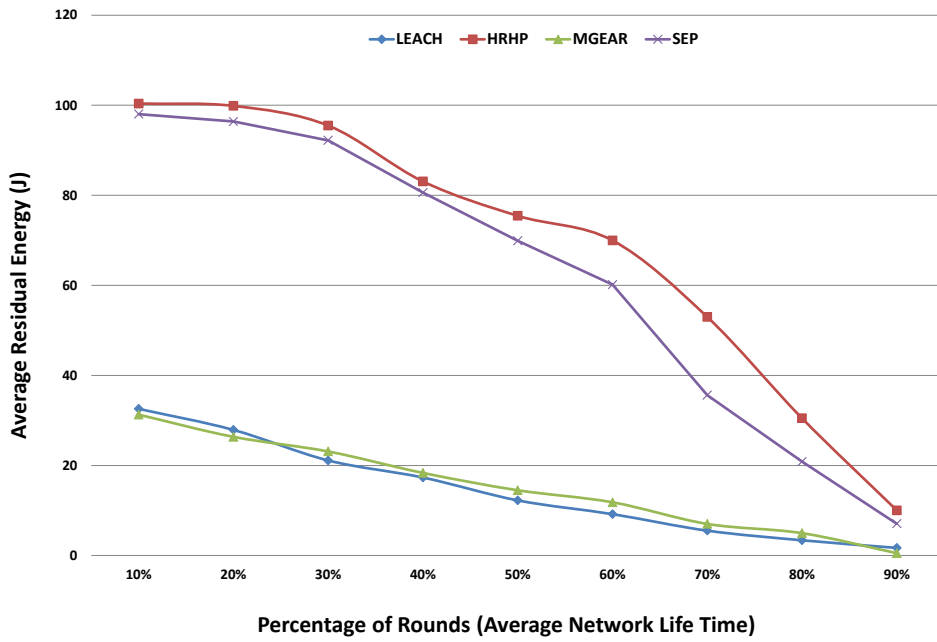
Algorithm	Results obtained for 100 nodes			Results obtained for 200 nodes		
	FND	HND	LND	FND	HND	LND
LEACH	12	82	416	12	71	810
HRHP	30	152	5218	50	355	5450
MGEAR	14	102	1912	8	79	4367
SEP	19	140	4867	29	158	5057

HRHP indicators for 100 nodes as follows: (FND: at round 30) which the highest compared to the other protocols, (HND: at round 152) longer operational time than the other protocols and (LND: at round 5218) the longest life time among the protocols and to be compared with the previous two cases it is almost the same performance. HRHP performance improved for the same area when the number of nodes increased to 200 nodes, were (FND extended to round 50), (HND extended to round 355) longer operational time, and (LND extended to round 5450) which is the longest network life time compared to other protocols. When the nodes number increases to 200, HRHP showed and increase improvement in the network stability by 66.67% which the highest compared to other protocols were: LEACH did not show any improvement, MGEAR had a decreased change in the network stability of 42.86% and SEP showed an increase of 52.63%.

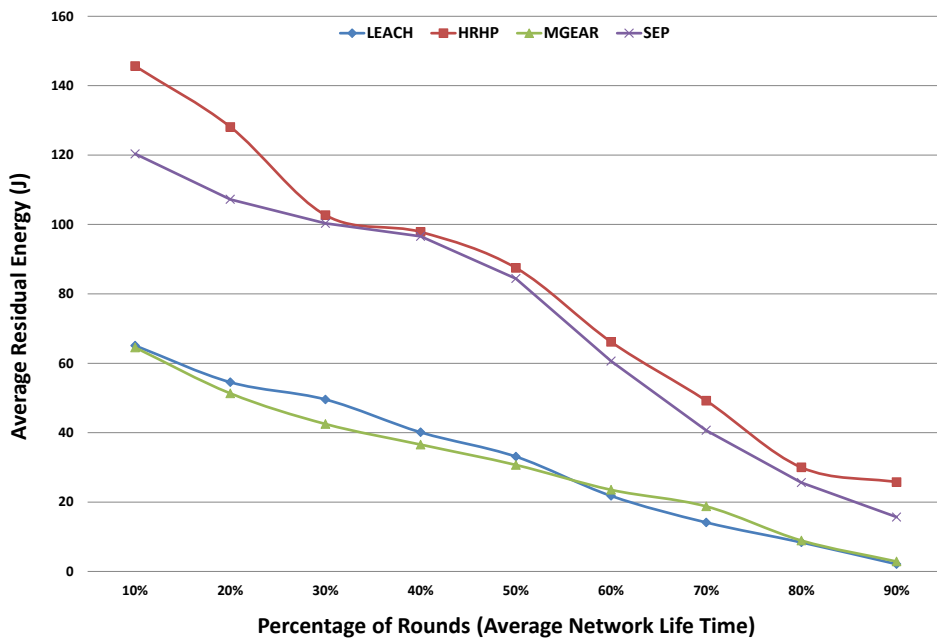
The stability period time in terms of FND for HRHP is extended compared with that of LEACH by an average of 68%, MGEAR by an average of 69% and SEP by an average of 39% with the different number of deployment, which higher performance than the area $300 \times 300 m^2$. Furthermore, an improvement in operational time value in terms of HND is extended compared with that of LEACH by an average of 63%,

MGEAR by an average of 55% and SEP by an average of 32% with the different number of deployment, i.e more balanced energy dissipation for the different number of nodes deployment. Finally, HRHP has the longest network life in terms of LND when compared with the other protocols, HRHP network life time is extended compared with that of LEACH by an average of 89%, MGEAR by an average of 42% and SEP by an average of 46% with the different number of deployment.

In order to compare the remaining energy levels for the different time slots, Fig 3.10 illustrates the results obtained for measuring the energy efficiency for the area of deployment with size 500×500 . Fig. 3.10a showing the results for 100 nodes deployment and Fig. 3.10b shows the results for 200 nodes. HRHP also outperform other protocols in terms of residual energy levels as can be seen from the figures.



(a) Average residual network energy levels for $N = 100$.



(b) Average residual network energy levels for $N = 200$.

Fig. 3.10 Average residual network energy levels scenario 3, $Area = 500 \times 500$

3.4.4 Scenario 4

In this scenario, the BS is located in the corner of the network boundaries and the nodes are randomly deployed over area of $(200 \times 200 m^2)$ with two node density cases (100 and 200 nodes distribution). The main idea behind choosing this scenario is to exploit the effects of BS location, network size and node density among algorithms. HRHP performance is compared to LEACH, MGEAR, and SEP protocols in terms of protocol stability (FND), the operational time (HND) and in terms of network life time (LND). The simulation results for the two cases are given in Table 3.5.

Table 3.5 Network life time results obtained from scenario 4 with BS location (210,210)

Algorithm	Results obtained for 100 nodes			Results obtained for 200 nodes		
	FND	HND	LND	FND	HND	LND
LEACH	196	510	1146	141	572	1531
HRHP	378	1201	5869	417	1325	6952
MGEAR	55	1132	2450	57	1293	2442
SEP	403	1172	5072	328	1322	5521

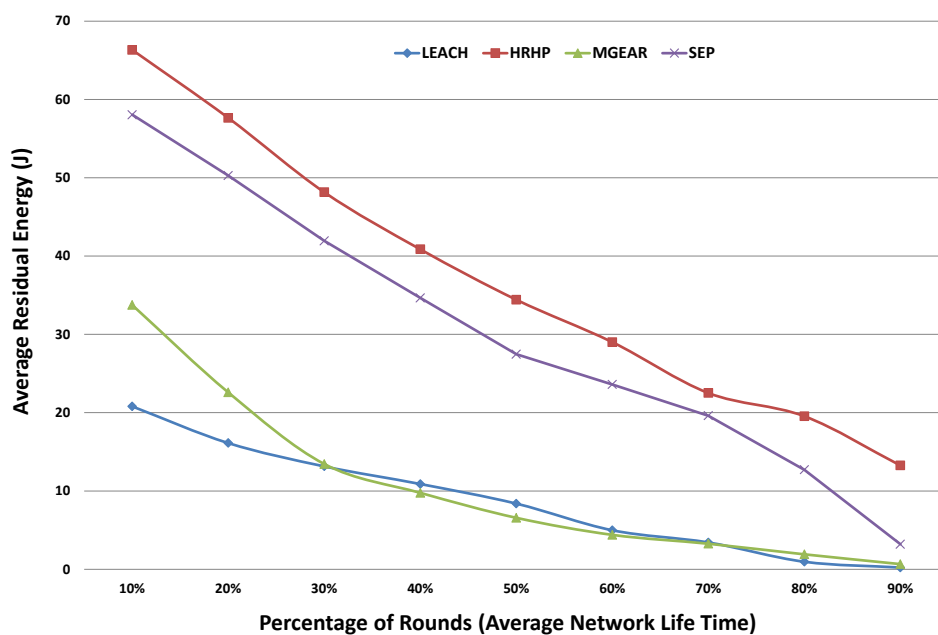
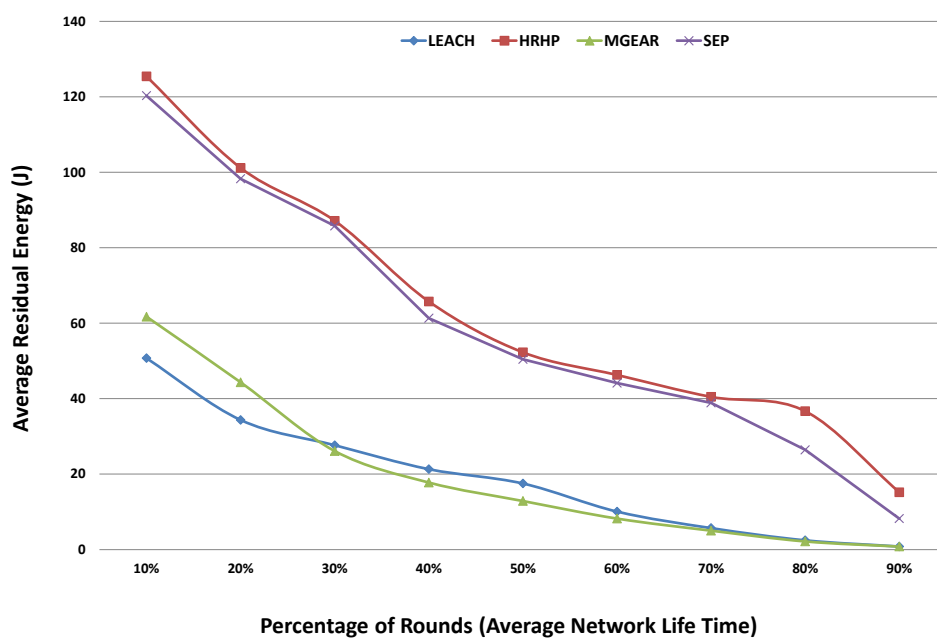
Changing the BS location to the corner of the field affected the performance of HRHP in terms of stability period (FND) and operational time (HND), however, it did not affect the network life time (LND) for the case of 100 nodes. The stability period of HRHP stability period decreases by 22.86%, the operational time decreases by 6.25% and the overall network life time have an increase of 3.69% compared to scenario 1 for the same case. While for 200 nodes case, the stability period was changes by a percentage decrease of 49.15%, the operational time percentage change decreases by 15.87% while the overall network life time percentage change increases by 19.86%.

However, HRHP maintain better performance compared to the other protocols as can be seen from Table 3.5. HRHP nodes starting death (FND: at round 378 for 100 nodes) leading to longest stability period, (HND: at round 1201 for 100 nodes) meaning longer operational time and (LND: at round 5869 for 100 nodes) producing the longest life time among the protocols. HRHP performance improved for the same area when the number of nodes increased to 200 nodes, were (FND extended to round 417) which is around double the stability period, (HND extended to round 1325) longer operational time, and (LND extended to round 6952) indicating that HRHP has better control with node distribution over $(200 \times 200 m^2)$ area.

From Table 3.5, when the number of nodes increases to 200, HRHP performance improved compared to 100 nodes deployment case for the stability period, operational time and the network life time. The stability period and the operational time increase by a percentage change of 10.32% and the network life time increases by a percentage change of 18.45%. From these results, HRHP improves its performance when the number of nodes in the field increases.

HRHP stability period time in terms of FND is extended compared to LEACH by an average of 57%, MGEAR by an average of 86% and SEP by an average of 7% with the different number of deployment. The operational time for HRHP in terms of HND is extended compared with that of LEACH by an average of 57%, MGEAR by an average of 4% and SEP by an average of 1% with the different number of deployment, i.e more balanced energy dissipation for the different number of nodes deployment. Moreover, HRHP has the longest network life in terms of LND when compared with the other protocols, HRHP network life time is extended compared with that of LEACH by an average of 79%, MGEAR by an average of 62% and SEP by an average of 46% with the different number of deployment.

Fig. 3.11 shows the total remaining energy depletion at certain average time percentage of the total network time. In both deployment cases, HRHP maintain the highest residual residual energy levels for the different times of network life. HRHP outperform other protocols over area($200 \times 200 m^2$) in energy efficiency due to its suitable choice of cluster size and CHs as observed in Fig 3.11 for node deployment of 100 nodes (Fig. 3.11a) and with 200 nodes (Fig. 3.11b), in this figure the network residual energy is measured accordantly to the percentage of average network life time (represented by rounds).

(a) Average residual network energy levels for $N = 100$.(b) Average residual network energy levels for $N = 200$.Fig. 3.11 Average residual network energy levels scenario 4, $Area = 200 \times 200$

3.4.5 Scenario 5

In this scenario, the BS is located in the corner of the network boundaries and nodes are randomly deployed over area of ($300 \times 300 m^2$) with two node density cases (100 and 200 nodes distribution). The simulation results for the two cases are given in Table 3.6.

Placing the BS in the corner for a $300 \times 300 m^2$ area further reduced the stability, operational time and network life time for HRHP in comparison with Scenario 2. The percentage change of the stability of the network has decreased by 57.8%, the operational time decreases by 46.08% and the life time has decreased by 8.49%. However, from the results in Table 3.6, HRHP performance is the best compared with other protocols.

Table 3.6 Network life time results obtained from scenario 5 with BS location (310,310)

Algorithm	Results obtained for 100 nodes			Results obtained for 200 nodes		
	FND	HND	LND	FND	HND	LND
LEACH	37	201	908	27	186	1108
HRHP	119	378	4837	180	588	6720
MGEAR	11	348	2110	12	502	2311
SEP	81	327	4758	72	422	6184

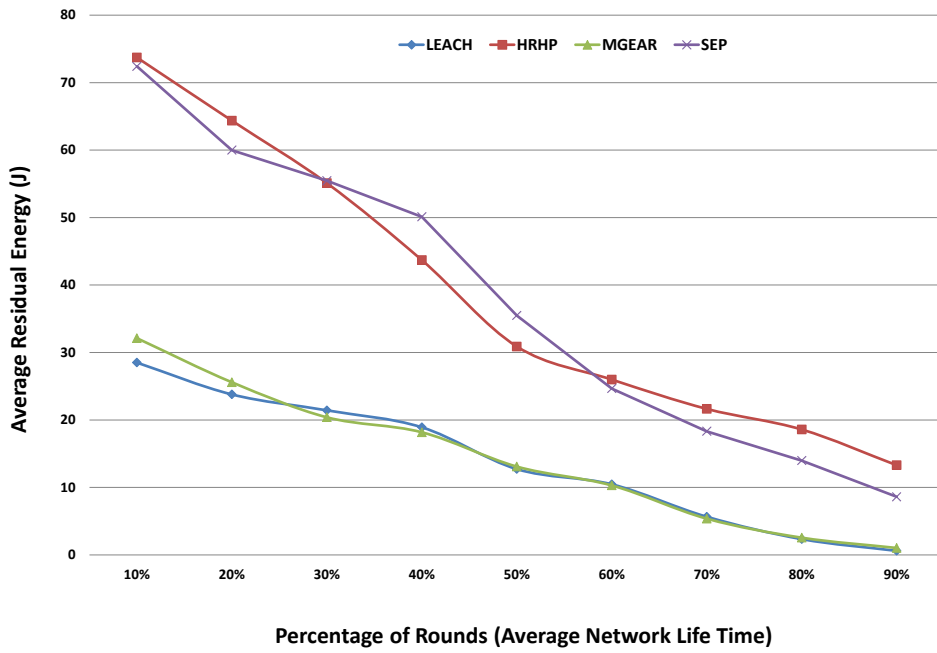
HRHP has the highest round rate for nodes starting death (FND: at round 119 for 100 nodes) leading to longest stability period, (HND: at round 378 for 100 nodes) meaning longer operational time and (LND: at round 4837 for 100 nodes) producing the longest life time among the protocols. HRHP performance improved for the same area when the number of nodes increased to 200 nodes, were (FND extended to round 180) which is around double the stability period, (HND extended to round 588) longer operational time, and (LND extended to round 6720) indicating that HRHP has better control with node distribution over ($300 \times 300 m^2$) area.

The stability period in terms of FND is extended in HRHP compared with LEACH by an average of 77%, MGEAR by an average of 92% and SEP by an average of 46% with the different number of deployment. The operational time in terms of HND is extended compared with LEACH by an average of 58%, MGEAR by an average of 11% and SEP by an average of 21% with the different number of deployment, i.e more balanced energy dissipation for the different number of nodes deployment. Moreover, HRHP has the longest network life in terms of LND when compared with the other protocols, HRHP network life time is extended compared with that of LEACH by an

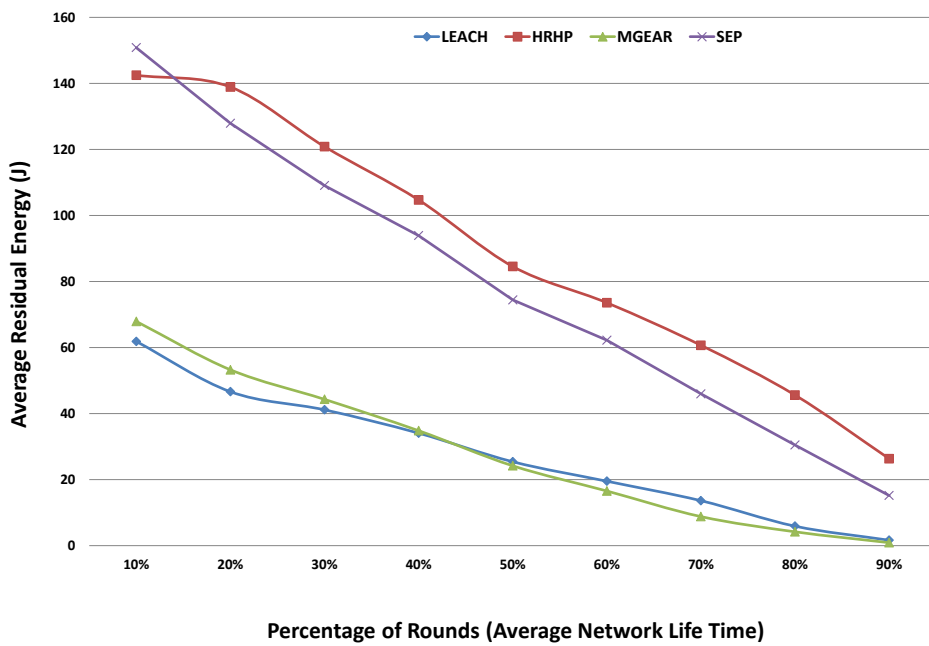
average of 82%, MGEAR by an average of 61% and SEP by an average of 43% with the different number of deployment.

Furthermore, HRHP performance improved for the same settings when the number of the nodes increased to 200. Hence, the stability period percentage change increased by 51.26%, the operational time percentage change has an increase of 55.56% and the overall network time percentage change has an increase of 38.93%.

Fig. 3.12 depicted the total remaining energy depletion at certain average time percentage of the total network time. In both deployment cases, HRHP maintain the highest residual residual energy levels for the different times of network life. SEP protocol had unstable energy dissipation for 100 nodes as shown in Fig. 3.12a, while HRHP maintain a stable and smooth energy dissipation. The same for 200 nodes, although SEP started point with higher energy; however, it dissipate energy faster than HRHP (Fig. 3.12b).



(a) Average residual network energy levels for $N = 100$.



(b) Average residual network energy levels for $N = 200$.

Fig. 3.12 Average residual network energy levels scenario 5, $Area = 300 \times 300$

3.4.6 Scenario 6

In this scenario, the BS is located in the corner of the network boundaries and nodes are randomly deployed over area of ($500 \times 500 m^2$) with two node density cases (100 and 200 nodes distribution).

The affect of changing of the BS location on HRHP was higher on the network with size $500 \times 500 m^2$, were the stability percentage change show a decrease of 53.33%, the operational time shows a decrease of 51.32% and the overall life shows a decrease of 56.25%, in comparison with the case of 100 nodes from scenario 3. Further, when compared to the case of 200 nodes deployment, HRHP shows a decrease of 62% for the stability period, a decrease of 64.51% for the operational time and decrease of 13.65% for the overall life time. Despite these results, when comparing the behaviours of HRHP with other protocols it shows better performance as can be seen from Table 3.7.

Table 3.7 Network life time results obtained from scenario 6 with BS location (510,510)

Algorithm	Results obtained for 100 nodes			Results obtained for 200 nodes		
	FND	HND	LND	FND	HND	LND
LEACH	2	40	575	2	31	828
HRHP	14	74	2283	19	126	4706
MGEAR	3	71	1150	3	35	417
SEP	3	70	2093	2	74	4703

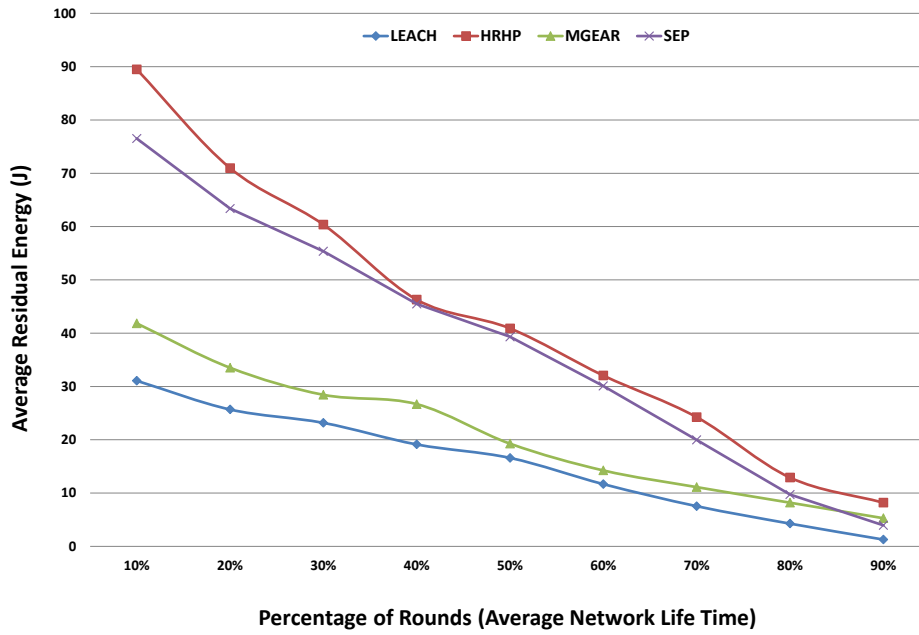
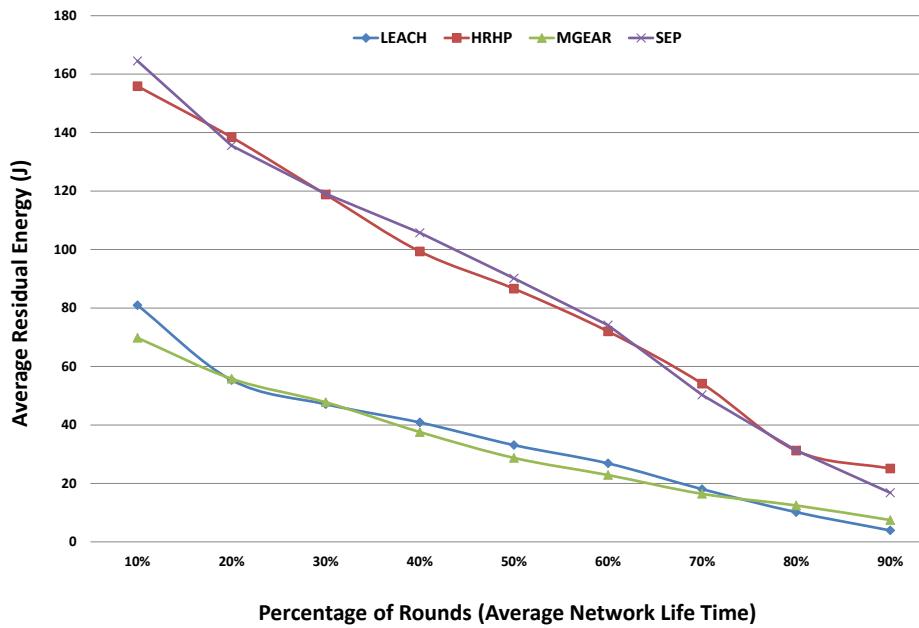
HRHP has the highest round rate for nodes starting death (FND: at round 14 for 100 nodes) leading to longest stability period, (HND: at round 74 for 100 nodes) meaning longer operational time and (LND: at round 2283 for 100 nodes) producing the longest life time among the protocols. HRHP performance improved for the same area when the number of nodes increased to 200 nodes, were (FND extended to round 19) which is around double the stability period, (HND extended to round 126) longer operational time, and (LND extended to round 4706) indicating that HRHP also has better control with node distribution over ($500 \times 500 m^2$) area.

HRHP stability period time in terms of FND is extended compared with LEACH by an average of 61%, MGEAR by an average of 38% and SEP by an average of 23% with the different number of deployment. The operational time in terms of HND is also extended compared with LEACH by an average of 58%, MGEAR by an average of 11% and SEP by an average of 21% with the different number of deployment, i.e more balanced energy dissipation for the different number of nodes deployment. Moreover,

HRHP has the longest network life in terms of LND when compared with the other protocols. HRHP network life time is extended compared with LEACH by an average of 79%, MGEAR by an average of 70% and SEP by an average of 45% with the different number of deployment.

In addition, when the number of nodes increases to 200 HRHP performed better in terms of the stability period, the operational time and the network life time. HRHP shows an increase in the percentage change of 35.71% for the stability period. An increase of 70.27% for the operational time and an increase of 106.13% for the overall network life time.

Fig. 3.13 shows the total remaining energy depletion at certain average time percentage of the total network time. In both deployment cases, HRHP maintains the highest residual energy levels for the different times of network life. SEP protocol had unstable energy dissipation for 100 nodes as shown in Fig. 3.13a, while HRHP maintains a stable and smooth energy dissipation. The same for 200 nodes, although SEP started point with higher energy; however, it dissipates energy faster than HRHP (Fig. 3.13b).

(a) Average residual network energy levels for $N = 100$.(b) Average residual network energy levels for $N = 200$.Fig. 3.13 Average residual network energy levels scenario 6, $Area = 500 \times 500$

3.5 Summary

Clustering is an important factor in developing efficient routing protocols to prolong the lifetime of wireless sensor networks, thus, a hybrid self-adaptive routing protocol (called HRHP) was proposed in this chapter for heterogeneous large-scaled WSNs.

HRHP divided the sensing area into two regions and combined centralized and deterministic clustering approaches for the selection of CHs depending on the network region. CHs selection was made based on several attributes, including the residual energy, the net distance from the base station, and the density of nodes. Moreover, A positive T-cell selection process was implemented to select the CHs. Positive selection ensures that cells expressing harmful or useless antigen receptors do not mature into active T-cells.

The performance of the proposed algorithm was tested in six different scenarios with different BS location, network size and node density. The algorithm significantly improved the stability period, extend the network life time and maintain the highest energy beyond that achieved by existing protocols including LEACH, MGEAR, and SEP. However, HRHP performed better when increasing the number of nodes to 200 regardless of the BS location and the network size, which desirable for IoT systems.

In the next chapter, we will introduce a multi level routing algorithm MLHP which seeks to extend the network life time with reducing energy consumption to the minimum.

Chapter 4

Multi Layer Hierarchical Routing Protocol (MLHP)

In this chapter, a multi-level hybrid clustering routing protocol algorithm (MLHP) for heterogeneous wireless sensor networks (WSNs) is presented. MLHP proposed several techniques to prolong the overall network life time and to fairly distribute the energy load among nodes. It logically divides the sensing area into three levels. A centralized selection is proposed for Level One, in which the base station (BS) plays a great role in selecting cluster heads (CHs) for the first round, then the next CH will be independently chosen among the cluster-members (CMs). In Level Two, CH selection is proposed based on the Grey Wolf Optimizer (GWO), where nodes select the best route to the BS for saving more energy. Herein, grey wolves represent the sensor nodes in Level Two and the prey is the CH. Finally, a distributed clustering based on a cost function is proposed for Level Three. The main idea target in MLHP is to minimize the communication distance to further prolong the network life time. The algorithm was evaluated through tests of a network's energy efficiency, lifetime, and stability period.

The next section gives a brief introduction and section 4.1.1 provides an overview about the Grey Wolf Optimizer. Section 4.2 exhibits the details of the proposed MLHP algorithm, section 4.6 presents the performance results of the proposed algorithm and finally, section 4.8 summarizes the chapter.

4.1 Introduction

New infrastructure systems are connecting the world: systems such as smart grid, smart homes, smart water networks, and intelligent transportation. These systems are associated with a single concept, the internet of things, in which sensors are the key components, closely coupled with information and communication technologies; devices are interconnected to transmit useful information and control instructions via sensor networks [84]. WSNs can provide cheap, appropriate solutions for a range of applications from military to medical [82, 109].

Bio inspired metaheuristic algorithms are proposed by researchers as WSN routing becomes more challenging and complex, like Ant Colony Optimization (ACO) [110–112], Particle Swarm Optimization (PSO) [113][114], Artificial Bee Colony Optimization (ABC) [115][116], and Fuzzy Logic [117][118], are used to provide prolonged network lifetime for WSNs. Grey Wolf Optimizer algorithm (GWO) [119] is a new evolutionary optimizing algorithm that used for modest applications such as optimum feature subset selection [120], when compared with PSO and genetic algorithms showed better performance. Authors of [121] proposed improved version of GWO for training q-Gaussian Radial Basis Functional-Link nets neural networks and a competitive results were obtained comparing to other metaheuristic methods.

4.1.1 Grey Wolf Optimizer (GWO)

Bio-inspired metaheuristics have been efficient in solving problems and finding the best solution. GWO is a new bio-inspired metaheuristic introduced in 2014 by Mirjalili et al. [119] [122]. It is inspired by the social hierarchy and hunting behaviour of grey wolf packs. Wolves live in a hierarchical society of 5 to 12 members and can be categorized into four types: alpha (α) wolves are on top of the societal pyramid (Fig. 4.1); they are responsible for making hunting decisions, deciding where to sleep and when to wake up, etc.

α wolves can be male or female and are not necessarily the strongest but rather the best at finding possible prey locations. Beta (β) wolves are the α wolves' consultants, and in the absence of α they take responsibility for the pack. Delta (δ) wolves are the last ones to eat and they play a devotee role. If a wolf does not belong to the

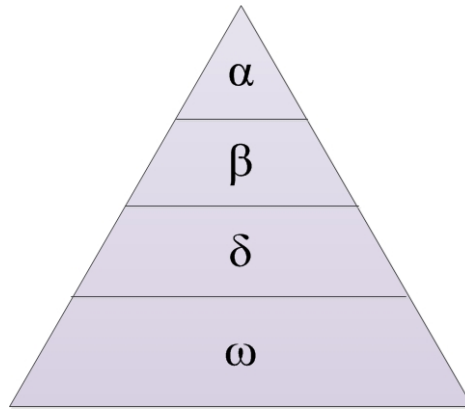


Fig. 4.1 Grey wolf social hierarchy.

previous groups then it is an omega (ω) wolf; ω wolves are responsible for protecting the boundaries and alerting the pack in case of emergency.

In the GWO algorithm illustrated in (Fig. 4.2) [119], the search starts with a population of wolves (solutions) randomly generated: α is the best solution, β is the second-best solution, and δ is the third-best solution within the search space. During the hunting (optimization), the prey's location (optimum) is estimated by the three best solutions through an iterative procedure. Each grey wolf's position is denoted in a vector form $X = x_1 + x_2 + \dots + x_n$, where n is the search-space dimension. Search (hunting) is guided by the α , β , and δ wolves, and the ω wolves follow. The hunting behaviour consists of three main stages: (1) Searching (Hunting), (2) encircling, and (3) attacking the prey.

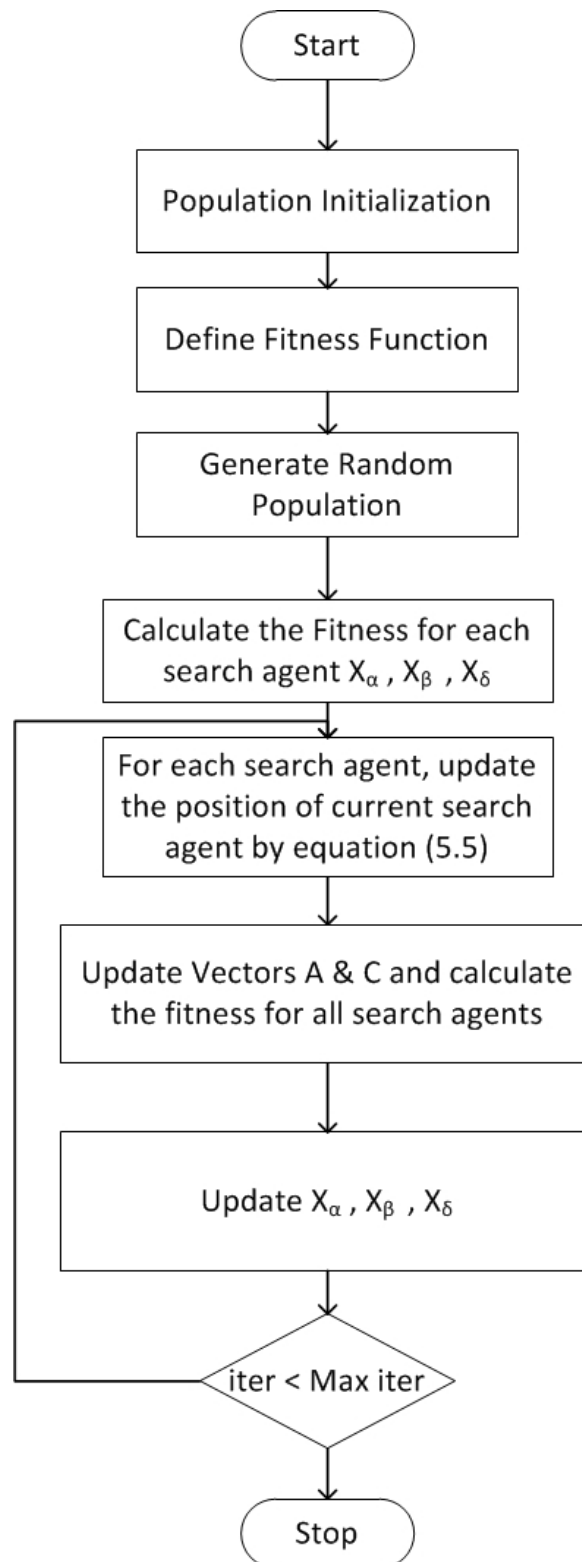


Fig. 4.2 Grey Wolf Optimizer Flowchart.

4.1.1.1 Searching (Hunting) Prey

GWO hunting behaviour is led by the α , β , and δ wolves because they have better knowledge of potential prey locations. Therefore, the three best solutions obtained so far are used by the ω to update their positions as follows:

$$\begin{aligned} D_\alpha &= |C_1 \cdot X_\alpha - X| \\ D_\beta &= |C_2 \cdot X_\beta - X| \\ D_\delta &= |C_3 \cdot X_\delta - X| \end{aligned} \quad (4.1)$$

Where t indicates the current iteration, X represents the position of the current solution, X_α shows the position of α wolf, D_α is the updated α position, X_β shows the position of β wolf, D_β is the updated β position, X_δ shows the position of δ wolf, and D_δ is the updated δ position.

After defining the distances, the final positions of the current solutions X_1 , X_2 , and X_3 are calculated as follows:

$$\begin{aligned} X_1 &= X_\alpha - A_1 \cdot D_\alpha \\ X_2 &= X_\beta - A_2 \cdot D_\beta \\ X_3 &= X_\delta - A_3 \cdot D_\delta \end{aligned} \quad (4.2)$$

$$X^{t+1} = \frac{X_1 + X_2 + X_3}{3} \quad (4.3)$$

where, A_1, A_2, A_3 are random vectors, and t indicates the number of iterations.

4.1.1.2 Encircling Prey

Wolves update their positions imitating the encircling behaviour during the optimization, around α , β , or δ . This is mathematically modelled by the following equations:

$$D = |C \cdot X_p^t - X^t| \quad (4.4)$$

$$X^{t+1} = X_p^t + A \cdot D \quad (4.5)$$

where t is the current iteration, X_p is the prey position, and X is the wolf's position; D is the distance between the position vector of the prey and a wolf and it is calculated in Eq. 4.4; A and C are coefficient vectors calculated in Eqs. 4.6 and 4.7, respectively:

$$A = 2d.r_1 - a \quad (4.6)$$

$$C = 2d.r_2 \quad (4.7)$$

where the a components are linearly decreased from 2 to 0 over the course of the iterations, and r_1, r_2 are random vectors in the range $[0,1]$.

4.1.1.3 Attacking Prey

Grey wolves diverge from each other when searching for prey (exploration) and converge when attacking prey (exploitation). A mathematical model of divergence uses A with random values greater than 1 or less than -1 to oblige the search agent to diverge from the prey, allowing GWO to search globally. That is, $|A| > 1$ forces the grey wolves to diverge from the prey hoping to find better prey, while $|A| < 1$ forces the grey wolves to converge and attack the prey.

4.2 MLHP Initialization

This section describes the network model and the energy model of MLHP in details.

4.2.1 Network Model in MLHP

Nodes that reside far from BS tend to lose their power more quickly due to the far distance communication between nodes and BS. Therefore, the network is logically divided into three equal rectangular spaces based on distance threshold d_{th} to minimize the transmission distance. Level One is closest to the BS and Level Three is farthest away, Fig. 4.3.

MLHP considers a heterogeneous network with three stationary types of nodes in terms of their initial energy and their processing capabilities, m_1 nodes equipped with β times more energy acting as advanced nodes and m_2 nodes equipped with α times

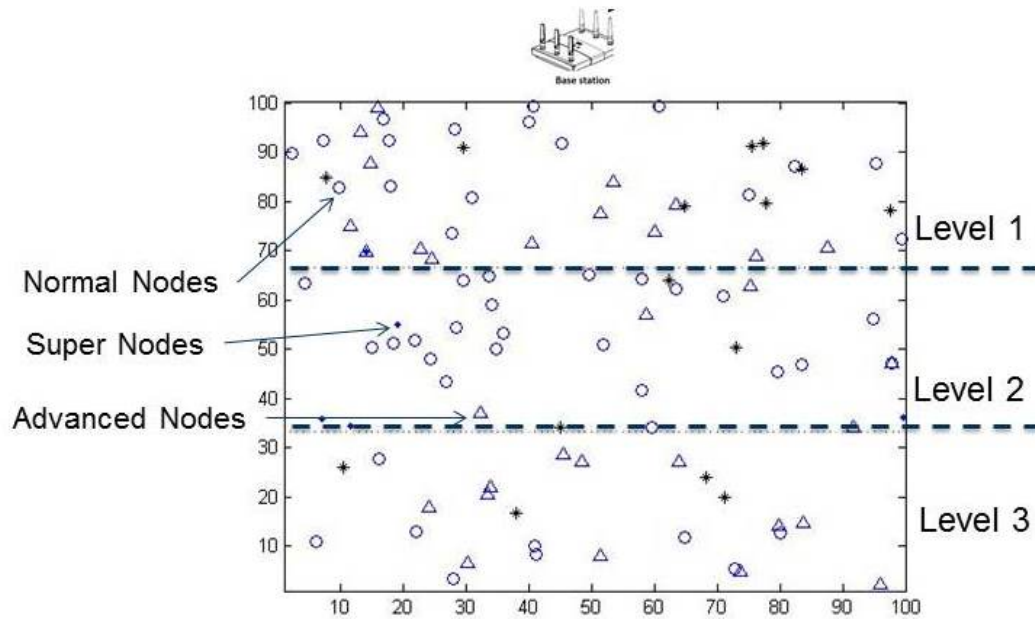


Fig. 4.3 Network Model.

more energy acting as super nodes. The BS is stationary and located in the central upper area. Sensor nodes have a limited and irreplaceable battery. And, sensor nodes can aggregate the l packets into a single packet. In order to keep total energy equivalent with other algorithms for comparison, the total number of nodes is calculated as in Eq. 3.1 in Chapter 3.

After the network is deployed, the BS asks the nodes for their location by broadcasting a message; it calculates the net distance of a particular node from other nodes and from the BS, Net_{dtoBS} , for every node, plus the maximum Net_{dtoBS} , then broadcasts back $(d_{node}, Net_{dtoBS}, D_{Max}, L)$ once, where d_{node} is the node's distance from the BS, D_{Max} is the maximum Net_{dtoBS} , and L is the node's level, which is determined by the BS depending on the signal transmission.

4.2.2 Energy Model

The energy model used for this algorithm as previously explained in Chapter 3, section 3.3.2, Fig. 3.3, where the energy consumed to send a k -bit message over distance d is

$$E_{TX}(k, d) = \begin{cases} k.E_{elec} + k\epsilon_{fs}d^2, & d < d_0 \\ k.E_{elec} + k\epsilon_{mp}d^4, & d > d_0 \end{cases} \quad (4.8)$$

In LEACH, the cluster formation was created to ensure that the expected number of clusters is k . However, the CH's selection depends on the random number generated by the sensor node, and instability of the random number leads to instability of the number of sensor nodes. Calculation of the optimal cluster number (k_{opt}) gives an expected value that may differ greatly from the value in the real WSN. The proposed algorithm calculates an optimal number of clusters that guarantees a CH in every round for Level One nodes by calculating the real k_{opt} , thus ensuring that nodes in Level Two can forward data if no CH was found in Level Two.

4.3 Cluster Number Calculation

MLHP operates in rounds to minimize energy consumption and to evenly distribute energy load over the network. The proposed algorithm suggested several different approaches to improve the network performance and prolong the network life time, which is:

- ***Optimal number of clusters in the network:*** Finding the optimal number of CH's is a key factor that has strong effect on both the life cycle and energy consumption of the network. Lacking suitable number of CH's would cause either redundant selection to nodes or no CH selected, where both situations will lead to power lose.
- ***Different CH selection strategies based on node's level:*** in the proposed scheme three selection techniques were proposed. A centralized CH selection based on node's suitability for Level One, where nodes with the highest suitability make good candidates to be selected as CH. A probabilistic GWO-based CH selection for nodes in Level Two to fairly distribute energy load among nodes.

And, a distributed tree based CH selection is performed in Level Three based on a cost function.

The main reason behind the clustering technique is to reduce the energy consumption rate so that the life time of a wireless network extends. For the hierarchical topologies used in WSNs clustering, they are generally preferred to have a fixed (K) number of sensor nodes working as CHs in each round of the collection process to equally balance the energy load and to save more energy.

4.3.1 Optimal number of CHs ($k1$) for Level One

In the proposed network, nodes are randomly deployed over the network area. Level One nodes (m) are scattered near the BS over the area ($A = M\ddot{O}M/3$) with ($d < d_0$) which is set based on the distance threshold (d_{th}). Therefore, the energy dissipation to transmit an l -bit message in the Level One CH is

$$E_{CH} = lE_{elec}\left(\frac{m}{k1} - 1\right) + lE_{DA}\frac{m}{k1} + lE_{elec} + l\epsilon_{fs}d_{toBS}^2 \quad (4.9)$$

where d_{toBS} is the distance from the CH node to BS, and a perfect data aggregation has been assumed:

$$E_{non-CH} = lE_{elec} + l\epsilon_{fs}d_{toCH}^2 \quad (4.10)$$

Since nodes are equally distributed, we put d_{toCH}^2 to $E[d_{toCH}^2] = A/(2\pi.k1)$ and substitute into Eq. 4.10:

$$E_{non-CH} = lE_{elec} + l\epsilon_{fs}\frac{A}{2\pi.k1} \quad (4.11)$$

Now, the energy dissipated in a cluster in one frame is

$$E_{Cluster} = l\left(E_{CH} + \frac{m}{k1}E_{non-CH}\right) \quad (4.12)$$

and the total energy is

$$\begin{aligned} E_{total} &= k1E_{Cluster} \\ &= l\left(E_{elec}m + E_{DA}m + E_{elec}m + k1\epsilon_{fs}d_{toBS}^2 \right. \\ &\quad \left. + \epsilon_{fs}\frac{A}{2\pi.k1}\right)m \end{aligned} \quad (4.13)$$

To find the optimal number of clusters k_1 , we equate Eq. 4.13 to zero and differentiate with respect to k_1 :

$$k_1 = \sqrt{\left(\frac{m \cdot A}{2\pi}\right)} \cdot \frac{1}{d_{toBS}} \quad (4.14)$$

where m is the node number in Level One and the average distance from a CH to the BS is given by [123] $E[d_{toBS}] = 0.765 \times \frac{A}{2}$.

4.3.2 Optimal number of CHs (k_2) for the rest of the network

As for the rest of the network (Level Two and Level Three), the same formula as in LEACH-C [81] has been considered:

$$k_2 = \sqrt{\frac{n}{2\pi}} \sqrt{\frac{\epsilon_{fs}}{\epsilon_{mp}} \frac{M}{d_{toBS}^2}} \quad (4.15)$$

where ($n = N - m$), M is the sensed area, and $d_{toBS} = 0.765 \times \frac{M}{2}$.

Given n nodes in a network structured as in Fig. 1.7, the expected energy to send k bits from level 1 SNs to Level 2 CHs will be [124]:

$$E_1 = kE_{elec} + k\epsilon_{fs}d_{toCH}^2 \quad (4.16)$$

The researchers in [124] left the multi-level as an open research issue and this is what we applied in CH Wolf.

4.4 Cluster Heads Selection

Improper cluster formation may results in overload for some CHs; this overload may degrade the performance of the entire network due to the high energy consumption of the CHs. Therefore, proper CH selection is the most important concern for clustering in WSNs and designing an energy efficient clustering algorithm is crucial issue and has many challenges. In this section, the selection of CHs is performed by proposing different strategies depending on the node's level to minimize the energy consumption and enhance the performance of the network.

4.4.1 Centralized selection of CHs for Level One

In level One, the BS calculates the suitability of each node which represents the chance of the node to become CH. BS will only select $K1$ nodes with the highest suitability to be declared as CHs. As depicted in Eq. 4.17, the selection is based on the node's location from the BS, the residual energy, and the energy consumption ratio.

$$Suitability(m) = \frac{E_r}{ECR \times Net_{dtoBS}} \quad (4.17)$$

where E_r is the node's residual energy and $ECR = \frac{E_0}{E_0 - E_r}$ is the energy consumption ratio. And the net distance is calculated in Chapter 3, Algorithm 1. [108]

Nodes will be sent a control message from their BS stating the ID of the CHs, the CHs locations and the nodes suitability ratio, the nodes will send join requests to the nearest CH and form the cluster. This process takes place at the first round of the simulation only and when the current CH reaches a predefined energy threshold, an inner cluster decision to select the next CH among the cluster members will occur. By following this approach, nodes will save communication energy through communicating to their CH instead of with the BS to select the next CH, Fig.4.4 provides a detailed description to the CH selection procedure in Level One.

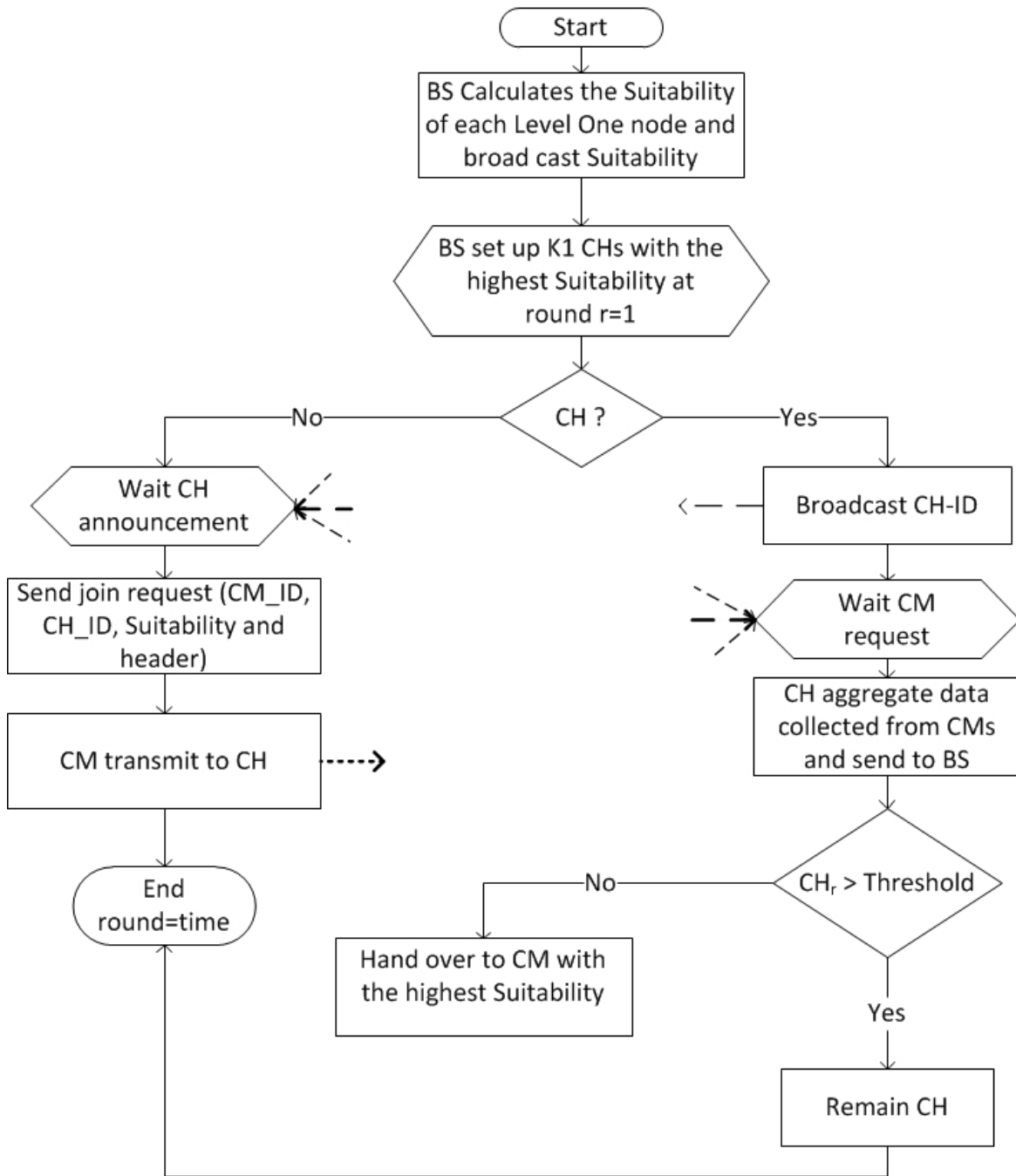


Fig. 4.4 Centralized Selection in Level One.

4.4.2 Probabilistic GWO-based selection of CHs in Level Two

The proposed GWO implementation targets the randomly deployed stationary nodes in Level Two. It assumes m nodes that represent the CH search agents (wolves), $(CH = CH_1, CH_2, \dots, CH_m)$. In order to mimic the positions of the wolves in GWO,

and since changing the position of a static sensor node is not possible, the search agent's position (candidate CH) is represented by \overrightarrow{CH}_i in a two-dimensional space that represents the nodes' positions ($Pos_i(t) = x_i(t), y_i(t)$). The final solution is obtained by considering the nearest node to the best search agent position (α position). Algorithm 2 describes the Level Two GWO-based CH selection.

The CH selection is determined by a fitness function; in the GWO algorithm, the fitness function has the most important role in the searching-for-prey mechanism. The input for this function is the node's characteristics, including its residual energy (E_r) and the number of neighbours; the output is a value expressing how fit the node is to become a CH.

$$f(CH_i) = p_1 |N(CH_i)| + p_2 \sum CH_E, p \in N(CH_i) \quad (4.18)$$

where p_1 and p_2 are random numbers in the range $[0,1]$, $N(CH_i)$ is the list of sensor neighbours for a particular CH_i , and CH_E is the neighbour node's residual energy.

The successful candidate is the one with the highest f , meaning the node with the highest residual energy and sufficient adjacent neighbours will declare itself as a CH. After the selection is completed, CHs will broadcast a *HELLO_Msg* including the CH identification and the CH distance from BS, see Fig. 4.5. Then CH waits for cluster members to join.

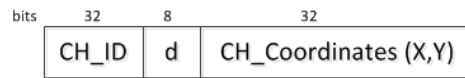


Fig. 4.5 *HELLO_Msg*.

When the current α CH reaches an energy threshold, the next CH selection will be in that cluster and the next CH will be chosen from β nodes. This process prevents energy loss in outer cluster communication if CH selection happens on a network level.

4.4.3 Distributed selection of CHs in Level Three

After receiving the *HELLO_Msg* from Level Two CHs, nodes in Level Three will start CH selection process, this may cause delay in the initialization phase of the algorithm however, it will grantee a maximum life time for the entire network as result for shortening the communication distances.

Algorithm 2 GWO-based CH Selection

```

1: Input  $\alpha$  and  $\beta$  start locations ▷ for each round  $r$ 
2: while  $r < r_{max}$  do
3:   for each search agent  $CH_i$  do
4:     Clone the nearest node to  $CH_i$ 
5:     Compute fitness according to (Eq. 4.18)
6:     Update leader nodes  $X_\alpha, X_\beta, X_\delta$ , the best three search agents
7:     Calculate the coefficient vectors according to (4.6) and (4.7)
8:     Update wolves' positions using (4.3)
9:   end for
10: end while
11:  $CH_{ID} =$  Nearest node to  $\alpha$  obtained.

```

The criteria for selecting the $L3_{CHs}$ depends on the node's distance from $L2_{CH}$ and the its energy. $L3_{node}$ calculates the approximate distance d from each $L2_{CH}$ then build CH_Neighbour_Table as shown in Table 4.1 below.

Table 4.1 CH_Neighbour_Table

CH_Neighbour_ID	d_{toBS}	d
1	62	15
...

A successful CH candidate will have a minimum communication cost, and its residual energy will be greater than half E_0 . None-CH nodes decide its parent within neighbours based on a cost function (Eq. 4.20), where the parent node selection criteria are:

1. The distance between the parent and the BS should be shorter than between itself and BS.
2. If the node can't find a neighbour CH which satisfies criteria 1, it selects the nearest $L2_{CH}$ as its parent.
3. The process of tree constructing phase can be regarded as an iterative algorithm. Using energy level, MLHP chooses the $L3_{CH}$ with more residual energy to transmit data to $L2_{CH}$ if the sensor node cannot find a suitable parent node it will transmit its data directly to BS.

Assume the current node is i , the communication radius is R , and the set of its CH_Neighbours is S ; then its parent node, P_{arent} , is chosen by the following formula:

$$P_{arent} = \begin{cases} BS, & \text{if } d(i, BS) < R \\ L2_{CH}, & \text{if } \min(cost(j) \text{ where } j \in S \text{ and} \\ & d(j, BS) < d(i, BS)) \end{cases} \quad (4.19)$$

$$cost(j) = \frac{P \times Net_{dtoBS}}{D_{max}} + ((1 - P) \times (E_0 - E_r)) \quad (4.20)$$

Where, P is a probability factor chosen by CHs, Net_{dtoBS} is the net distance between the CH and BS and between itself and $L2_{CH}$, D_{max} is the maximum distance to BS, E_r is the residual energy and E_0 is the initial energy. The pseudocode for generating the parental tree is given in Algorithm 3.

Algorithm 3 Pseudocode for creating the tree

```

1: Sending HELLO_Msg (CH_ID,  $d_{toBS}$ )
2: On receiving a HELLO_Msg from node  $j$  by node  $i$ 
3: Add  $j$  to the CH_Neighbour_Table
4: for  $i = 1 : N$  do
5:   if  $Node.L == 3$  &  $Node.Energy > E_0/2$  then
6:      $Node.Live = 1$ 
7:      $Node.p = 0$ 
8:      $Node.d = 0$ 
9:      $min_{cost} = 1$ 
10:    for  $j = 1 : S(i)$  do
11:      if  $Node(i).d_{toBS} < R$  then
12:         $Node(i).p = BS$ 
13:      else  $Node(i).d_{toBS} > Node(j).d_{toBS}$ 
14:         $cost = P \times (Net_{dtoBS}/D_{max}) + ((1 - P) \times (E_0 - E_r))$ 
15:        if  $cost < min_{cost}$  then
16:           $min_{cost} = cost$ 
17:           $Node(i).p = j$ 
18:           $Node(i).d = d(i, j)$ 
19:        end if
20:      end if
21:    end for
22:  end if
23: end for

```

4.5 Performance Evaluation

The motivation of designing MLHP is to further improve the network energy consumption and to extend the network life time than of HRHP (proposed in Chapter 3). In this section, MLHP is compared HRHP in terms of network stability (FND), operational time (HND), network life time (LND) and the total remaining energy. Two cases are conducted to test the performance of both protocols when changing the sensing area and the network density. The base station located in the middle far of the network and the heterogeneity parameters were set to ($\alpha = 2$ and $\beta = 1$) which will give fair testing environment:

- **Case1:** $Area = 100 \times 100 m^2$, the number of nodes $N = 100$ and $N = 200$.
- **Case2:** $Area = 200 \times 200 m^2$, the number of nodes $N = 100$ and $N = 200$.

MLHP reduces the communication distance by dividing the area into three levels and applies a tree-based CH selection for level 3. In the first level of the network, MLHP applies the same techniques used in HRHP, however, different CH selection technique is used for the remaining area. Which improved the performance of MLHP compared to HRHP. Examining the results obtained from case1, MLHP performance outperformed HRHP for the stability period by a percentage change of 78.03%, the operational time for MLHP is also increases by a percentage change of 74.06% and the network life was extended by a percentage change of 80.66%, as can be seen in Table 4.2.

Table 4.2 Case1: Network life time, Area= $100 \times 100 m^2$

Algorithm	Results obtained for 100 nodes			Results obtained for 200 nodes		
	FND	HND	LND	FND	HND	LND
MLHP	1848	3490	9353	1463	2406	6389
HRHP	1038	2005	5177	116	2096	5034

When increasing the number of nodes to 200, MLHP stability period increases compared to HRHP by a change of 25.58%, the operational time increases by a percentage change of 14.79% and the network life time increases by 26.92%.

Furthermore, MLHP has more energy balanced network compared to HRHP, MLHP successfully maintains higher energy levels for both node deployments. Fig. 4.6 shows the total remaining energy levels for a 100 nodes deployment and Fig. 4.7 shows the remaining energy for network deployment of 200 nodes.

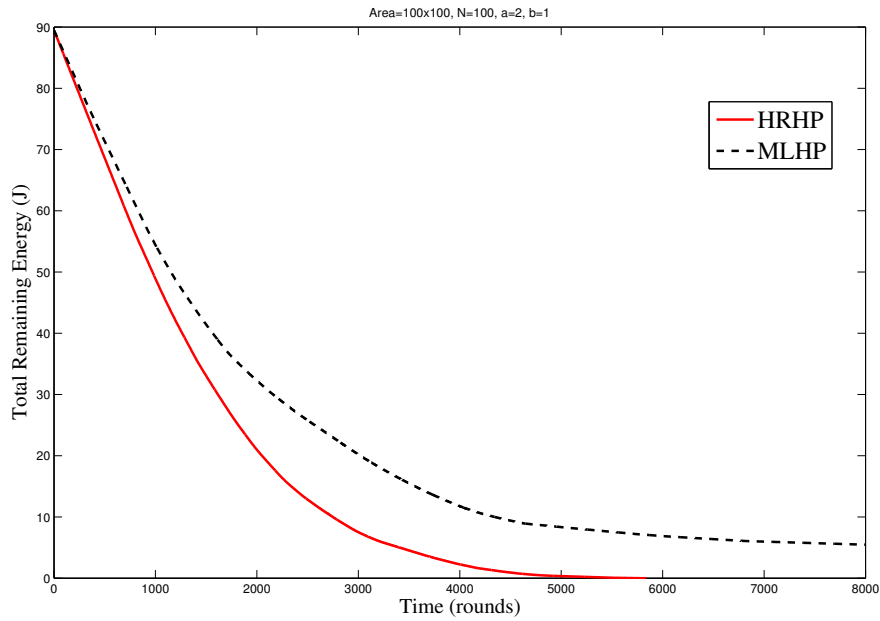


Fig. 4.6 Total network remaining energy for $100 \times 100 m^2$ area and $N = 100$.

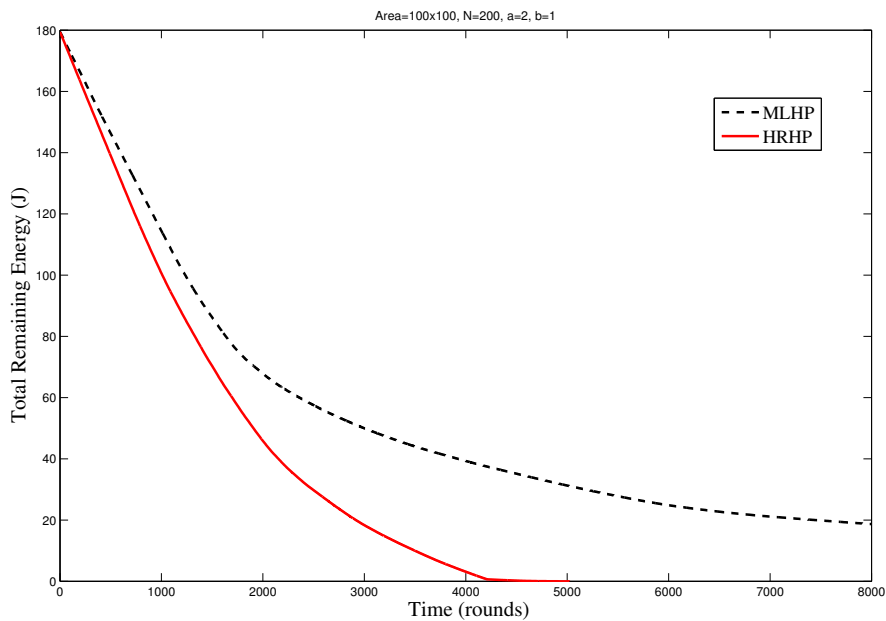


Fig. 4.7 Total network remaining energy for $100 \times 100 m^2$ area and $N = 200$.

Increasing the sensing area to $200 \times 200 m^2$ has affected the performance of both protocols in comparison with case1. However, MLHP remains to act better than HRHP.

For 100 nodes deployment, the stability period of MLHP increases by increase of 23.47%, the operational time increases by 2.62% and the network life time increases by 28.57%. In addition, when the number of nodes increases to 200, the stability period of MLHP increases by 12.2%, the operational time increases by 2.16% and the network life time increase by 43.07%. Table 4.3 presents the results obtained for case2.

Table 4.3 Case2: Network life time, Area= $200 \times 200 m^2$

Algorithm	Results obtained for 100 nodes			Results obtained for 200 nodes		
	FND	HND	LND	FND	HND	LND
MLHP	605	1212	7277	920	1609	8298
HRHP	490	1181	5660	820	1575	5800

The network remaining energy is further improved in MLHP when increasing the sensing area size. Fig. 4.8 presents the results for comparing the remaining energy for 100 nodes deployment and Fig. 4.9 shows the results obtained for 200 nodes deployment. The figures clearly show that MLHP performance in preserving the network energy is better than HRHP for both nodes deployment.

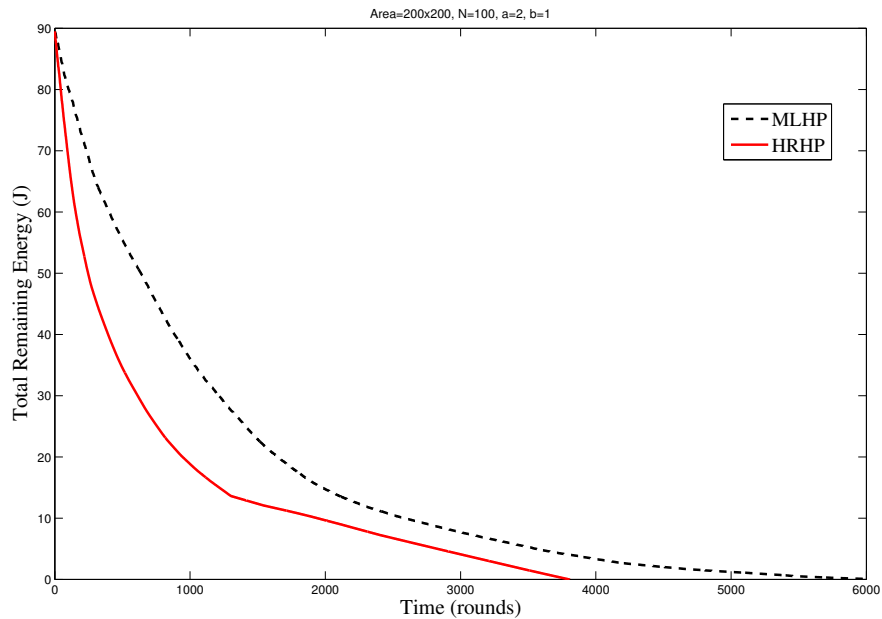


Fig. 4.8 Total network remaining energy for $200 \times 200 m^2$ area and $N = 100$.

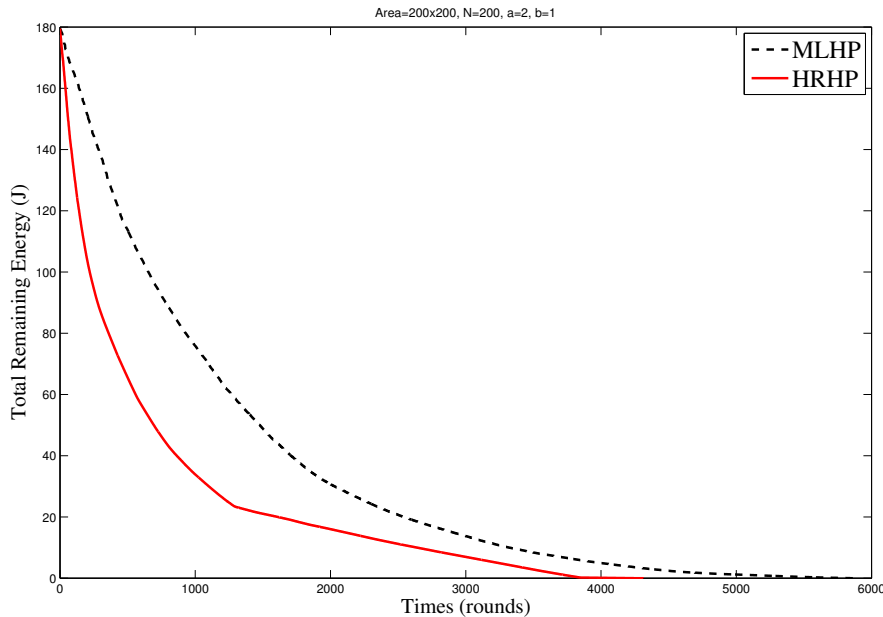


Fig. 4.9 Total network remaining energy for $200 \times 200 \text{ m}^2$ area and $N = 200$.

MLHP has fulfilled its purpose in comparison with HRHP. Therefore, we wanted to test MLHP against other protocols. MLHP is compared with LEACH, DEEC and SEP protocols in terms of stability period, operational time, network life time and the network remaining energy. In the next section, the simulation parameters and the settings are explained in details.

4.6 Simulation Parameters and Settings

Simulation can be defined as a representation or imitation of a system in its realistic form. It is a powerful tool for the evaluation and analysis of a new system design, modifications to existing systems. Employing simulation to study system performance incorporates different advantages. In networking field, simulation has been widely used to evaluate network algorithms under different conditions, and to provide a critical understanding for their behaviours and characteristics. The main scenarios involve results for different assumptions simulation scenarios and analyses the most significant performance results in terms of network stability, life time, percentage of nodes survival, residual energy, and data packets sent to the BS. This section illustrate the design

and implementation of the simulation parameters and the scenarios for comparing the performance of HRHP to other reported protocols.

4.6.1 Simulation Parameters

To evaluate the performance of MLHP, three extensive simulation studies was conducted using MatLab R2012b and compared with the performance of best-known algorithms. All simulations were conducted in randomly generated, static networks with different number of nodes and monitoring area size. The metric performance used in simulation is based on the number of *rounds* in which the first node deployed its energy, half of nodes are active and when all nodes are inactive. A *round* is a time interval where all the Cluster Members (CMs) have to transmit their data to the associated Cluster Head (CH). To represent the heterogeneity of the network, three types of nodes are used with different initial energy as illustrated in Section 4.2.1. The common simulation parameters settings are listed in Table 4.4 and the performance indicators are defined below:

1. **Network Stability Period:** is the number of rounds lapsed from the start of the network operating till the energy of the *First Node Dead (FND)* is insufficient to transmit data. High value of FND indicates more balanced energy consumption among sensor nodes [125].
2. **Operational Time:** is defined as the number of rounds for which 50% of the total nodes are active, *Half Node Dead (HND)*.
3. **Network Life Time:** referred to as the *Last Node Dead (LND)*, which indicates the number of rounds after which all nodes in the network deployed their energy and no longer able to establish communication with other nodes.
4. **Energy Dissipation:** this parameter indicates the average energy dissipated by the network over the period of operating time.
5. **Packets Delivery:** which is the total data transmitted by CH's and received by the BS.

Table 4.4 Simulation Parameters

Parameter	Value
Initial Energy (E_o Normal)	0.5J/bit
Cluster Head Probability (P)	0.1
Data Aggregation Energy cost (EDA)	5nJ/bit/signal
Packet Size	4000 bits
Transmitter/ Receiver Electronics (E_{elec})	50nJ/bit
Transmit amplifier (ϵ_{fs})	10pj/bit/m ²
Transmit amplifier (ϵ_{mp})	0.0013pj/bit/m ⁴
Fitness function probability (p_1)	0.7
Fitness function probability (p_2)	0.3

4.6.2 Simulation Settings

In this work, the scenarios were designed to give proper indication on the algorithm performance in terms of heterogeneity awareness to extend the network life time and thus the network performance. Three main scenarios were set to measure the performance of the proposed algorithm. The stability of the algorithms as well network operational time were tested in scenario-I for small-scale and large-scale networks with the minimum heterogeneity and for different number of nodes (100, 300, and 500) as illustrated in Table 4.5, the performance of the protocols in terms of network life time, energy conception and packet delivery for small-scale networks is examined in scenario-II and the parameters are set accordingly as illustrated in Table. 4.6. Finally, the performance over large-scale networks in terms of network life time, energy conception and packet delivery is measured in scenario-III and the parameters settings are shown in Table. 4.7.

Table 4.5 Scenario-I Settings: Network Stability and Operational Time

Case	Area	Nodes (N)	β	α	m	mo
1	$100 \times 100 m^2$	100 nodes	0.5	1	0.5	0.4
2	$100 \times 100 m^2$	300 nodes	0.5	1	0.5	0.4
3	$100 \times 100 m^2$	500 nodes	0.5	1	0.5	0.4
4	$200 \times 200 m^2$	100 nodes	0.5	1	0.5	0.4
5	$200 \times 200 m^2$	300 nodes	0.5	1	0.5	0.4
6	$200 \times 200 m^2$	500 nodes	0.5	1	0.5	0.4

Table 4.6 Scenario-II Settings: Heterogeneity over Small-Scale Network)

Case	Area	Nodes (N)	β	α	m	mo
1	$100 \times 100 m^2$	100 nodes	0.5	1	0.5	0.4
2	$100 \times 100 m^2$	100 nodes	1	2	0.5	0.4
3	$100 \times 100 m^2$	200 nodes	0.5	1	0.5	0.4
4	$100 \times 100 m^2$	200 nodes	1	2	0.5	0.4

Table 4.7 Scenario-III Settings: Heterogeneity over Large-Scale Network

Case	Area	Nodes (N)	β	α	m	mo
1	$200 \times 200 m^2$	100 nodes	0.5	1	0.5	0.4
2	$200 \times 200 m^2$	100 nodes	1	2	0.5	0.4
3	$200 \times 200 m^2$	200 nodes	0.5	1	0.5	0.4
4	$200 \times 200 m^2$	200 nodes	1	2	0.5	0.4

where, m is the ratio of normal nodes, mo is the ratio of advanced and super nodes combined, α is the percentage of energy for the super nodes, and β is the percentage of energy for the advanced nodes.

The usage of these factors are explained in the following **Example**: in scenario-I, when the total number of nodes ($N = 100$) and $m = 0.5$, this means the ratio of normal nodes is 50%, therefore the network will have 50 normal nodes, the same ratio division applies to ($N = 300$ and $N = 500$). When $mo = 0.4$, then the number of advanced nodes (N_a) in the network can be calculate as:

$$\begin{aligned}
 N_a &= N \times m \times (1 - mo) \\
 &= 30 \text{ nodes}
 \end{aligned}
 \tag{4.21}$$

And the rest of the nodes are super nodes ($N - N_a \Rightarrow 50 - 30 = 20 \text{ nodes}$), now the initial energy of the advanced nodes is calculated as: $E_a = E_o * (1 + \beta)$, meaning when

$\beta = 0.5$ that means there are 30 advanced nodes equipped with initial energy equals to $0.75 J/bit$, and when $\alpha = 1$ that means there are 20 nodes equipped with initial energy equals to $1 J/bit$. The same ratio settings apply for ($N = 200, 300,$ and 500).

In scenario-II and scenario-III when $\beta = 1$, the initial energy of the advanced nodes, equals to $1 J/bit$ and when $\alpha = 2$ the initial energy of the super nodes equals to $1.5 J/bit$. Which is the highest energy level allowed for the nodes, this will provide a clear vision for the algorithms behaviour under worst case scenarios when the heterogeneity of the network is low.

4.7 Simulation Results

In the first stages of the network setup, MLHP sets the number of CHs based on the Eq. 4.14, then selects the nodes with the highest suitability using Eq. 4.17 for Level One. In Level Two, the selection is made based on the proposed fitness function (Eq.4.18) which guarantee the selection of the best fitted nodes. Lastly, it reduces the communication distance in Level Three by selecting the nearest CH in Level Two to act as the parent of Level Three CH based on the cost function which is proposed in Eq. 4.20. Three main scenarios were set in Table 4.7 to compare the performance of MLHP against three known protocols namely LEACH, DEEC and SEP.

In this section, the evaluation performance of MLHP and the simulation results are presented. Each result represents an average of 30 simulation runs to provide accurate results. The first set of results investigate the network stability and the operational time in small-scale and large-scale networks (Section 4.7.1). Section 4.7.2 presents the results obtained to find the affect of changing the network heterogeneity in small-scale networks. Finally, Section 4.7.3 display the results collected to find the affect of changing the network heterogeneity in large-scale networks.

4.7.1 Network Stability and Operational Time

In order to test the algorithms' behaviour over a scaled network deployed with different node density (100, 300, and 500 nodes) and low heterogeneity parameters ($\alpha = 1$ and $\beta = 0.5$), the stability of the network and the network operational time are evaluated for two different areas ($100 \times 100 m^2$ and $200 \times 200 m^2$). The obtained results are illustrated in Table 4.8 and Table 4.9 respectively.

In Table 4.8, for a small network area ($100 \times 100 \text{ m}^2$) deployed with 100 nodes, MLHP first node has lost its activity in round 1213, LEACH in round 955, DEEC in round 1205, and SEP in round 1019. This indicates that MLHP had the longest network stability, which will give the systems that are implemented in a small area more stable environment to operate. When the number of nodes increases to 300, the stability time percentage change for MLHP increases by 12.7%, LEACH by 1.99% and SEP by 16.58% while DEEC decreases by 2.66%. Further, when the deployment of the nodes increases to 500 nodes, the stability time percentage change for MLHP increases by 18.47% and SEP by 20.22% while LEACH decreases by 1.57% and DEEC further decreases by 5.39%. MLHP and SEP took the advantage of choosing CHs that can support the network which made them maintain higher increase stability regardless of the network density for small scaled networks.

However, when we examine the operational time represented by Table 4.9, we can see that MLHP HND took place at round 2765 for $100 \times 100 \text{ m}^2$ area deployed with 100 nodes, and SEP in round 1753 which represents an increased percentage change by 36.6% for MLHP over SEP. When the same area is deployed by 300 nodes, MLHP percentage change increased by 15.19% while SEP only increases by 0.74%. The same improvement is noticed when deploying the area with 500 nodes, MLHP shows an increased percentage change by 37.03% and SEP by 1.08%. MLHP scored better performance because it consider the characteristics of the nodes when selecting a CH, which include the node's location in the network, the node's distance from the BS and the node's residual energy. Therefore, when we increased the number of nodes, MLHP had more range of nodes to select from, which is important for IoT applications were there will be billions of nodes connected together.

Moreover, MLHP keeps the communication distance to the minimum when considering a CH. Therefore, when the sensing area increases to $200 \times 200 \text{ m}^2$, MLHP successfully preserve the highest stability period. For an area deployed with 100 nodes, MLHP percentage change increased by 16.53%, while LEACH by 0.34%, DEEC by 15.12% and SEP by 4.01%. Furthermore, for deployment of 500 nodes, stability period percentage change increased in MLHP by 6.62%, LEACH by 0.68%, DEEC by 8.54% and SEP by 1.34%. This will reflect on the operational time for HND (Table 4.9) were MLHP had the highest improvement for operational time, which will guarantee that the system operates MLHP have longer time to collect more data from the field. The operational time percentage change has increased for MLHP by 49.34% for a network deployed with 300 nodes and 43.65% for a network deployed with 500 nodes.

For LEACH an increase of 13.07% for 300 nodes and increase of 11.7% for 500 nodes. DEEC showed an increase of 25.6% for 300 nodes and 25.16% for 500 nodes. Finally, SEP showed an increase of 19.51% for 300 nodes and 11.67% for 500 nodes.

As a result, MLHP successfully preserves good stability period and the longest operational time for both small-scale and large-scale area networks, regardless the nodes number and for minimum heterogeneity. It also has the longest operational time for both areas, which means that MLHP has more balanced network.

Table 4.8 Network Stability: Average number of communication rounds at which the first node in the network dies for small-scale and large-scale networks with different node density.

Protocols	100 Sensor nodes		300 Sensor nodes		500 Sensor nodes	
	$100 \times 100 m^2$	$200 \times 200 m^2$	$100 \times 100 m^2$	$200 \times 200 m^2$	$100 \times 100 m^2$	$200 \times 200 m^2$
MLHP	1213	484	1367	564	1437	529
LEACH	955	295	974	296	940	297
DEEC	1205	480	1173	553	1140	521
SEP	1019	449	1188	467	1225	455

Table 4.9 Network Operational Time: Average number of communication rounds at which half of nodes in the network dies for small-scale and large-scale networks with different node density.

Protocols	100 Sensor nodes		300 Sensor nodes		500 Sensor nodes	
	$100 \times 100 m^2$	$200 \times 200 m^2$	$100 \times 100 m^2$	$200 \times 200 m^2$	$100 \times 100 m^2$	$200 \times 200 m^2$
MLHP	2765	1212	3185	1810	2911	1741
LEACH	1130	658	1153	744	1158	735
DEEC	1820	1178	1778	1354	1750	1362
SEP	1753	1174	1740	1403	1734	1311

4.7.2 Heterogeneity over Small-Scaled Networks

MLHP had high stability period and the longest operational times for a small-scale network sized $100 \times 100 m^2$, for different node intensities (100, 300 and 500) with the minimum heterogeneity parameters ($\alpha = 1$ and $\beta = 0.5$).

In this section, the results obtained in order to find the affect on the performance of MLHP when increasing the heterogeneity parameters. The performance of MLHP is compared to LEACH, DEEC and SEP in terms of network life time, network residual energy and the number of packets delivered to the BS.

4.7.2.1 Network Life Time

The majority of the literature compare the network lifetime in terms of last dead node (LND) only, which may not give a full indication on the performance of the algorithms and the ratio of the active nodes during different life time stages. In the presented results for this scenario, a time slots are set to provide a better image for the number of active nodes during the life time of the network.

Case1: When the network was deployed with 100 nodes with low heterogeneity parameters ($\alpha = 1$) and ($\beta = 0.5$).

Fig. 4.10 illustrates the average communication rounds at which a certain nodes percentage death happen, which is presented by the x-axis. When comparing the nodes' death point of MLHP with those of LEACH and SEP, MLHP nodes died later for the entire life time points. MLHP 10% of nodes died at round 1463, LEACH at round 1025 and SEP at round 1230. However, when comparing with DEEC (at round 1472), the 10% death of MLHP happened slightly before that of DEEC because MLHP had more active nodes at the first rounds. While when comparing the remaining time slots, we can see that MLHP had slower death than DEEC which means that MLHP adjust its selection of CHs to preserve the number of active nodes. The improvement percentage of MLHP over all compared algorithms is presented in Table 4.10.

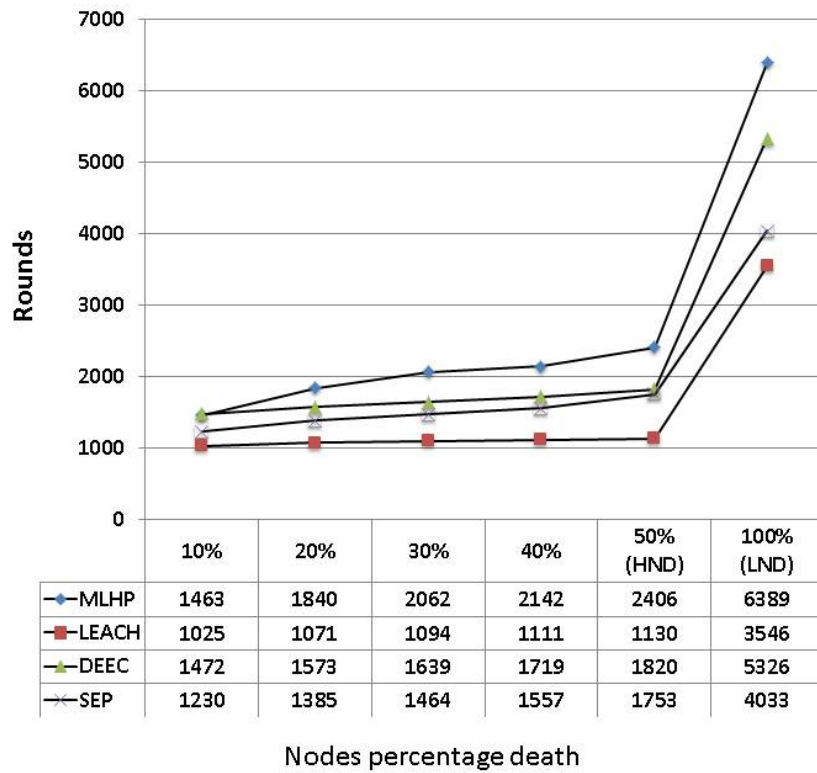


Fig. 4.10 Network lifetime for small-scale network, $N = 100$, $\alpha = 1$, $\beta = 0.5$.

Table 4.10 Average life time percentage improvement over other protocols for small-scale network ($N = 100$, $\alpha = 1$, $\beta = 0.5$)

Percentage of dead nodes	Improvement over LEACH	Improvement over DEEC	Improvement over SEP
10%	43%	-1%	19%
20%	72%	17%	33%
30%	88%	26%	41%
40%	93%	25%	38%
50% (HND)	113%	32%	37%
100% (LND)	80%	20%	58%

Case2: When increasing the heterogeneity parameters ($\alpha = 2$) and ($\beta = 1$) for 100 nodes.

Fig. 4.11 presents the results obtained for the case2. MLHP life time extended rapidly to reach round 9353 (for LND) compared to other protocols. LEACH network stopped working early at round 2108 which is even less than the first case, this is

due to LEACH does not consider the heterogeneity of the network, instead it assign random CHs in the network. Network life time in SEP ended at round 6236 and DEEC at round 8276. Table 4.11 presents the average percentage improvement for MLHP compared to other protocols.

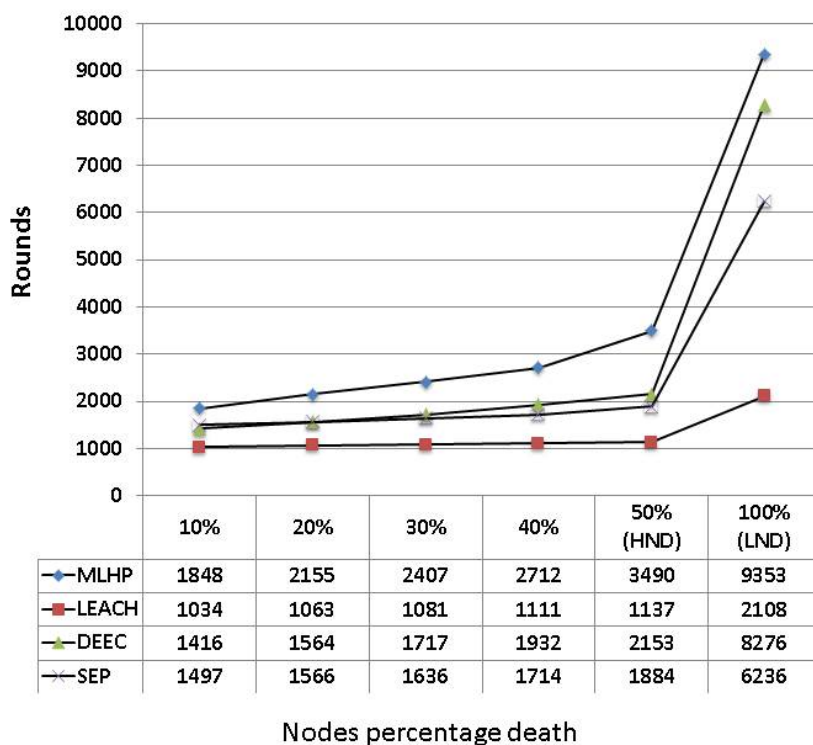


Fig. 4.11 Network lifetime for small-scale network, $N = 100$, $\alpha = 2$, $\beta = 1$.

Table 4.11 Average life time percentage improvement over other protocols for small-scale network ($N = 100$, $\alpha = 2$, $\beta = 1$)

Percentage of dead nodes	Improvement over LEACH	Improvement over DEEC	Improvement over SEP
10%	77%	31%	23%
20%	90%	38%	38%
30%	113%	40%	47%
40%	165%	40%	58%
50% (HND)	231%	62%	85%
100% (LND)	341%	13%	50%

Therefore, when increasing the heterogeneity parameters, the performance of MLHP increases compared to case1. For 10% death point, MLHP improved by a percentage change of 26.32% which indicates better network stability. For 50% death point, MLHP improved by an increase of 45.05% which is longer operational time. As for the entire network life (LND), MLHP increased its performance by 46.39%. This behaviour showed that when increasing the heterogeneity, the performance of MLHP increases, which is expected and wanted when applying IoT systems.

Case3: When increasing the number of nodes to 200 with low heterogeneity parameters ($\alpha = 1$) and ($\beta = 0.5$).

This case was set to find the affect when increasing the network intensity in regards with changing the network heterogeneity. Fig. 4.12 illustrates the results obtained for the case of low heterogeneity ($\alpha = 1$ and $\beta = 0.5$). When increasing the number of nodes to 200, MLHP 10% death point increased compared to case1 by 25.22%, for 50% death point increased by 56.61% and an increase by 45.59% for LND. Based on these results, MLHP improved its performance by having longer network stability, operational time and overall network life time.

When comparing MLHP performance to other protocols, MLHP outperformed them in terms of network stability, operational time (HND) and life time (LND) as illustrated in Fig. 4.12. The average life time percentage improvement of MLHP over the compared algorithms is presented in Tables 4.12.

Table 4.12 Average life time percentage improvement over other protocols for small-scale network ($N = 200$, $\alpha = 1$, $\beta = 0.5$)

Percentage of dead nodes	Improvement over LEACH	Improvement over DEEC	Improvement over SEP
10%	75%	27%	19%
20%	87%	30%	27%
30%	109%	34%	40%
40%	162%	47%	71%
50% (HND)	228%	69%	94%
100% (LND)	403%	10%	57%

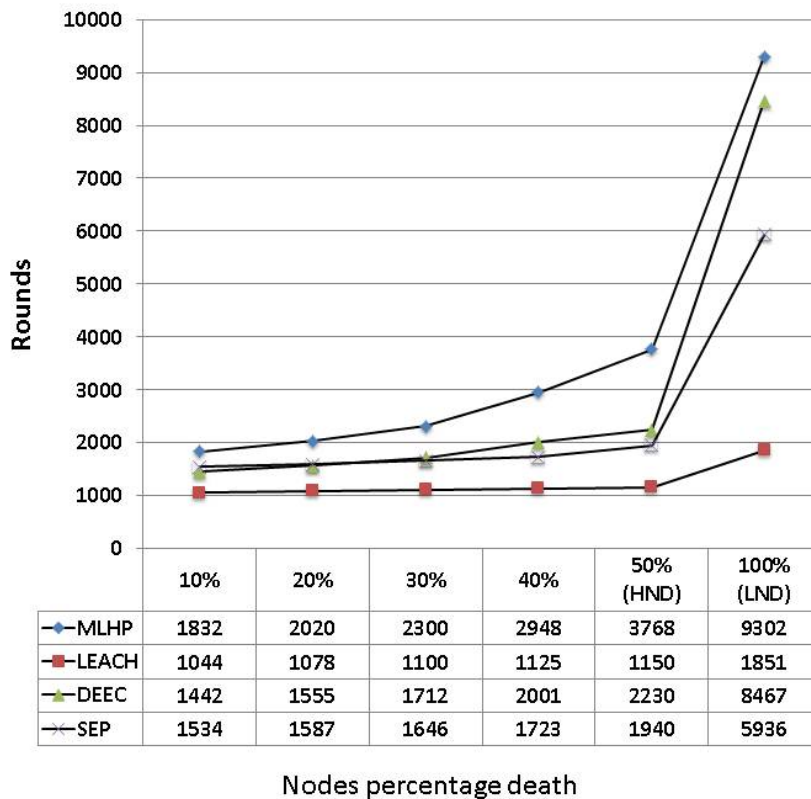


Fig. 4.12 Network lifetime for small-scale network, $N = 200$, $\alpha = 1$, $\beta = 0.5$.

Case4: When increasing the number of nodes to 200 with higher heterogeneity parameters ($\alpha = 2$) and ($\beta = 1$).

When increasing the heterogeneity of the network, MLHP showed a decreased percentage change for 10% death point compared to case2 by 1.89%, and increase for the HND by 4.27% and by 0.56% for the network life time. This is due to larger number of nodes deployed over small-scale network, which will shorten the distances between nodes and the BS. Therefore, more nodes to be treated as best nodes in Level Two and this means larger number of working CHs in the first rounds. However, after 30% of nodes death point, MLHP shows better control and longer life time.

Comparing MLHP to the other protocols, MLHP have outperformed other protocols in terms of stability, operational time and network life time as shown in Fig. 4.13. Table 4.13 provides the average life time percentage improvement of MLHP over the compared algorithms.

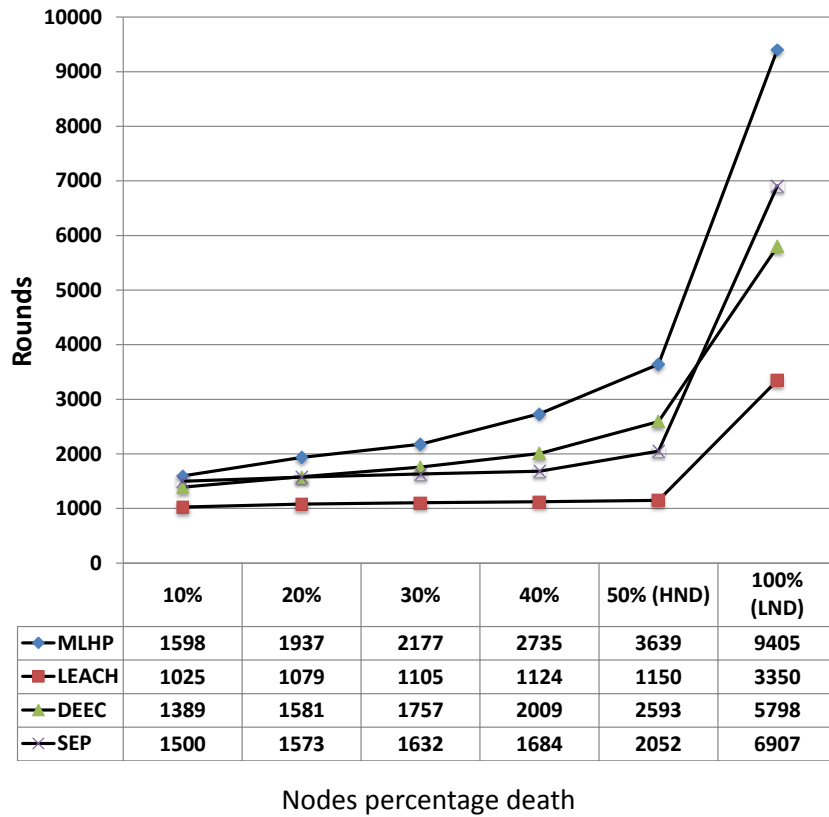


Fig. 4.13 Network lifetime for small-scale network, $N = 200$, $\alpha = 2$, $\beta = 1$.

Table 4.13 Average life time percentage improvement over other protocols for small-scale network ($N = 200$, $\alpha = 2$, $\beta = 1$)

Percentage of dead nodes	Improvement over LEACH	Improvement over DEEC	Improvement over SEP
10%	70%	2%	-10%
20%	98%	1%	-6%
30%	98%	1%	1%
40%	125%	11%	8%
50% (HND)	214%	50%	60%
100% (LND)	431%	26%	48%

4.7.2.2 Energy Consumption

Fig. 4.14 through Fig. 4.17 show the per-round energy consumption of the four cases mentioned in the previous section. In all different cases, MLHP has a higher level of remaining energy in the network compared to LEACH, DEEC and SEP during the

operational time after (HND) and through the end of life time (LND). MLHP preserved the network energy by reducing the communication distances between the nodes and the BS, it also reserve the energy through the selection of CHs which guarantees only the best nodes to be selected.

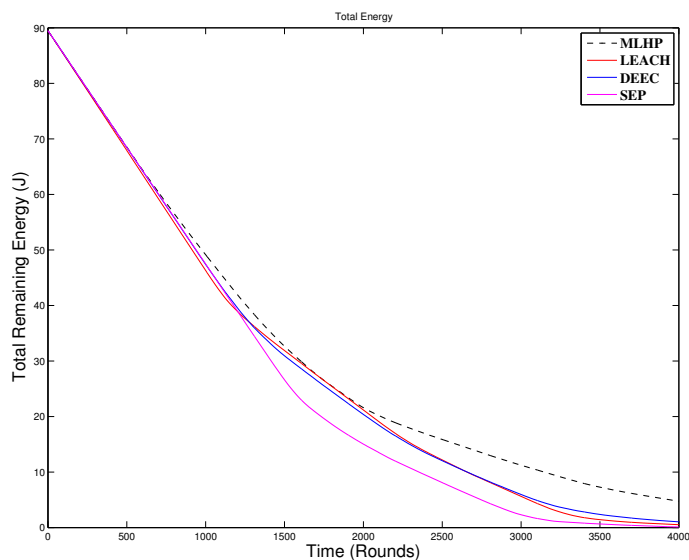


Fig. 4.14 Case1: Total residual energy, $N = 100$, $\alpha = 1$, $\beta = 0.5$.

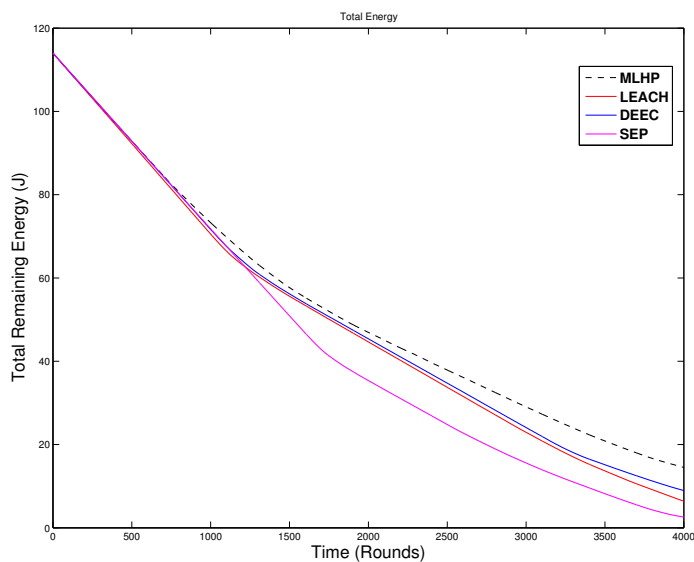


Fig. 4.15 Case2: Total residual energy, $N = 100$, $\alpha = 2$, $\beta = 1$.

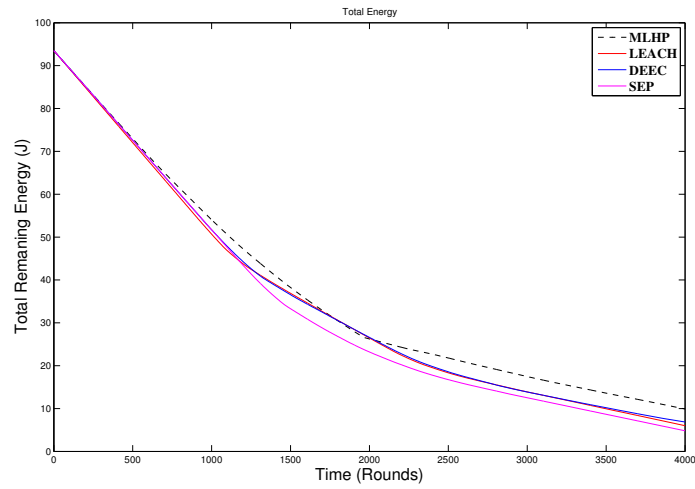


Fig. 4.16 Case3: Total residual energy, $N = 200$, $\alpha = 1$, $\beta = 0.5$.

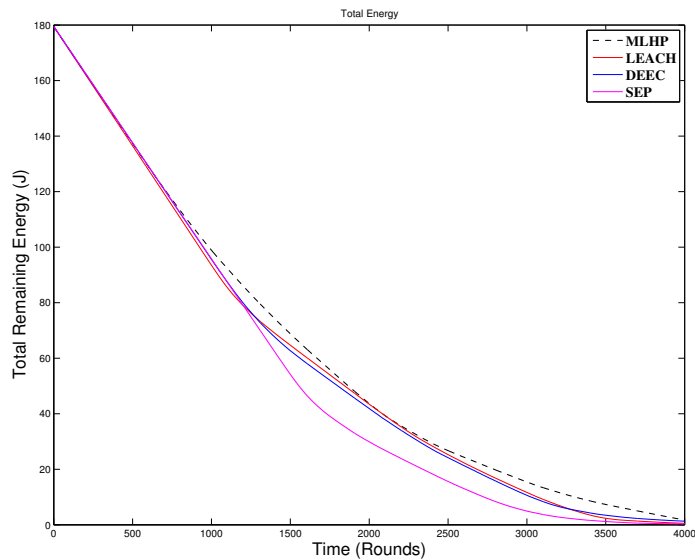


Fig. 4.17 Case4: Total residual energy, $N = 200$, $\alpha = 2$, $\beta = 1$.

4.7.2.3 Packet Delivery

Packet delivery ratio to BS is another metric considered in the evaluation of the proposed MLHP. Fig. 4.18 shows the average accumulative number of data packets sent to the BS for the different cases. In all the different cases, MLHP has longer life time and thus longer time to detect and sent packets (data) to the BS therefore the ratio of packets sent by MLHP algorithm is greater than for the compared algorithms.

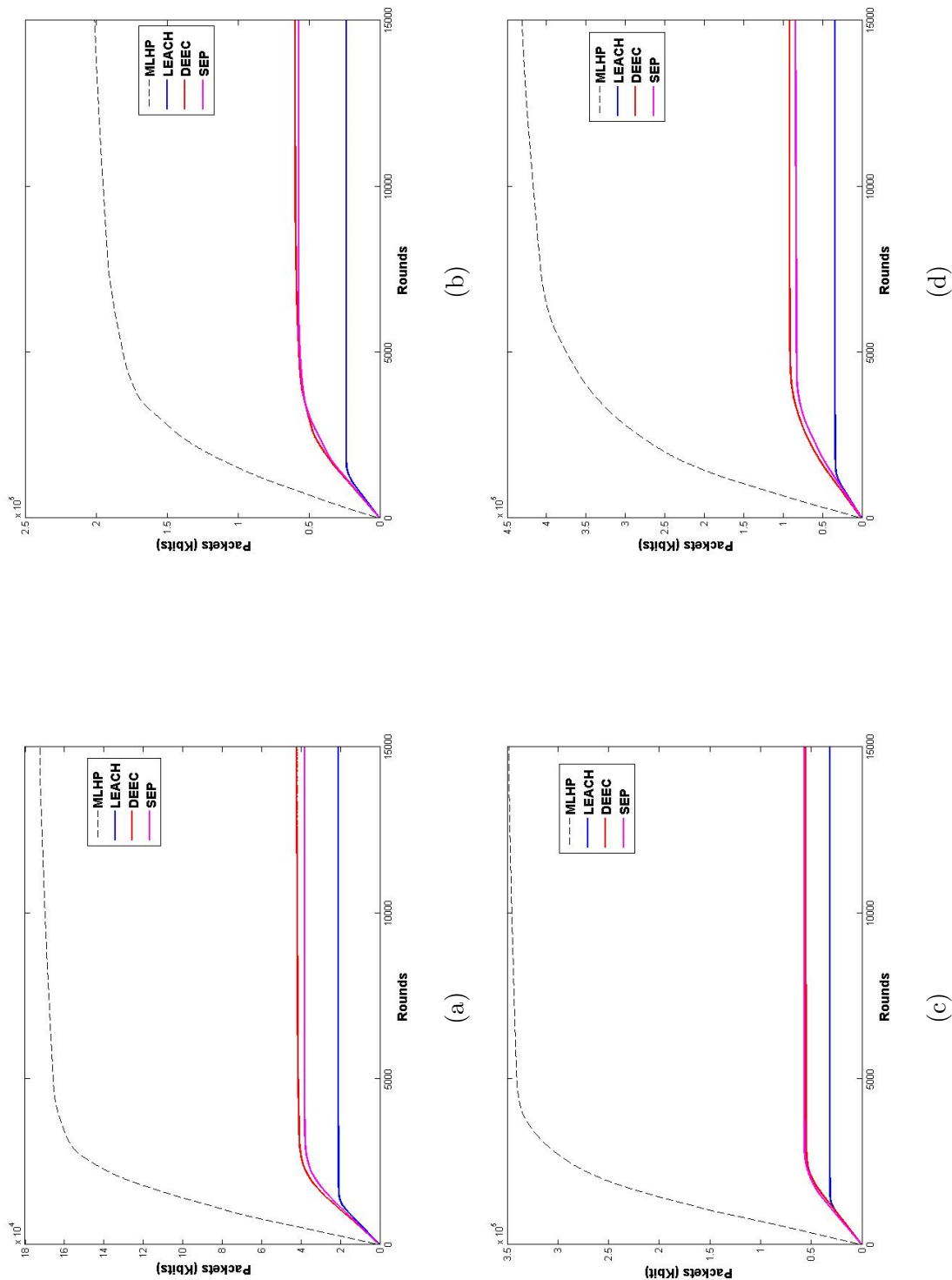


Fig. 4.18 The total number of packets sent to the BS for small-scale area with heterogeneity: (a) ($\alpha = 1$ and $\beta = 0.5$) for 100 nodes. (b) ($\alpha = 2$ and $\beta = 0.5$) for 100 nodes. (c) ($\alpha = 1$ and $\beta = 1$) for 200 nodes. (d) ($\alpha = 2$ and $\beta = 1$) for 200 nodes.

4.7.3 Heterogeneity over Large-Scaled Networks

In this section, the results obtained in order to find the affect on the performance of MLHP when increasing the heterogeneity parameters for an area of $200 \times 200 m^2$. The performance of MLHP is compared to LEACH, DEEC and SEP in terms of network life time, network residual energy and the number of packets delivered to the BS.

4.7.3.1 Network Life Time

Case1: When the network was deployed with 100 nodes with low heterogeneity parameters ($\alpha = 1$) and ($\beta = 0.5$).

For a larger area deployed with 100 nodes and low heterogeneity, MLHP performed better than LEACH during the nodes death time points. When MLHP compared to DEEC and SEP, the nodes started to die earlier until 40% death point. However, MLHP succeeded to have the longest operational time (HND) and longer network life time (LND). Compared to other protocols' LND, LEACH network stop functioning at the round 1259, DEEC at round 4496 and SEP at round 4240.

Fig. 4.19 shows the results for case1, the average communication rounds at which a certain nodes percentage die is represented by the x-axis. The percentage improvement of MLHP over all compared algorithms is presented in Table 4.14.

Table 4.14 Average life time percentage improvement over other protocols for large-scale network ($N = 100$, $\alpha = 1$, $\beta = 0.5$)

Percentage of dead nodes	Improvement over LEACH	Improvement over DEEC	Improvement over SEP
10%	35%	-22%	-17%
20%	23%	-22%	-25%
30%	37%	-16%	-24%
40%	67%	0%	-2%
50% (HND)	84%	3%	3%
100% (LND)	283%	7%	14%

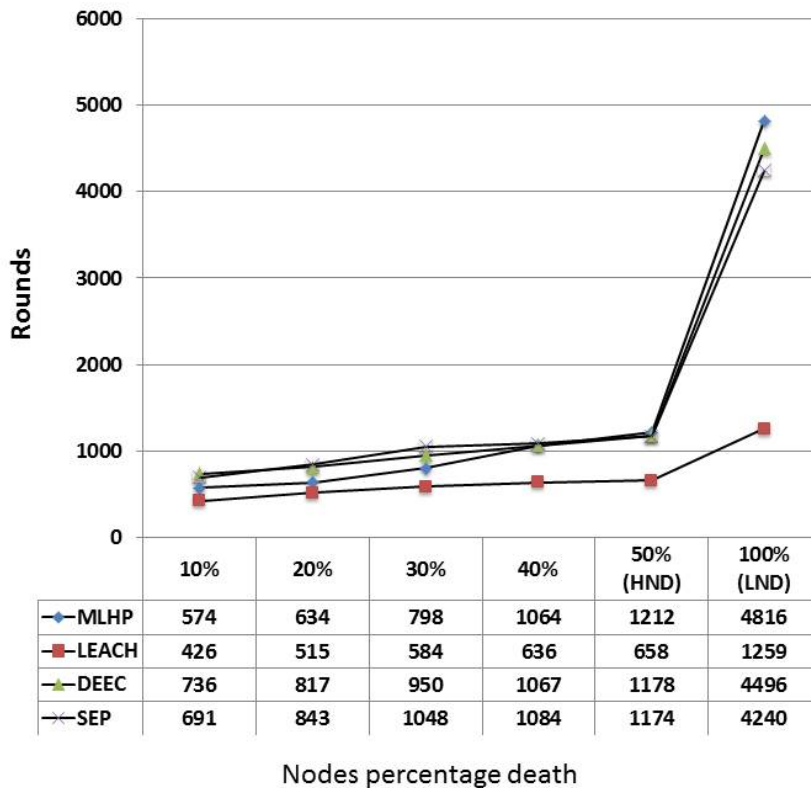


Fig. 4.19 Network lifetime for large-scale network, $N = 100$, $\alpha = 1$, $\beta = 0.5$.

Case2: When the network was deployed with 100 nodes with higher heterogeneity parameters ($\alpha = 2$) and ($\beta = 1$).

By increasing the heterogeneity factors to ($\alpha = 2$ and $\beta = 1$) for 100 nodes, MLHP performance is enhanced as shown in Fig. 4.20. The life time was extended to reach round 7277 (LND) which is the highest compared to other protocols. LEACH network LND at round 1370, DEEC LND at round 6798 and SEP life time ended at round 4907. Table 4.15 presents the average percentage improvement for MLHP compared to other protocols.

Comparing the performance of MLHP to case1 for the 10% death point, MLHP increased its performance by a percentage change of 5.4%. It also increased the network life time by 51.1%. This behaviour is expected since MLHP take the advantage of the network heterogeneity in selecting the CHs in the network which make it more effective for large-scaled networks with small nodes density.

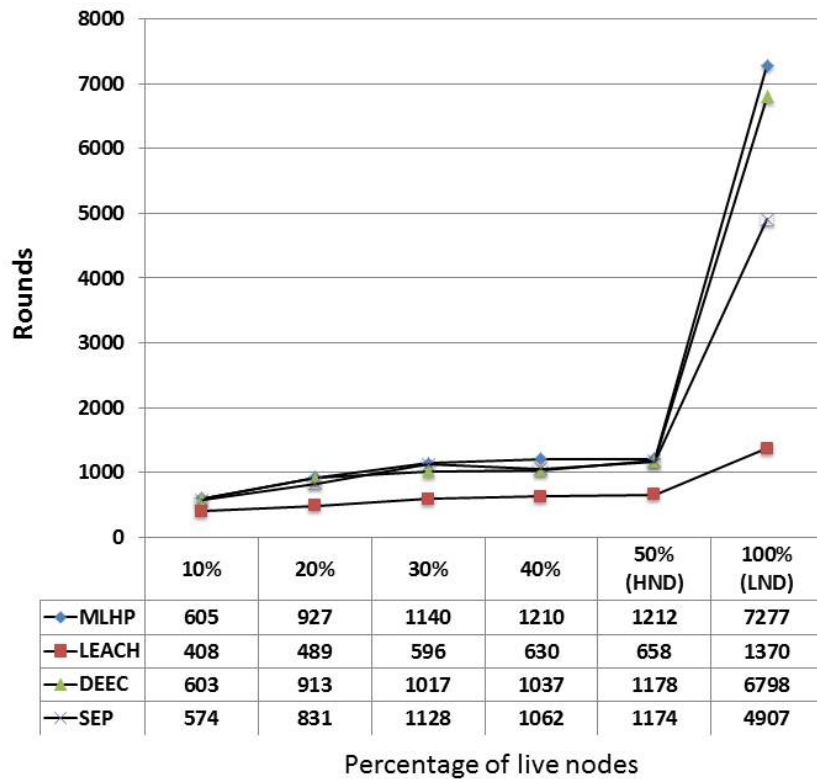


Fig. 4.20 Network lifetime for large-scale network, $N = 100$, $\alpha = 2$, $\beta = 1$.

Table 4.15 Average life time percentage improvement over other protocols for large-scale network ($N = 100$, $\alpha = 2$, $\beta = 1$)

Percentage of dead nodes	Improvement over LEACH	Improvement over DEEC	Improvement over SEP
10%	68%	-6%	20%
20%	155%	37%	80%
30%	230%	75%	128%
40%	303%	117%	167%
50% (HND)	364%	154%	183%
100% (LND)	366%	8%	95%

Case3: When increasing the number of nodes to 200 with low heterogeneity parameters ($\alpha = 1$) and ($\beta = 0.5$).

MLHP performs better when there are larger number of nodes deployed in the sensing field. which is the aim of designing this protocol, in order to offer the systems with tense nodes and operating on a large-scaled areas better choice. MLHP showed

an increase of 19.51% for network stability, 34.57% increase in terms of operational time and an over all network life time has a percentage increase of 3.32%. Fig. 4.21 illustrates the results obtained for comparing MLHP to the other protocols. MLHP has the maximum life time among all protocols. The percentage improvement of MLHP over the other protocols are presented in Table 4.16.

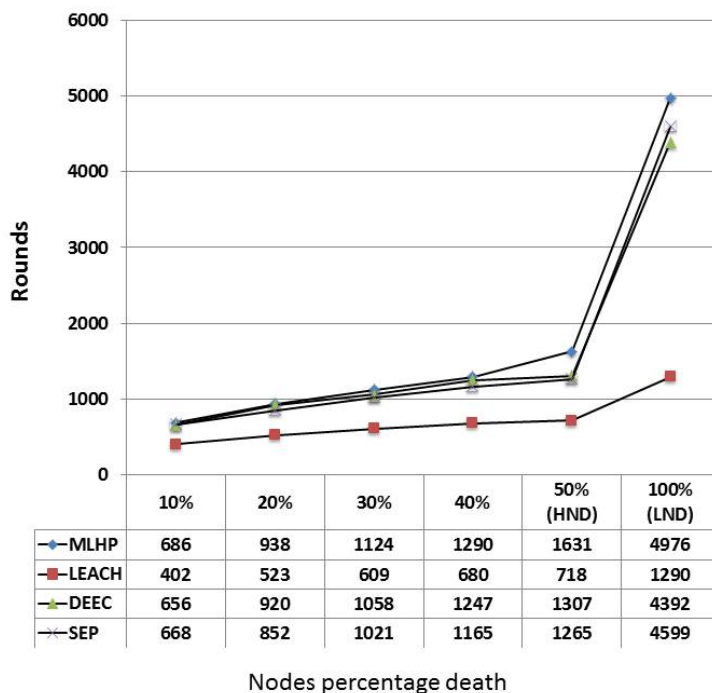


Fig. 4.21 Network lifetime for large-scale network, $N = 200$, $\alpha = 1$, $\beta = 0.5$.

Table 4.16 Average life time percentage improvement over other protocols for large-scale network ($N = 200$, $\alpha = 1$, $\beta = 0.5$)

Percentage of dead nodes	Improvement over LEACH	Improvement over DEEC	Improvement over SEP
10%	117%	7%	54%
20%	137%	17%	63%
30%	128%	13%	52%
40%	127%	13%	41%
50% (HND)	167%	38%	59%
100% (LND)	338%	46%	52%

Case4: When increasing the number of nodes to 200 with higher heterogeneity parameters ($\alpha = 2$) and ($\beta = 1$).

Increasing the number of nodes improved the performance of MLHP compared to that of 100 nodes by a percentage change of 10.25% for the 10% death point, an increase of 32.76% for the operational time and 14.03% percentage change increase for the network life time. Moreover, comparing MLHP to other protocols MLHP performed better than other protocols when the number of nodes increases in a large scaled network. as illustrated in Fig. 4.22. As evident from the results shown in the previous cases, The percentage improvement of MLHP over the other protocols are presented in Table 4.17.

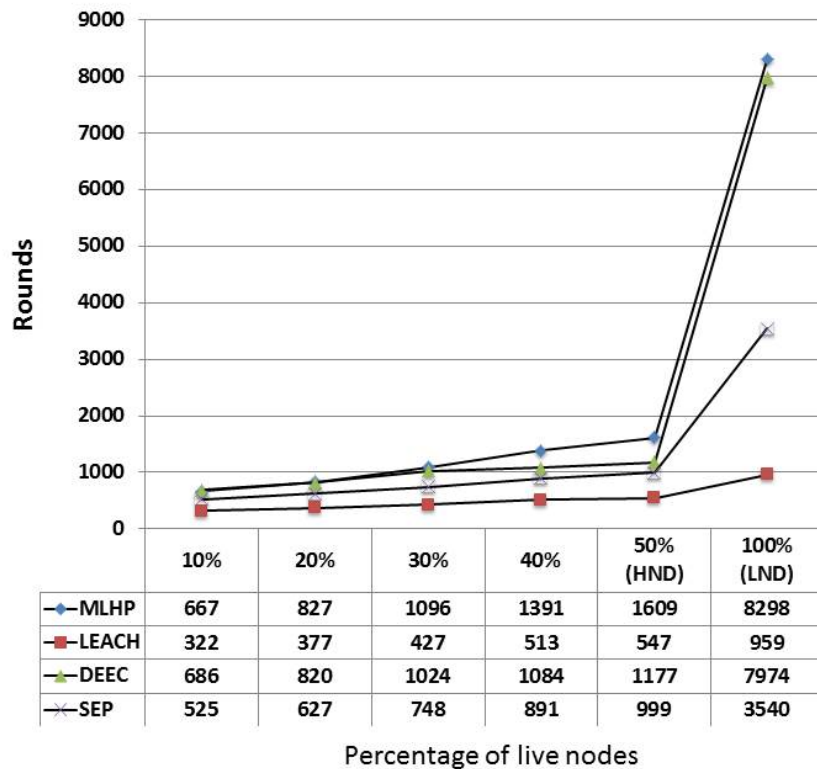


Fig. 4.22 Network lifetime for large-scale network, $N = 200$, $\alpha = 2$, $\beta = 1$.

Table 4.17 Average life time percentage improvement over other protocols for large-scale network ($N = 200$, $\alpha = 2$, $\beta = 1$)

Percentage of dead nodes	Improvement over LEACH	Improvement over DEEC	Improvement over SEP
10%	166%	16%	129%
20%	199%	30%	80%
30%	192%	34%	81%
40%	232%	52%	80%
50% (HND)	263%	72%	97%
100% (LND)	485%	1%	95%

4.7.3.2 Energy Consumption

Fig. 4.23 through Fig. 4.26 show the per-round energy consumption of the network with different node deployment with different heterogeneity factors. As can be seen from the figures, MLHP has a higher level of remaining energy in the network compared to LEACH, DEEC and SEP during the operational time after (HND) and through the end of life time (LND). However, for the stability time when the number of nodes is 100 with low heterogeneity, HRHP had less remaining energy compared to the other. This is because not all the nodes are active in MLHP to preserve the energy for the longer time. While when increasing the heterogeneity parameters or the number of nodes, MLHP preserved higher energy levels compared to the other protocols. Which prove that MLHP works better when the network has more variety of nodes or when the network has large node density.

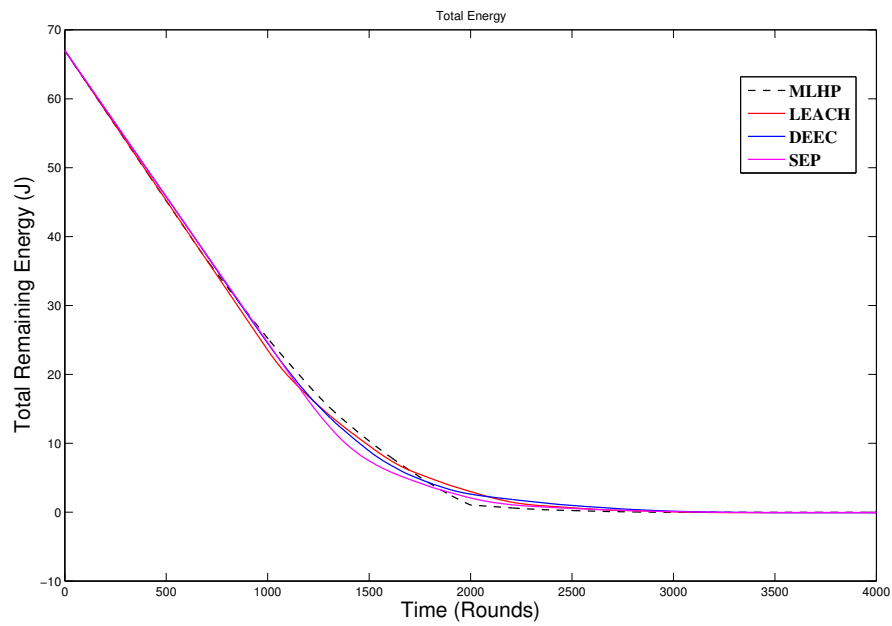


Fig. 4.23 Total residual energy, $N = 100$, $\alpha = 1$, $\beta = 0.5$.

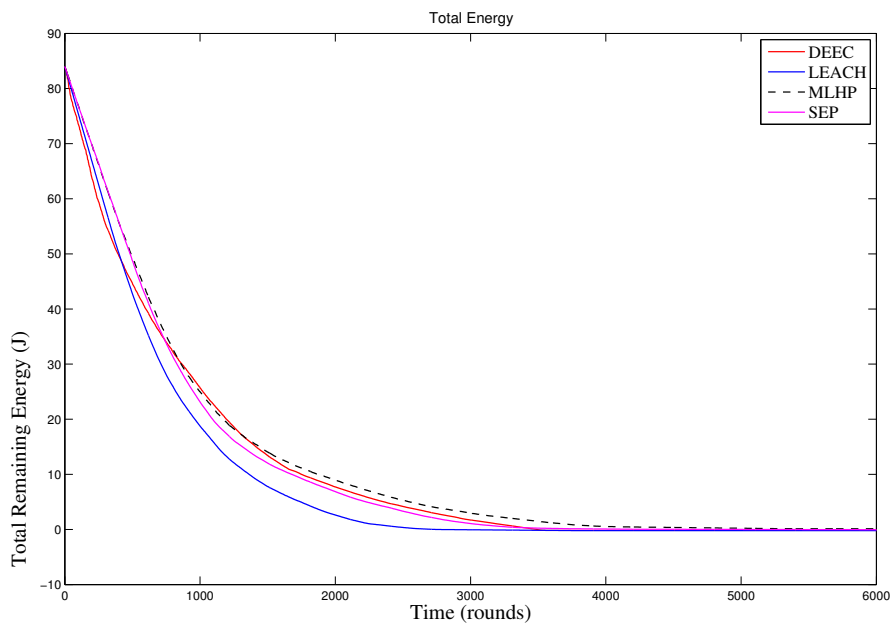


Fig. 4.24 Total residual energy, $N = 100$, $\alpha = 1$, $\beta = 2$.

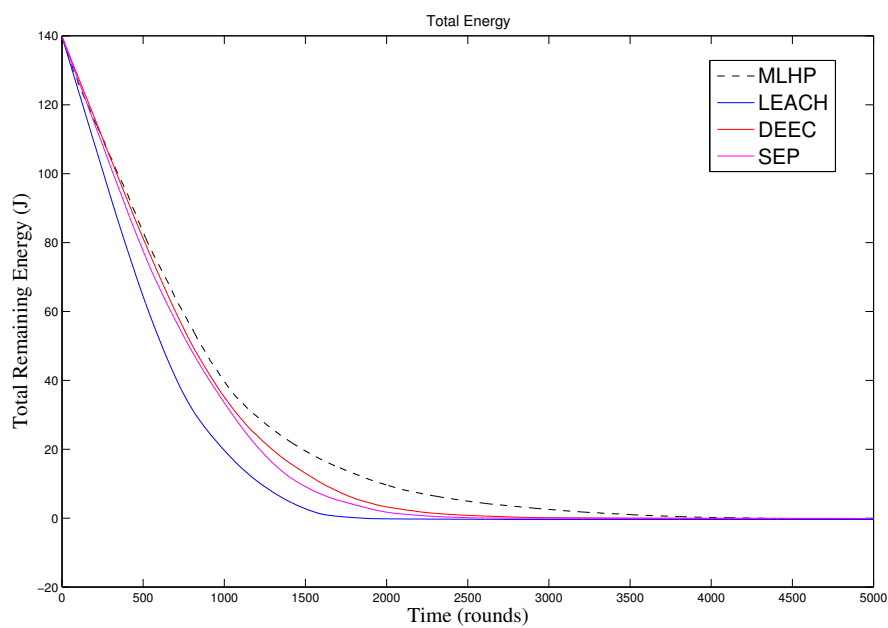


Fig. 4.25 Total residual energy, $N = 200$, $\alpha = 1$, $\beta = 0.5$.

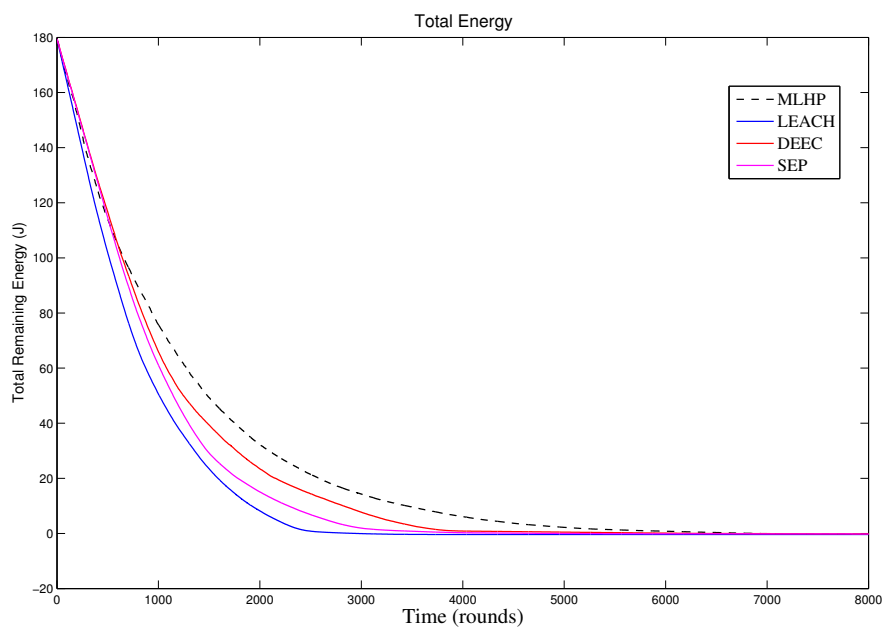


Fig. 4.26 Total residual energy, $N = 200$, $\alpha = 1$, $\beta = 2$.

4.7.3.3 Packet Delivery

Packet delivery ratio to BS is the last metric considered in the evaluation of the proposed MLHP. Fig. 4.27 shows the average accumulative ratio of data packets sent to the BS for the different cases. In all the different cases, MLHP has longer life time and thus longer time to detect and sent packets (data) to the BS therefore the ratio of packets sent by MLHP algorithm is greater than for the compared algorithms.

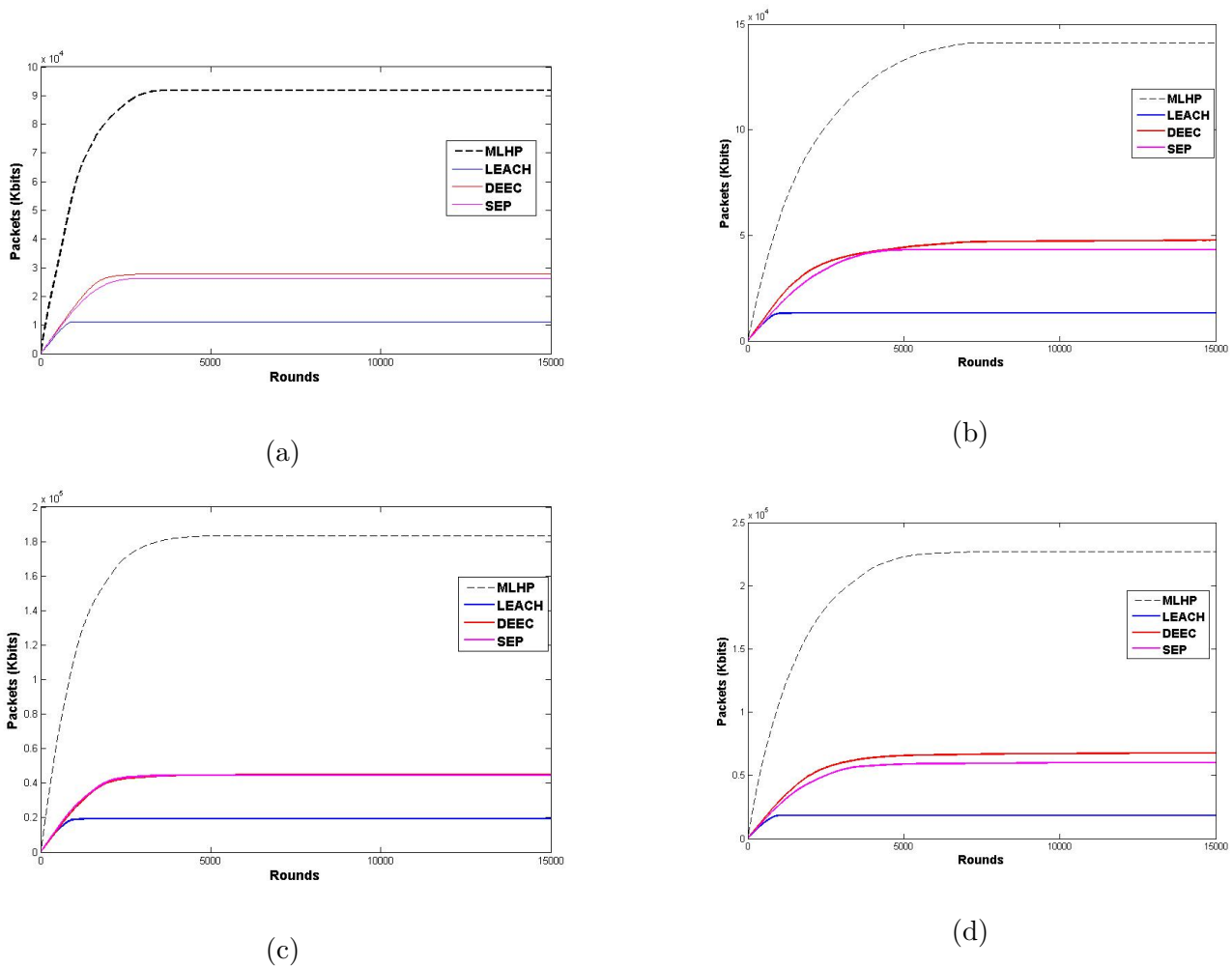


Fig. 4.27 The total number packets sent to the BS for large-scale area with heterogeneity: (a) ($\alpha = 1$ and $\beta = 0.5$) for 100 nodes. (b) ($\alpha = 2$ and $\beta = 1$) for 100 nodes. (c) ($\alpha = 1$ and $\beta = 0.5$) for 200 nodes. (d) ($\alpha = 2$ and $\beta = 1$) for 200 nodes.

4.8 Summary

In this chapter, a multi level algorithm (called MLHP) was presented for the use in heterogeneous wireless sensor networks. It combines the advantages of clustering in hierarchical and tree-based routing techniques with the metaheuristic technique, it takes the power of centralized as well distributed cluster-heads (CH) selection. The key idea in MLHP is to keep a low transmission distances between CH and the BS and among the cluster-members and their associated CH. The algorithm significantly extends the network lifetime, network stability beyond that achieved with existing protocols and kept energy consumption to the minimum.

The performance of the algorithm was tested in three different scenarios. The first scenario presented the stability of the network for two sizes networks deployed with different number of nodes with the minimal heterogeneity. The results showed that MLHP has the highest stability period for FND and HND for both small-scale and large-scale area networks with different node density, which means that MLHP has more balanced network by having the highest ratio of active nodes.

The two other scenarios showed the affect of changing the network heterogeneity in small-scale and large-scale networks respectively. The performance of MLHP was tested against other protocols in terms of network life time, energy consumption and packet delivery ratio. In all the different cases, MLHP has more surviving nodes over time than other protocols and hence longer life time. MLHP had more surviving nodes over time than other protocols and hence longer life time in all different cases. However, the best performance of MLHP in terms of network life time for small scale networks was when the network heterogeneity parameters are set to ($\alpha = 2$ and $\beta = 1$) with 100 nodes and when ($\alpha = 1$ and $\beta = 0.5$) with 200 nodes, this confirms that MLHP can operate in crucial cases with enough amount of heterogeneity for small number of nodes and with the minimal heterogeneity for larger number of nodes.

Finally, MLHP had higher levels of remaining energy in the network compared to LEACH, DEEC and SEP during the operational time after (HND) and through the end of life time (LND). However, for the stability time in the first few rounds, not all the nodes are active in MLHP to preserve the energy for the longer time, therefore it show less average energy than DEEC and SEP but always show more energy than LEACH.

Chapter 5

Adaptive Real-time Clouded Sensor Network-based Approach for Emergency Navigation (ARTC-WSN)

In this chapter, a real-time, autonomous emergency evacuation approach that integrates cloud computing with wireless sensor networks in order to improve evacuation accuracy and efficiency is proposed. The approach is designed to perform localized, autonomous navigation by calculating the best evacuation paths in a distributed manner using two types of sensor nodes. In addition to distributed path finding, sensor nodes identify the occurrences of a common evacuation problem that happens when evacuees are directed to safe, dead-end areas of a building. These areas are characterized as safe because they are far from the incident, but they are also far from the exit. Eventually, these areas become no longer safe, especially if the incident is intense. When such a situation is identified, our approach employs cloudification to efficiently and carefully handle this problem. The performance of the proposed localized WSN-based evacuation approach is also compared to its cloudified version in terms of number of survivors, evacuation time, and efficiency. We also compare the performance of our two approaches to one of the existing, widely used evacuation approaches that relies on a distance metric to find the shortest path to the closest exit. Simulation shows both proposed approaches have improved evacuation efficiency and accuracy.

The rest of this chapter is organized as follows: next, a brief introduction is presented, section 5.2 presents some of the existing related work in the literature. In section 5.3, the design of the proposed approaches has been presented. In section 5.4, the analysis and simulation results has been discussed. Finally, the summary of this chapter is presented in section 5.5.

5.1 Introduction

An emergency is a situation or condition that causes hazard to an environment, life, company, community, or property. Emergency management (EM) is vital for any organization today. It aims to create plans by which communities reduce their vulnerability to hazards and cope with disasters. It does not avert or eliminate the threats; instead, it focuses on creating plans to decrease the effect of disasters [126].

Emergencies can be caused by several intentional or unintentional natural or man-made acts. In most cases, emergencies are unpredictable in terms of occurrence, scope, impact, and intensity which significantly increases their impact on safety, property, economy, infrastructure, and environment. Therefore, emergency planning, preparedness, and evacuation are quite important for safeguarding national security and economy to control the hazard and to provide autonomous evacuation solutions during an emergency [127].

The practice of evacuating people threatened by a disaster has a very long history. Generally speaking, coping with a threat or an incident includes three strategies: (1) controlling the threatening event; (2) controlling human settlement patterns; and/or (3) development of forecasting techniques and warning systems that generate a protective response by those threatened. Table 1 shows the cross classification of evacuation based on two important dimensions: Timing and period, which generates a tentative classification format for distinguishing four kinds of evacuation: preventive, protective, rescue, and re-constructive. Nowadays, information and communication technologies (ICTs) play a significant role in each of these four phases. However, the rescue evacuations are considered the most critical type of evacuation, as they require the provision of powerful, real-time actions under risk and time constraints, sometimes with the least possible human interaction. Most of the automated emergency evacuation and navigation systems, including our approach, are targeted to act as rescue evacuation systems [126].

Table 5.1 A classification scheme of evacuation based on two dimensions: the timing and duration of evacuation.

Timing of Evacuation	Period of Evacuation	
	Short-Term	Long-Term
Pre-impact	Preventive	Rescue
Post-impact	Protective	Reconstructive

Emergency navigation (EN) concentrates on combining mathematical models or algorithms with the underlying sensing, communication, and distributed, real-time computation to guide evacuees to safety in a built environment [128]. Wireless sensor networks (WSNs) have been widely employed for environmental monitoring and control [129] [38]. Using WSNs, the deployed sensors collect and report results to a central repository [9]. WSNs have been recently integrated with other communication and intelligent technologies, such as cloud computing, smartphones, and robots, in order to implement systems with more powerful, advanced, and accurate solutions [130]. Such integration allows the efficient utilization of WSNs' advantages and overcomes almost all WSNs' limitations, including limited processing power, limited communication, and low accuracy for localized decisions.

The idea of integrating WSNs with cloud computing (CC) is quite promising [130]. A typical WSN consists of a large number of low-cost, low-power, multifunctional, and resource-constrained sensor nodes. Cloud services are a powerful, flexible, and cost-effective framework that provides real-time data to users with vast quality and coverage. A cloud typically consists of hardware, networks, services, storage, and interfaces that enable the delivery of computing as a service [131]. Clouds are designed with the flexibility to withstand harsh environmental conditions in some cases. Integrating CC with WSNs allows virtualization, which facilitates the shifting of data from WSNs to a cloud. Accordingly, it also allows cost-efficient applications and service provisioning in WSNs. Using the cloud, all WSNs' resources can be virtualized and provided as services to third parties depending on their demands. However, integration should be well designed and modeled in order to provide efficient, robust, and scalable infrastructure for several critical applications, including emergency management.

In an evacuation and emergency management context, the advantages of using WSNs include real-time oversight of complex first responses, advanced alerts, in-field data collection, communication, aggregation, collaborative processing and analysis, and configuration-dependent actuation. On the other hand, CC can provide complex/remote

data and situation analysis, on-demand centralized processing, and high-performance, wide-range communication. As a result, while WSNs can be implemented as part of a short-time first-response system for rescue evacuations, CC helps in making accurate, informed, and centralized decisions as a second-response system for rescue and reconstructive evacuations. CC also offers more advanced services to be provided in the service plane for local authorities and agencies [132–134]. The trade-off between centralized decisions made remotely by the cloud and localized, distributed decisions calculated by sensor nodes is important. Centralized decisions are generally expensive in terms of time and communication costs, but they could minimize damage and fatalities, especially when localized decisions lack in making proper evacuation decisions. This trade-off is affected by many factors, including timing, intensity (or perception) of the hazard, evacuees’ behavior, and environmental conditions, all of which are considered in tackling time-critical evacuation tasks.

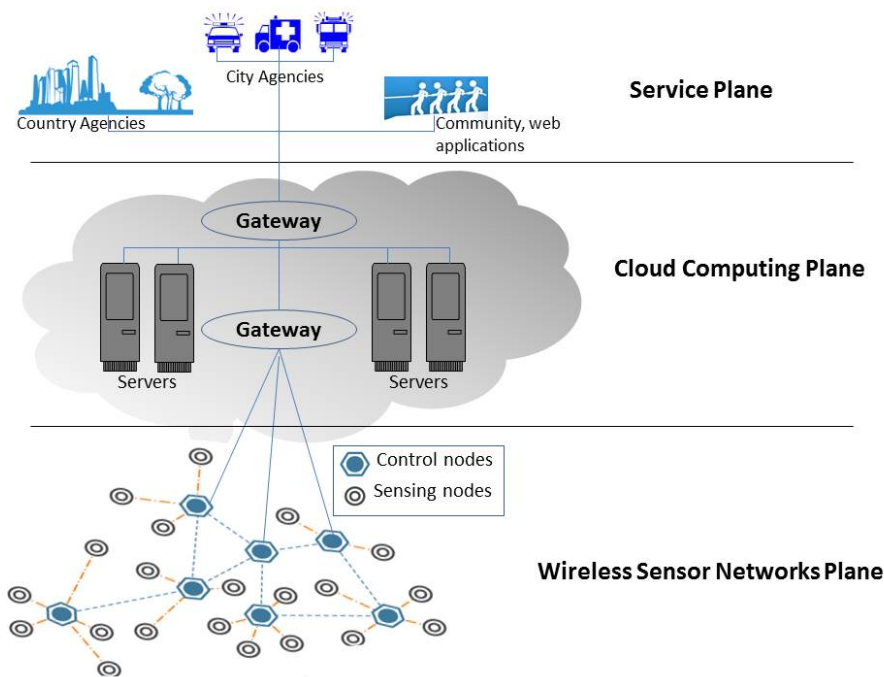


Fig. 5.1 A typical architecture of integrated WSNs and CC for emergency and evacuation management.

Fig. 5.1 shows a typical architecture for integrating WSNs with CC for emergency and evacuation management. The figure shows that WSNs act on the base plane, where low-cost sensing nodes are densely deployed in the targeted area. Sensing nodes collect and transmit data to control nodes. Control nodes are more capable than sensor

nodes, as they have higher computation and communication capabilities. However, they are usually deployed less intensely than sensor nodes to minimize the cost and communication overhead. Connection to the cloud gateway on the middle plane is done through control nodes to tackle complex computations or provide remote information. The cloud plane is connected to the upper service (or control) plane through another gateway.

5.2 Related Work

The investigation of emergency management and navigation was previously motivated by defense applications [135]. Emergency management has attracted many researchers in recent years as a result of increasing threats and unpredictable sources and types of hazards [136]. Accordingly, several approaches and models have been proposed in the literature to autonomously act during a hazard to improve evacuation efficiency. In this section, an overview of the existing emergency navigation algorithms used in emergency situations is provided.

Early emergency navigation systems were computer-aided information reporting systems to assist emergency managers in making decisions without decision-making capabilities due to their limited resources [128, 137]. Most of these emergency navigation algorithms were normally based on pure mathematical models that simplified evacuation processes. Evacuation was considered a minimum-cost network flow problem of converting a building graph into a time-expanded network. Evacuees could obtain optimal routes through solving the time-expanded network based on linear programming [128, 138].

Many approaches have been proposed to combine WSNs' advantages with the unlimited computing power of CC to improve navigational efficiency. For example, a cloud-enabled emergency navigation algorithm [139] was developed to achieve efficient evacuation. It considers changes in initial evacuation conditions over time including hazard source location, distribution of evacuees and occupancy rate. It performs faster-than-real-time simulation using the cloud. It mainly includes two layers: user and cloud layers. The user layer gathers on-site information while the cloud layer offers processing. During a hazard, evacuees take and upload photos to the cloud layer, using their mobile phones and a proper application that has previously installed. The cloud determines their locations and calculates evacuation paths using a WSN-Dijkstra-based

algorithm. The calculation of the best routes is also based on estimating the spread of the hazard, depending on the initial distribution of civilians, with the use of a fire model. Results showed that the developed system has an enhanced survival rate. However, this approach is unrealistic for evacuation for many reasons. First, it requires prior installation and configuration of an appropriate mobile application. It also relies on evacuees to react during the hazard. In addition, there is no on-site response system in this model.

A distributed CC-based evacuation approach for TinyOS in nesC [140] was proposed by designing and assessing two types of evacuees detection sensors. Evacuation data are displayed in a control room using control room software and then displayed using a building overlay and charts. Another approach for smart building evacuation was proposed in [141] using cognitive packet networks (CPNs) with time and distance metrics. This approach aims to evacuate people based on their health conditions. A simulation was conducted using 30 evacuees. The results showed that this approach outperformed the Dijkstra-based evacuation algorithm in terms of time and survival rate. Another approach for managing crowds in hazards using dynamic grouping was proposed in [128] which enhanced survival rates.

In [142], a WSN-based safe, ordered, and speedy (SOS) emergency navigation algorithm was presented to reduce the evacuation time and losses among evacuees. Using this approach, each evacuee is guided via sensor nodes located on the scheduled path. Simulation was performed to assess the SOS performance, results showed that SOS algorithm outperformed traditional approaches in terms of the evacuation time and network load.

In [143], an adaptive emergency protocol was proposed to navigate people in high-rise buildings based on dynamic computing. A study concerning the congestion level in the evacuation process was conducted in [144], it proposed a WSN-based indoor-congestion-aware algorithm. This algorithm decreases the direction oscillations resulting from the delay of the network communication and improves evacuation time compared to similar approaches. In [145], indoor-distributed, flow-based guiding approach was proposed to evacuate people to safe exits from dangerous zones using a WSN. In [145], indoor-distributed, flow-based guiding approach was proposed to evacuate people to safe exits from dangerous zones using a WSN. In [146], an efficient approach based on WSN was proposed to assist with monitoring a targeted region, controlling the crowd, and supporting the evacuation process from the overcrowded area.

This chapter proposes a real-time autonomous emergency evacuation approach that integrates cloud computing to wireless sensor networks in order to improve evacuation accuracy and efficiency. The approach is designed to perform a localized autonomous navigation by calculating the best evacuation paths in distributed manner using two types of sensor nodes. In addition to distributed path finding, sensor nodes identify the occurrences of a common evacuation problem which happens when evacuees are directed to safe dead-end areas of the building. These areas are characterized to be safe since they are far from the incident but they are also far from the exit. Eventually, these areas are no longer safe especially if the incident is intense. When such situation is identified, the proposed approach employs cloudification to efficiently and carefully handle this problem. This chapter also studies and compares the performance of the proposed localized WSN-based evacuation approach to its cloudified version in term of number of survivals, evacuation time and efficiency. It also compares the performance of the proposed two approaches to one of the existing widely-used evacuation approach, which relays on a distance metric in finding the shortest path towards the closest exit. Simulation shows both proposed approaches have an improved evacuation efficiency and accuracy.

The rest of this chapter is organized as follows: next section presents the design of the proposed approaches. Section 5.4 analysis and discuss simulation results. Finally, the summary of this chapter is presented in section 5.5.

5.3 Proposed Approach

In this section, the discussion of the conceptual model and the design of the proposed solution, called adaptive real-time clouded wireless sensor network-based (*ARTC – WSN*) emergency navigation approach, is presented. First the evacuation area model is discussed. Then, the conceptual model is illustrated representing the overall behaviour of the approach and discuss the design considerations, and approach design in details.

5.3.1 Modeling the Area of Evacuation

To model the underlying evacuation, a similar model to the described building model in [128] is used. A typical floor building model to the proposed approach includes two

types of wireless nodes to sense and process the information needed to provide safe paths to the evacuees:

- **Sensor Nodes (SNs):** are used to sense the presence of the hazard (e.g. fire, gas) and to detect the presence of the evacuees in their vicinity. In other word, these nodes present a combination of hazard and motion sensors. SNs communicate with their neighboring decision nodes in order to transmit the sensed data.
- **Control or Decision Nodes (DNs):** act as routers that execute the ARTC-WSN approach in order to calculate the best evacuation path to guide the evacuees in the nearby area. DNs are also able to communicate with the cloud in specific conditions, especially in the case of safe, dead-end areas; high personal risks; or detected fatalities. An assumption is made that DNs are connected to installed path signs (i.e., LCDs) in order to show the calculated evacuation directions to the evacuees.

Fig. 5.2 shows an exemplary model for the underlying area, which corresponds to the bottom-most plane in Fig. 5.1. The evacuation area has been divided into zones covered by SNs and DNs. SNs and DNs were deployed with alignment distances $(Step_x, Step_y)$ and $(Step_{dx}, Step_{dy})$, respectively. Each zone has been covered by four DNs and at least four SNs to provide full sensing coverage for the building. Two exits were suggested, one at the top right corner and the other at the bottom left corner of the building.

5.3.2 ARTC-WSN Conceptual Model

The conceptual model of the overall behavior of ARTC-WSN is presented in Fig. 5.3. ARTC-WSN emergency evacuation approach is triggered when a hazard is detected. Sensor nodes periodically collect and report data on hazards source, intensity and evacuees movements to the DNs. Decision nodes gather and combine data received from the nearby sensor nodes to the information provided by cloud. Then, DNs employ ARTC-WSN approach to locally find evacuation paths.

The calculation of evacuation paths at DNs is done in distributed manner through the following steps:

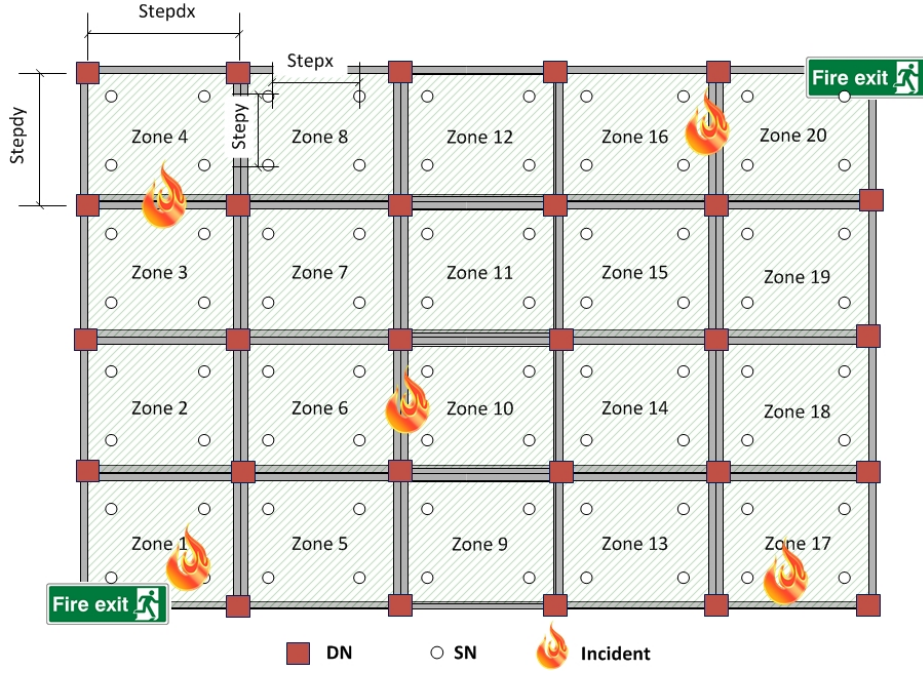


Fig. 5.2 Graph representation of the building.

Step 1: At time t , each DN (d_i) evaluates the nearby paths by calculating its safety metric, $S_{(i,t)}$, as follows:

$$WayOutIndicator(d_i) = distance(d_i, EX) \times ExitFactor \quad (5.1)$$

$$RiskIndicator(d_i) = distance(d_i, Incident) \times RiskFactor \times Intensity \quad (5.2)$$

$$S_{(i,t)} = \frac{RiskIndicator(i)}{WayOutIndicator(i)} \quad (5.3)$$

Where, $ExitFactor$ is a scalar number between (1-2) calculated as $(1+(1/numberofexits))$. $distance(d_i, EX)$ represents the distance between the DN (d_i) and its nearest exit (EX), $distance(d_i, Incident)$ represents the distance between the DN (d_i) and the incident, and intensity corresponds to the spreading out of the incident overtime between any point of time t and $(t - 1)$.

Step 2: Each DN (d_i) exchanges with its neighboring DNs its safety metric ($S_{(i,t)}$).

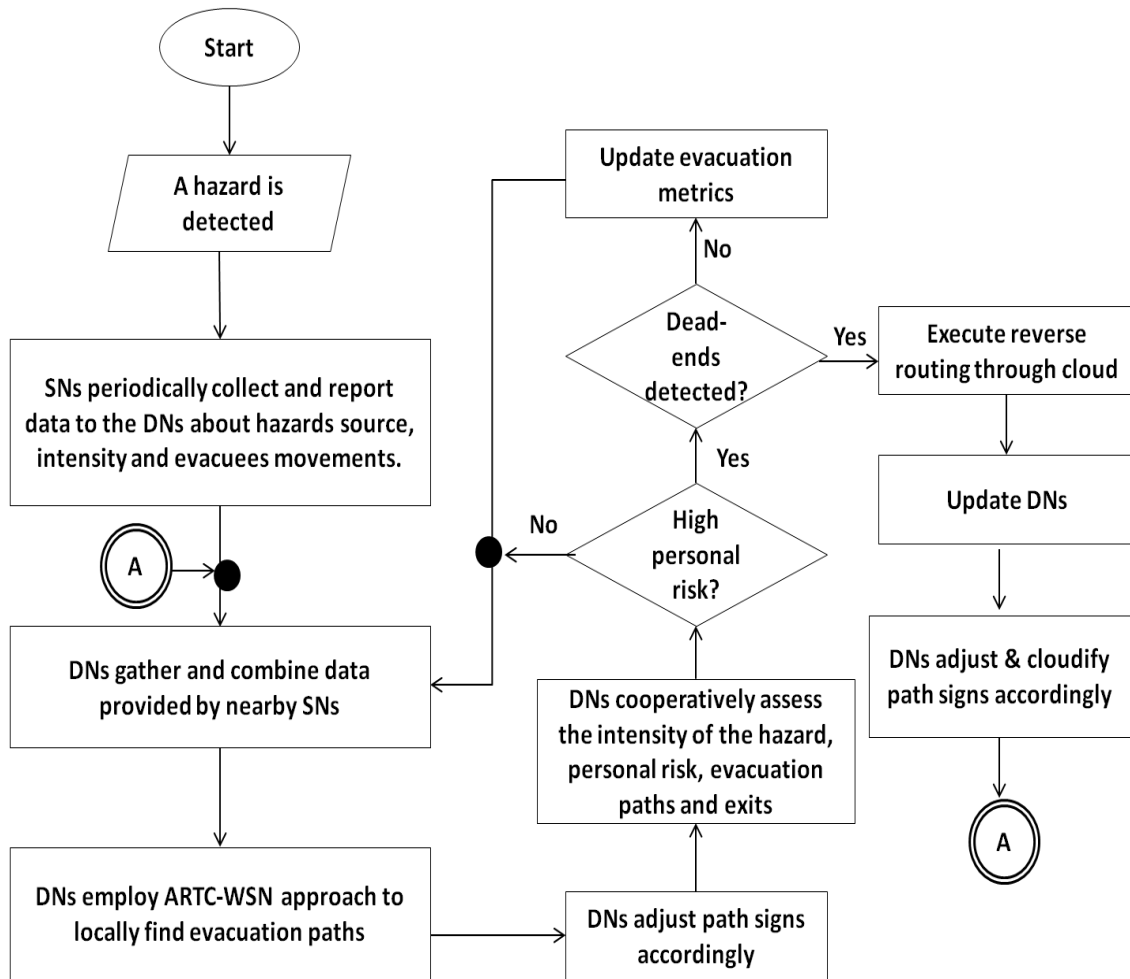


Fig. 5.3 The conceptual model of ARTC-WSN.

Step 3: Each DN (d_i) finds its best neighboring DN (j) among its neighbors by comparing its safety metric S_i with the safety metric ($S_{(j,t)}$) of all neighboring DNs (j). The best neighboring DN of any node is the one (including the node itself) that has the highest safety metric.

Step 4: At time t , each DN d_i adjusts its controllable path signs to point at leading to the best DN (j).

Step 5: Each DN (d_i) cooperatively assesses the intensity of the hazard, personal risk, evacuation paths and exists with its neighbor.

Step 6: If high personal risk is detected, the incident is closer or reached a nearby area where an evacuee exists, DN (d_i) communicates to the cloud in order to request help and update evacuation matrices.

Step 7: If high dead-end area is detected, DN (d_i) communicates to the cloud in order to perform reverse routing.

5.3.3 Cloudification Phase

In the ARTC-WSN model, all decision nodes periodically report important information to the cloud about the hazard and progress of evacuation. When high personal risk is detected, either by the cloud or locally by a decision node, the cloud acts either to rescue people in that area or to adjust evacuation metrics at specific decision nodes. The cloud also plays another important role in evacuating people at safe dead-end areas detected by any decision node d_i . *Safe dead-end conditions occur when evacuees can't be moved from their current location toward the exit because all other nearby areas are considered by the surrounding decision nodes to be more dangerous than their current location.* These safe dead-end areas are safe at that moment, say at time t ; however, the evacuees are, in fact, considered endangered because they have not been evacuated or reached the exit yet. Because DNs are performing in a distributed localized manner without human interaction, they cannot optimally solve this problem, which sometimes requires a global view of the whole evacuation area and communication with some authorities. In this situation, the *cloud server* executes the reverse routing phase of our approach (ARTC-RR), which attempts to find a route from the safest exit to the dead-end point, where evacuees are located, in order to find the best (shortest and safest) evacuation path for people in such areas. ARTC-RR path finding is a fast, greedy algorithm that executes the following steps:

Step 1: When a dead-end point is detected by decision a node d_i , it communicates to the cloud to request help in updating evacuation matrices and executing reverse routing.

Step 2: The cloud locates the nearest exit to the dead-end with highest safety metric as a starting pint of the reverse routing.

Step 3: Given the safety metric S_j and location of all decision nodes j , the cloud adds the decision node that is closer to the located dead-end area and has the highest safety among the other alternatives as a next hop.

Step 4: ARTC-RR keeps adding the safest next hop towards the dead-end.

Step 5: It terminates when the dead-end area is reached.

Accordingly, all DNs along this path adjust the path signs based on the calculated reverse path.

An important characteristic provided by ARTC-RR is that the evacuation matrices and calculated paths provided by the cloud can't be overwritten locally by DNs. This characteristic avoids recreating dead-end areas and leading evacuees to these areas. When changes are needed locally, DNs communicate with the cloud to get updates, if any. This grants avoiding any possible conflict between distributed decisions calculated cooperatively by DNs and global decisions that are calculated remotely by the cloud. Another interesting characteristic of this approach is that it only performs cloudification on demand when high personal risk and dead-end points are detected which eliminates the communication cost and delay encountered by centralization in normal situations.

5.4 Simulation Setup and Results

In order to study and analyze the performance of the proposed approaches, we implemented an event-driven simulator using MATLAB. This section presents the design and implementation of our simulation experiment. It discusses the different simulation scenarios, parameters and performance factors. It also shows and analyses the most significant performance results in terms of survival percentage, evacuation time and number of fatalities.

5.4.1 Simulation Design and Setup

In order to evaluate the performance of the proposed approaches in terms of adaptivity and real-time decision making quality, different simulation scenarios were considered and proposed. We considered a number of simulation variables in a way that mimic real life problems including: the location and the intensity rate of the hazard, the number of evacuees and the evacuation area. The presented results in this paper represent an average of 30 simulation runs with different levels of randomness. The considered simulation variables and their considered values are outlined next to give different simulation scenarios:

Hazard location, has a substantial impact on the performance of emergency navigation algorithms. A well-designed evacuation approach is one that predicts the path safety with respect to hazard location. When a hazard breaks out at a strategic location, such as an exit, it may result in poor evacuation performance if the employed autonomous approach doesn't consider or adapt to the hazard location. In order to critically evaluate the adaptability and autonomy of the proposed approach, a random hazard position was generated in each simulation run.

Hazard intensity, is very important for any evacuation approach in order to distinguish between different forms and intensities of hazards. In most cases, the incident itself and its side effects may spread at different rates and via different paths with complex correlations. For example, if a fire is the source of the hazard, the intensity is maximized because civilians are affected by two forms of danger: flames and smoke. In this simulation, four different intensity values were considered to represent the intensity of incident changes—3, 5, 7, and 9—in order to assess the behavior of the proposed approaches under different minor and major impact hazards. The intensity value 9 represents the highest. It means the hazard expands 9 units of area, i.e. meters, in each unit of time, i.e. seconds, in all directions.

The number of evacuees allows comparing the performance of different approaches under different evacuees' densities. We changed number of the evacuees in some scenarios. We considered 100, 300 and 500 evacuees. However, as certain metrics should be unified for each run in order to obtain accurate results, number of evacuees was fixed and given in each scenario in order to measure the impact of other factors. In most of the presented results, number of evacuees is 300 evacuees unless a different number is stated.

Evacuation area, the performance of the proposed approach was studied in small, moderate, and large evacuation areas. More specifically, the performance was evaluated for small evacuation area of size $(100 \times 100m^2)$, moderate area of size $(300 \times 300m^2)$, and large area of size $300 \times 300m$.

For exits availability, as illustrated in previous section, the proposed area modeling was assumed to mimic the model in [128] which has two exits. In addition, another model was examined in experiment 3 to analyze the behavior of the proposed algorithm in sever situations where only one exit is found.

The performance of the proposed approaches is compared to Dijkstra’s shortest path (DSP) algorithm with time and distance metrics [139]. All the reported simulation results are an average from 30 runs and described in terms of the following performance metrics:

- (a) **The overall survival rate (or *Percentage of survivals*):** This is the percentage of people in the evacuation area who were successfully evacuated and were still alive at the end of simulation compared to the total number of evacuees.
- (b) **Evacuation time,** which is the time taken to evacuate the entire civilian population from the hazardous area and locate them in safe zones where help could be provided. In this study, the evacuation time is calculated as the number of jumps needed until the evacuees reach the exit. Which is represented by the number of DNs passed in the rout.
- (c) **Civilian casualties or fatalities (*Number of dead Civilians*):** For accuracy purposes, two types of casualties are defined: initial casualties which represent evacuees who are located at the hazard in time 0. Actual or approach-resulted casualties which represent evacuees who lay within the hazard radius while spreading. In this study, we are more concerned about the actual approach casualties, which correspond to casualties caused by the evacuation approach, not those initially resulting from the hazard at the moment it occurred. The number of dead is calculated as the difference between the initial casualties and the total number of casualties at the end of the simulation.

In the below subsections, the performance of the three approaches is compared for randomly deployed evacuees and incidents in small-, moderate-, and large-scale evacuation areas with different hazard intensities.

5.4.2 Results: Evacuation Area and Hazard Intensity

This section reports the results obtained from comparing the proposed protocols to Dijkstra protocol. The results obtained from a total of 300 evacuees, over three different evacuation areas ($100 \times 100 \text{ m}^2$, $200 \times 200 \text{ m}^2$ and $300 \times 300 \text{ m}^2$) and with four hazard intensities (3, 5, 7 and 9).

DSP focuses on selecting the fastest paths to exits without considering hazards near these paths. For a given evacuation area, DSP shows a fixed evacuation time regardless of the intensity hazard. This is due to the DSP's main aim of preserving a short evacuation time without considering path safety. In contrast, the proposed algorithms give the path safety the highest priority. Both approaches direct evacuees to the safest exit through the path that has maximum safety.

As shown in Fig. 5.4, DSP always records the same and the shortest evacuation time for all hazard intensities, which reflects back on the safety of the evacuees. In contrast, the proposed algorithms show a variation in the evacuation time when the intensity of the hazards is changed. However, ARTC-RR requires longer time under higher-intensity hazards. Therefore, it has a longer evacuation time than ARTC-WSN approach for a hazard intensity 9. This variation is a result of communication and computation delays caused by remotely executing ARTC-RR in the cloud in order to evacuate civilians who are located in safe dead-end areas. Although DSP has the shortest evacuation time, it's survival percentage is the lowest for all hazard intensities compared to ARTC-RR and ARTC-WSN, as can be seen from Table 5.2.

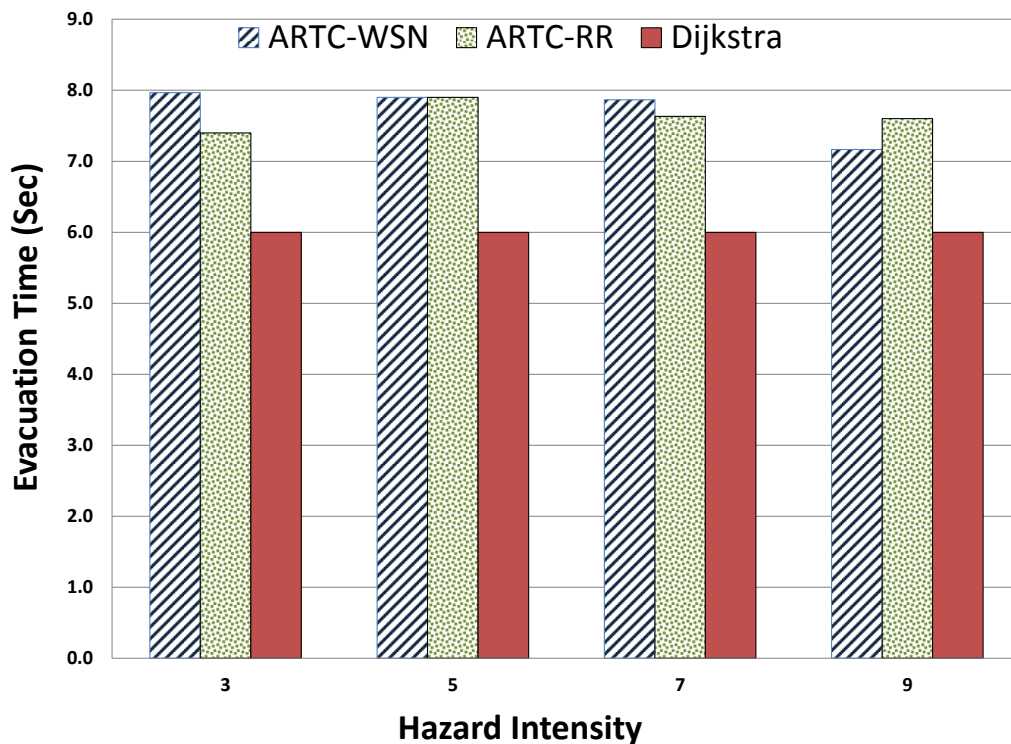
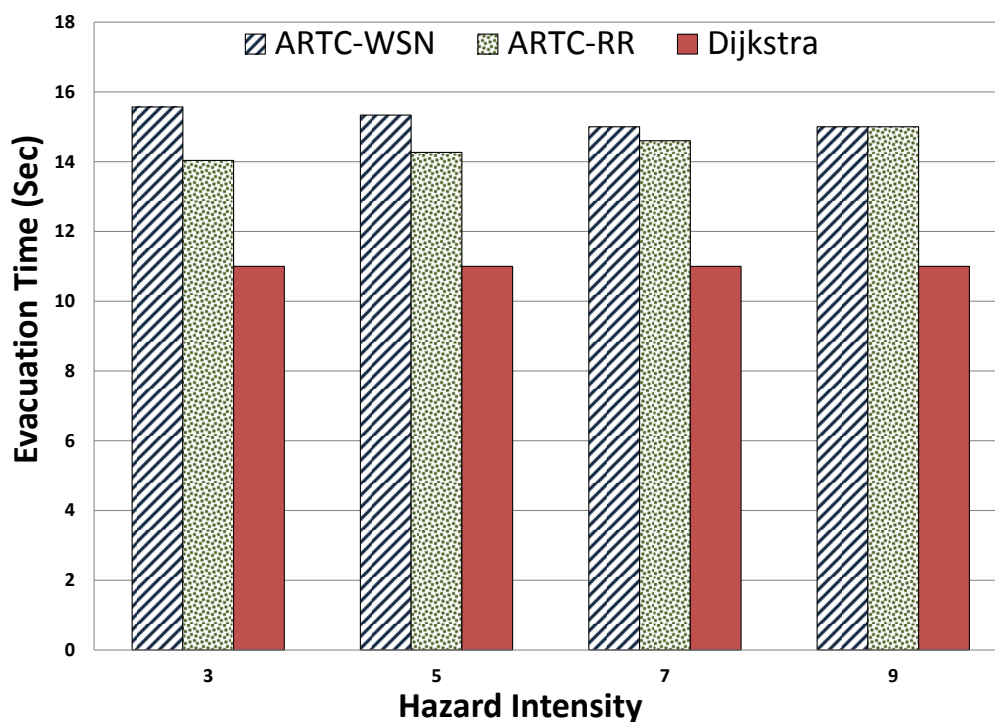


Fig. 5.4 Comparison of the average evacuation time for evacuation area of $100 \times 100 m^2$.

Table 5.2 The percentage of survivals for area of evacuation $100 \times 100 m^2$.

Hazard Intensity	Evacuation Approach		
	ARTC-WSN	ARTC-RR	Dijkstra
3	97%	98%	93%
5	96%	96%	85%
7	95%	96%	83%
9	96%	93%	87%

When the evacuation area increases to $200 \times 200 m^2$, ARTC-RR shows a better performance compared to its performance when the area was $100 \times 100 m^2$. This is expected because the evacuees are scattered on a larger area, this will reduce the possibility of safe dead end occurrence. Fig. 5.5 shows a comparison of the evacuation time between the protocols. It is apparent from the figure that DSP also has a fixed shortest evacuation time for all hazard intensities, which reflects on its percentage of survival illustrated in Table 5.3. DSP has the lowest survival percentage compared to the proposed algorithms.

Fig. 5.5 Comparison of the average evacuation time for evacuation area of $200 \times 200 m^2$.

Closer inspection to the table shows that both proposed algorithms has almost evacuate all the civilians, except the initial casualties or evacuees who were already located at the incident location. This confirms that, when there is no need to communicate to the cloud due a safe dead zone situation, both protocols will have the same well performance.

Table 5.3 The percentage of survivals for area of evacuation $200 \times 200 m^2$.

Hazard Intensity	Evacuation Approach		
	ARTC-WSN	ARTC-RR	Dijkstra
3	99%	99%	96%
5	99%	99%	96%
7	99%	99%	92%
9	98%	99%	89%

For an evacuation area of $300 \times 300 m^2$, the obtained results are provided in Fig. 5.6 for the evacuation time. ARTC-WSN and ARTC-RR adapt to the changes in the route as well as the environment, they can dynamically redirect evacuees along paths away from the hazard. When the intensity is low to moderate. ARTC-RR succeeded at having a 100% survival percentage and the ARTC-WSN achieved a 99% survival percentage (Table 5.4). However, at a high intensity within small areas, ARTC-WSN performed better than ARTC-RR in terms of evacuation time. This performance degradation was the result of the communication delay caused by cloud communication in addition to the computation overhead encountered in making centralized decisions in the cloud, which complicated evacuating civilians in dead-end areas when the hazard intensity was extremely high. Nevertheless, both proposed algorithms outperformed Dijkstra's approach in terms of survival percentage.

Table 5.4 The percentage of survivals for area of evacuation $300 \times 300 m^2$.

Hazard Intensity	Evacuation Approach		
	ARTC-WSN	ARTC-RR	Dijkstra
3	99%	100%	97%
5	99%	100%	95%
7	98%	94%	89%
9	98%	92%	87%

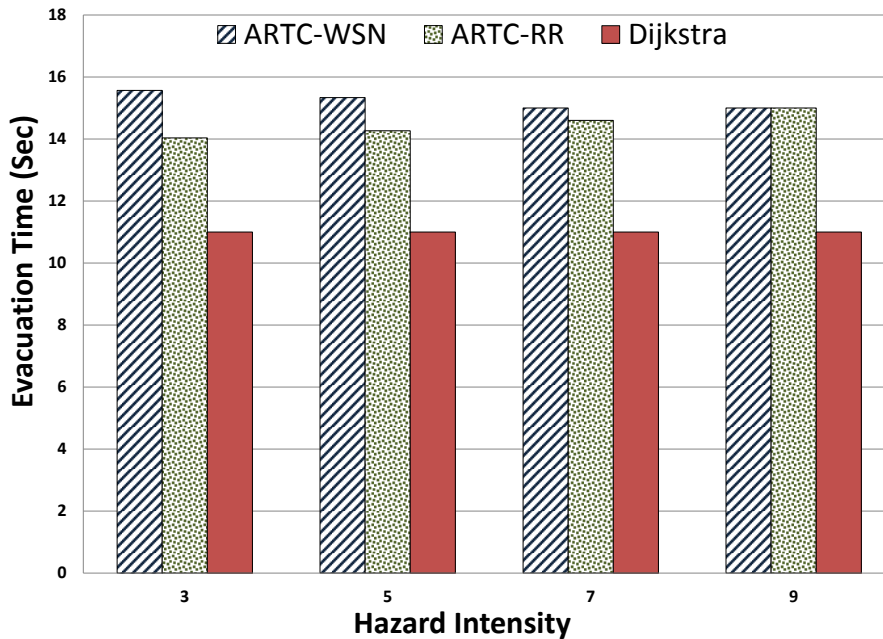


Fig. 5.6 Comparison of the average evacuation time for evacuation area of $300 \times 300 m^2$

Number of Fatalities: Another important performance factor to consider in evaluating the performance of any evacuation approach. Fig. 5.7, 5.8 and 5.9 respectively, show the average number of fatalities for small-scale, moderate-scale, and large-scale evacuation areas for different hazard intensities. As shown in the figures, both of our proposed approaches maintained the lowest death rate compared to DSP. This behavior indicates that the performance of the proposed approaches is stable in different evacuation areas. The results also show that when the hazard intensity was high and the area was large, DSP had the highest death rate compared to ARTC-WSN and ARTC-RR.

The results confirm that ARTC-WSN and ARTC-RR outperformed DSP by 75% and 91%, respectively, under low-intensity hazards. For high-intensity hazards, the ARTC-WSN and the ARTC-RR also outperformed the DSP by 85% and 39%, respectively, in different evacuation areas. This significant performance improvement proves that the ARTC-WSN and the ARTC-RR provide a good trade-off between the safety of the evacuees and the speed of the evacuation.

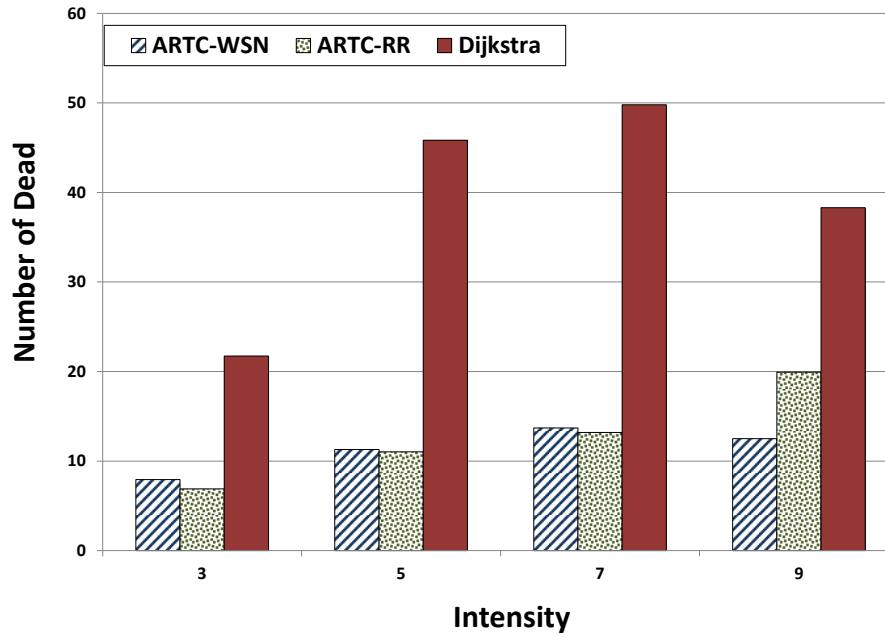


Fig. 5.7 Comparisons of total death ratio for small-scale evacuation areas.

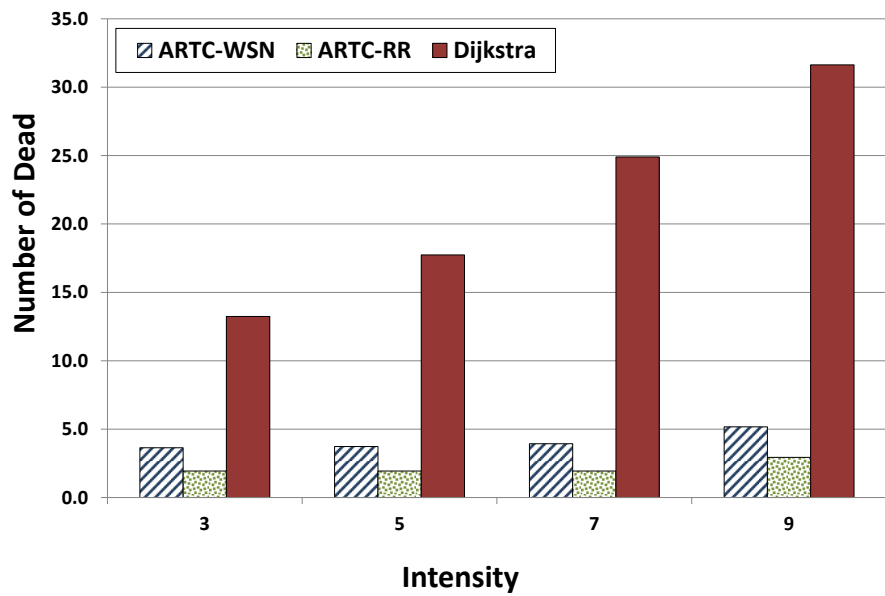


Fig. 5.8 Comparison of total death ratio for moderate-scale evacuation areas.

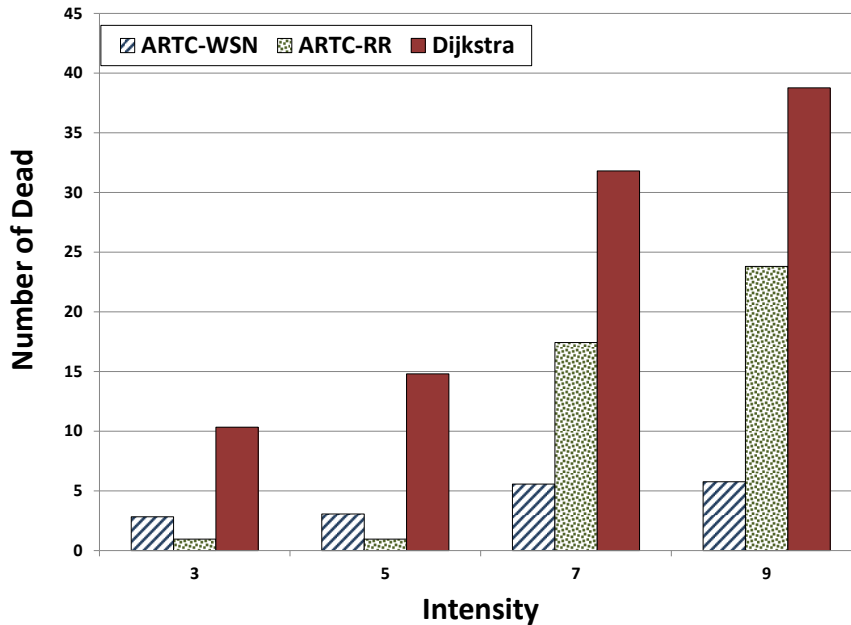


Fig. 5.9 Comparisons of total death ratio for large-scale evacuation area. simulation runs for 300 evacuees.

5.4.3 Results: The Number of Evacuees

The behaviour of the three approaches was tested for evacuee densities ranging between 100, 300, and 500 evacuees for a randomly located and low intensity hazard. The results show that ARTC-RR had the highest performance in terms of saving the largest number of evacuees, as seen in Table 5.5. However, with the large number of evacuees, a longer time was required to navigate all evacuees to the exit, as shown in Fig.5.10 when the population increased. The ARTC-WSN also had a high survival rate, reaching 97%, and an acceptable evacuation time compared to the DSP, which had the lowest survival rate and the highest death rate. Fig. 5.11 illustrates the death rate of the three approaches in Experiment

Table 5.5 The average percentage of survivals when number of evacuees ranges between 100 and 500.

Number of Evacuees	ARTC-WSN	ARTC-RR	Dijkstra
100	96%	97%	91%
300	97%	98%	93%
500	97%	97%	94%

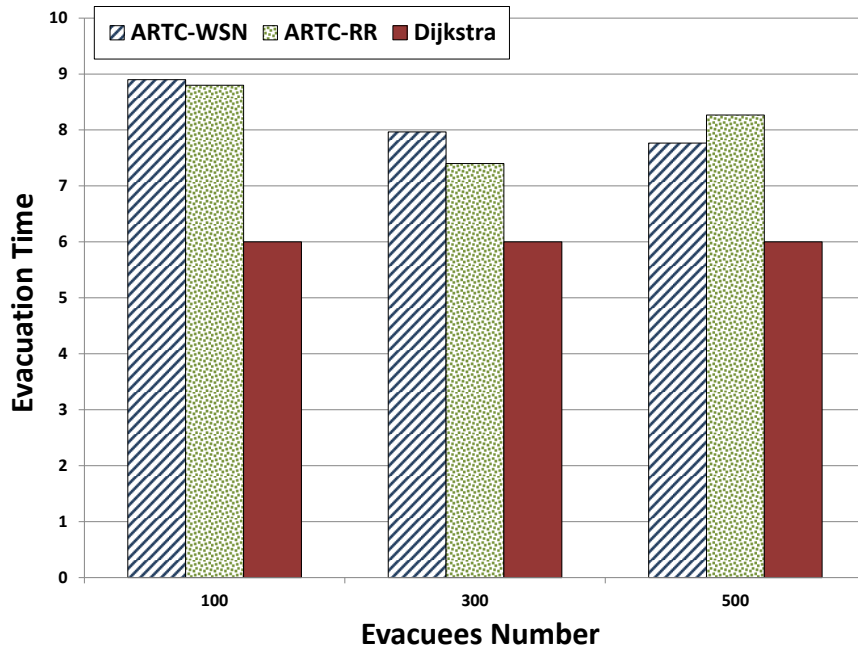


Fig. 5.10 Comparison of the evacuation time when number of evacuees ranges between 100 and 500.

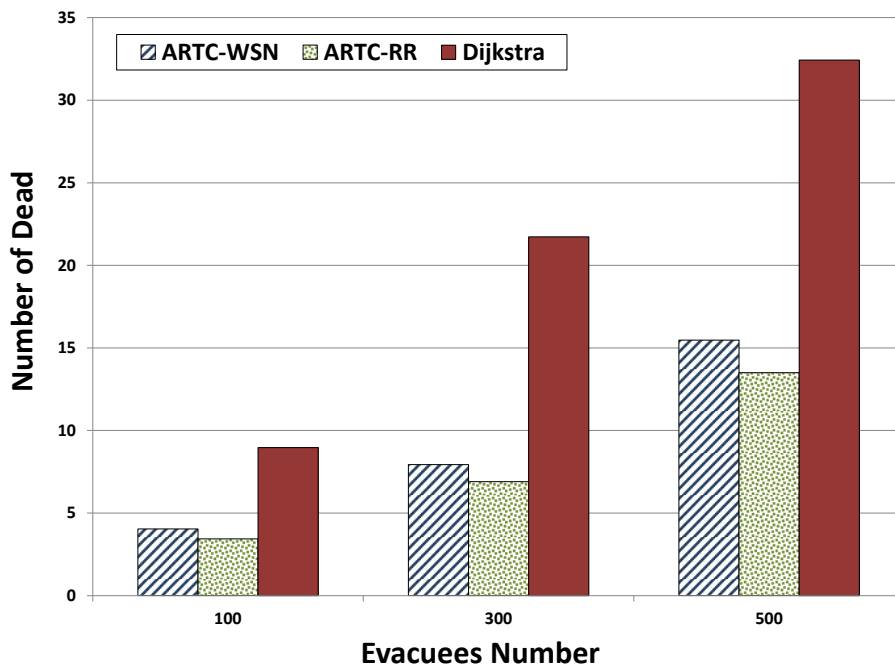


Fig. 5.11 Comparison of the number of dead for different occupation rates for experiment 4.

From the previous figures, it can be concluded that the DSP had the worst performance, especially in crowded areas where the number of civilians was high and they were scattered over small spaces such as office floors. In contrast, the proposed approaches performed very well in crowded areas.

5.4.4 Results: The Number of Available Exits

The performance of the proposed approaches is further evaluated when a smaller number of exits are available, or if one/all of the exits was blocked by a hazard. The evacuation area considered is $100 \times 100 \text{ m}^2$, which is occupied by 300 evacuees.

In severe circumstances, the highest priority is to evacuate the civilians with the minimum death rate. Under these circumstances, the simulation showed that the ARTC-RR had the highest survival rate and, hence, the lowest death rate, as shown in Table 5.6 and Fig. 5.12. ARTC-RR achieved good performance due to its priority assignment to the calculation of the safety of the path over the speed of evacuation.

Table 5.6 The average percentage of survivals for different number of exits

Exit Availability	ARTC-WSN	ARTC-RR	Dijkstra
Two Exits	96%	97%	91%
One Exit	79%	86%	81%

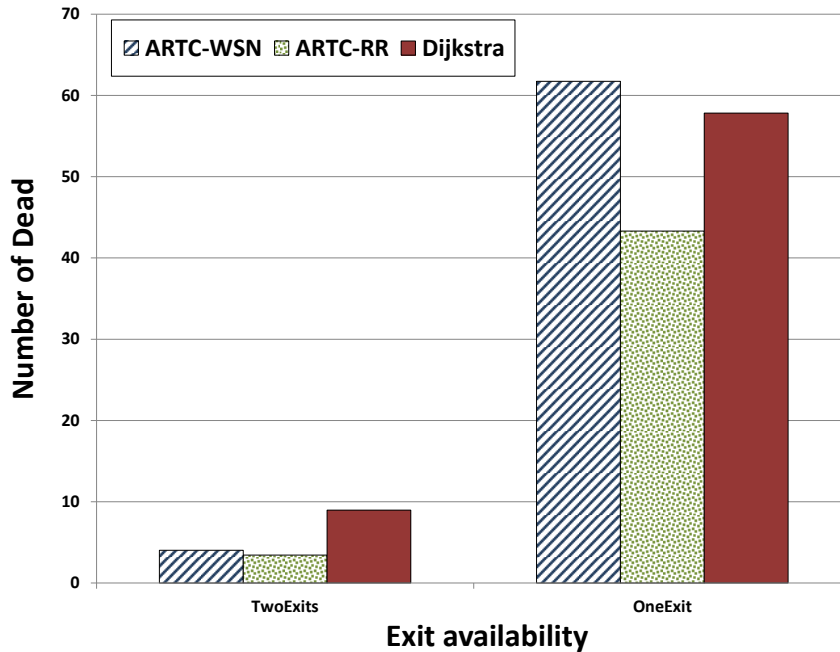


Fig. 5.12 Comparison of the percentage of death percentage for different exits availability.

In terms of the evacuation time and as expected, DSP had the same fixed shortest evacuation time, with the highest death rate due to its priority assignment to the evacuation time over the safety of the path as illustrated in Fig. 5.13.

In the proposed approaches, although they took a slightly longer time to evacuate all individuals, they considered the safety of the evacuation paths as higher in priority than the speed of the evacuation process. Thus, the proposed approaches might guide an evacuee to longer paths to avoid zones at higher risk of hazard. The main aim of the proposed approaches is to find the best (safest) path available, not the fastest path, like the DSP. Therefore, the DSP has a higher death rate mainly because it does not adapt to real-time changes to the hazard location and always directs evacuees to the nearest exit, searching for the fastest path with no prior hazard calculation.

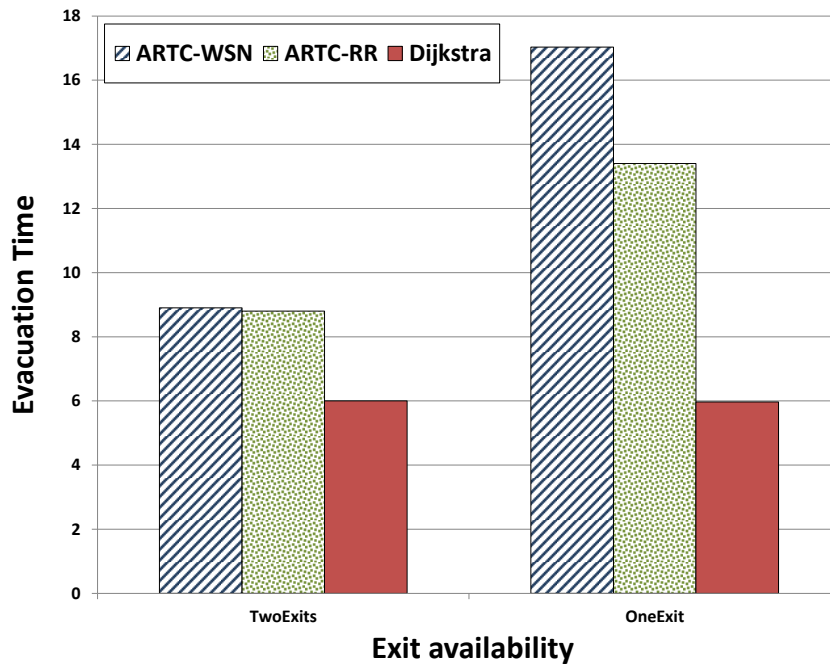


Fig. 5.13 Comparison of evacuation time for different exits availability for experiment 5.

To conclude, in comparison with the DSP, our proposed approaches had overall higher survival rates as a result of their ability to tailor paths to evacuees with respect to the safety of the path leading them farthest from the hazard. This reflects the use of cloud communication in severe cases where evacuees trapped in safe dead-ends have a positive impact on the performance of the algorithm. The reason is that the use of cloud-centralized reverse routing can generate a safe distance between evacuees and the spreading hazard.

5.5 Summary

In this chapter we proposed simulation-based, real time routing algorithms to increase the survival rate of an evacuation process that uses a cloud based control to predict the dead safe ends and re-calculate optimal paths for civilian evacuation. The main aim of the proposed approaches is to find the best (safest) path available not the fastest path as DSP. Therefore, DSP has a higher death ratio mainly because it does not adapt to the real-time changes to the hazard location and always direct evacuees to the nearest exit and searching for the fastest path with no prior hazard calculation.

Five experimental scenarios were proposed to give a clear indication on the performance of the proposed evacuation approaches over small, medium and large scaled areas. Moreover, a fire model was used to predict the hazard spread and the calculation of safe routes is based on the initial distribution of evacuees, the distance from the hazard, the distance to the exit, and the intensity of the hazard, differing from the traditional algorithms, including DSP, that normally calculate the fastest path only regardless to the safety of the path. Furthermore, the intensity of the hazard was represented by using four value rates to represent low and high intensity hazards.

In comparison with DSP, the proposed approaches achieved an overall survival rates up to 98%, this is due to their ability to tailor paths to evacuees with respect to the safety of the path leading them farthest from the hazard.

Although the proposed approaches took a slightly longer evacuation time to evacuate all individuals, they consider the safety of the evacuation paths as higher priority than the speed of evacuation process. Therefore, the proposed approach might guide the evacuee into longer paths to avoid zones at higher risk of hazard.

This reflects that the use of cloud communication in severe cases where evacuees trapped in safe dead ends has a positive impact on the performance of the algorithm. The reason is because the use of cloud centralized reverse routing can generate a safe distance between evacuees and the spreading hazard.

Chapter 6

Conclusions and Future Research Directions

6.1 Conclusions

Many clustering and routing protocols have been proposed for Wireless Sensor Networks (WSNs). This thesis explored some energy optimization methods and clustering schemes that have been employed in both homogeneous and heterogeneous WSNs to improve the energy efficiency. Among the bottlenecks often encountered in order to achieve a robust protocol design is energy-heterogeneity and transmission distances optimization. If the heterogeneity is not properly managed in the network, it can result in shorter lifetime and an uneven spread of energy consumption, thus facilitating coverage loss in the network. In the same concept, transmitting data over large distances for both inter- and intra- communication results in more energy consumption and thus shorter lifetime.

A hybrid routing protocol (called **HRHP**) was proposed for large-scaled heterogeneous WSNs to reduce energy consumption and prolong the network life time. It combined centralized and deterministic clustering approaches; a positive T-cell selection process was implemented to select a cluster head (CH) based on the positive selection in human T-cells mechanism that ensures cells expressing harmful or useless antigen receptors do not mature into active T-cells. In HRHP, nodes that succeed to demonstrate its powerfulness are selected as CHs. The selection was made based on several attributes including the residual energy, the net distance from the base station (BS), and the density of nodes. The performance of HRHP was tested in six scenarios

with different BS location, network size and node density in terms of stability period, operational time, network lifetime and network residual energy.

When tested over area of interest $200 \times 200 m^2$, HRHP extended its stability period in terms of first node dies (FND) by an average of 48% better than LEACH protocol, an average of 53% better than MGEAR, and an average of 26% better than SEP. Also, HRHP showed an improvement in operational time value in terms of half node dies (HND) by an average of 39% better than LEACH, an average of 14% better than MGEAR and an average of 2% better than SEP which indicates that HRHP has more balanced energy dissipation compared to other protocols. Moreover, HRHP has the longest network life in terms of last node dies (LND) when compared with the other protocols, HRHP network life time is extended compared with that of LEACH by an average of 78%, MGEAR by an average of 58% and SEP by an average of 50%. Furthermore, HRHP maintained the highest residual energy levels for the different times of network life.

And over area of interest $300 \times 300 m^2$, HRHP stability period time in terms of FND was rapidly extended compared with that of LEACH by an average of 77%, MGEAR by an average of 80% and SEP by an average of 43%. Improvement in operational time value in terms of HND was also extended compared with that of LEACH by an average of 41%, MGEAR by an average of 28% and SEP by an average of 8%. HRHP had the longest network life in terms of LND when compared with LEACH by an average of 79%, MGEAR by an average of 47% and SEP by an average of 44%. Also, it outperformed other protocols in terms of residual energy levels.

Finally, when tested over area of interest $500 \times 500 m^2$, the stability period time in terms of FND for HRHP is extended compared with that of LEACH by an average of 68%, MGEAR by an average of 69% and SEP by an average of 39%. Operational time value improved in terms of HND compared to LEACH by an average of 63%, MGEAR by an average of 55% and SEP by an average of 32%. HRHP had the longest network life in terms of LND when compared with that of LEACH by an average of 89%, MGEAR by an average of 42% and SEP by an average of 46%. From the test results, HRHP is able to function effectively on large-scaled networks longer than the compared protocols which crucial for a different number of WSNs applications that varies in nodes deployment numbers.

Having realized the importance of energy heterogeneity awareness and keeping communication distance to the minimum, and to further achieve an energy-efficient

optimized protocol, we embarked on designing a multi-level clustering routing algorithm (called **MLHP**) for heterogeneous WSN. It combined the advantages of clustering in hierarchical and tree-based routing techniques with the metaheuristic technique. The strength in MLHP came from using centralized as well distributed CHs selection. The key idea in MLHP was to keep a low intra-transmission distance between CHs and the BS, and inter-transmission distance among the cluster-members and their associated CH.

When comparing MLHP performance to HRHP, MLHP outperformed HRHP in terms of stability period, operational time, network life time and the remaining energy. For an area of interest size $100 \times 100 \text{ m}^2$ and with 100 nodes deployment, MLHP results showed an increase in the stability period by a percentage change of 78.03%, the operational time for MLHP is also increases by a percentage change of 74.06% and the network life was extended by a percentage change of 80.66%. Moreover, when the number of nodes increased to 200, MLHP stability period increases compared to HRHP by a change of 25.58%, the operational time increases by a percentage change of 14.79% and the network life time increases by 26.92%. Furthermore, MLHP showed an improved performance when the area of interest was increase to $200 \times 200 \text{ m}^2$. For 100 nodes deployment, the stability period of MLHP increases by increase of 23.47%, the operational time increases by 2.62% and the network life time increased by 28.57%. In addition, when the number of nodes increases to 200, the stability period of MLHP increased by 12.2%, the operational time increases by 2.16% and the network life time increase by 43.07%. Finally, MLHP has maintained more balanced energy consumption by having higher remaining energy.

The performance of MLHP was tested against LEACH, DEEC and SEP protocols in three different scenarios with total of fourteen cases to present heterogeneity awareness of MLHP. In the first scenario, the stability of MLHP and its operational time were tested over small-scaled and larged-scaled networks with three different nodes density (100, 300, and 500 nodes). MLHP proved that it had better stability and operational time for small-scale and large-scale networks deployed with different nodes density and having the minimal heterogeneity compared to LEACH, DEEC and SEP protocols.

In the second scenario, MLHP was tested over small-scaled networks sized ($100 \times 100 \text{ m}^2$) with two nodes deployments (100 and 200 nodes) and with two heterogeneity parameters ($\alpha = 0.5$, and 1, $\beta = 1$, and 2) in terms of live nodes, network residual energy and packet delivery ratio. MLHP had more surviving nodes over time than

other protocols and hence longer life time in all different cases. However the best performance of MLHP in terms of network life time for small scale networks was when the network heterogeneity parameters are set to ($\alpha = 2$ and $\beta = 1$) with 100 *nodes*. MLHP performance was 200 times better than LEACH in terms of HND, also it succeed to have 62% better improvement than DEEC and 85% than SEP in terms of HND. For 200 *nodes*, MLHP performed the best when ($\alpha = 1$ and $\beta = 0.5$), it also achieved 200 times better than LEACH, an improvement of 69% better than DEEC and 94% than SEP. This confirmed that MLHP can operate in crucial cases with enough amount of heterogeneity for small number of nodes and with the minimal heterogeneity for larger number of nodes. MLHP had a higher level of remaining energy in the network compared to LEACH, DEEC and SEP during the operational time after (HND) and through the end of life time (LND). MLHP had longer time and more energy to detect and sent packets (data) to the BS therefore the ratio of packets sent by MLHP algorithm was greater than the compared algorithms.

In the last scenario, MLHP was tested over large-scaled networks sized ($200 \times 200 m^2$) with two nodes deployments (100 *and* 200 *nodes*) and with two heterogeneity parameters ($\alpha = 0.5$, *and* 1, $\beta = 1$, *and* 2) in terms of live nodes, network residual energy and packet delivery ratio. The best performance for MLHP in large-scaled networks was when the network deployed with 200 nodes regardless of the heterogeneity parameters values. When $\alpha = 0.5$ and $\beta = 1$, MLHP achieved 300 times better than LEACH, and outperform DEEC by 46% and SEP by 52%. Moreover, when $\alpha = 1$ and $\beta = 2$, MLHP achieved 400 times better than LEACH, and outperform DEEC by 1% and SEP by 95%. Because MLHP had longer life time, the ratio of packets sent by MLHP algorithm is greater than for the compared algorithms for large-scaled networks. Finally, MLHP had higher levels of remaining energy in the network compared to LEACH, DEEC and SEP during the operational time after (HND) and through the end of life time (LND). However, for the stability time in the first few rounds, not all the nodes were active, therefore it show less average energy than DEEC and SEP but always show more energy than LEACH.

Following the attempts on improving the network lifetime and energy consumption in WSNs, we continue to develop routing technique for emergency evacuation systems using WSNs in smart buildings. A real-time, autonomous emergency evacuation approach that integrates cloud computing with WSNs was proposed (namely **ARTC-WSN**). It is designed to perform localized, autonomous navigation by calculating the

best evacuation paths in a distributed manner using two types of SNs, a sensing node and a decision node.

In addition to distributed path finding, SNs identify the occurrences of a common evacuation problem that happens when evacuees are directed to safe, dead-end areas of a building. These areas are characterized as safe because they are far from the incident, but they are also still far from the exit. Eventually, these areas become no longer safe, especially if the incident is intense. When such a situation is identified, ARTC-WSN employed cloudification to efficiently and carefully handle this problem. A fire model was used to predict the hazard spread, and the calculation of safe routes was based on the initial distribution of evacuees, the distance from the hazard, the distance to the exit, and the intensity of the hazard. ARTC-WSN was tested over five experiments, the first three were designed to test the performance of ARTC-WSN over small-, medium-, and large-scaled networks with four different hazard intensities. The results showed that ARTC-WSN outperformed the compared algorithms by 97% for small hazard intensity and 96% for high hazard intensity over small-scaled network. Also, 99% for small hazard intensity and 98% for high hazard intensity over medium-scaled network. Finally, 99% for small hazard intensity and 98% for high hazard intensity over large-scaled network in terms of survival ratio.

The fourth experiment was designed to find the behaviour of the proposed algorithm when applied over dense areas when evacuees numbers ranging between 100 and 500 with random deployment of the hazard. The results showed that ARTC-WSN outperformed the compared algorithms in terms of survival ratio by 96% when the evacuation area was occupied by 100 evacuees, 97% when occupied by 300 evacuees, and 97% when occupied by 500 evacuees. From these results, it is concluded that ARTC-WSN can perform better in small and crowded areas of evacuation.

The last experiment was designed to find the behaviour of ARTC-WSN when limited number of exits are available or when the exit is blocked by the hazard. The evacuation area considered ARTC-WSN outperformed the compared algorithms in terms of survival ratio by 96% when there was two available exits and by 79% when only one exit was available. However, when ARTC-WSN employed cloudification and applied a reverse routing it achieved 97% when two exits were available and 86% when only one exit was available. This confirms that when ARTC-WSN is used in small congested area with minimum access to exits, it perform better than compared algorithms and can achieve even better results when employing cloudification.

6.2 Future Research Directions

During our research work, we have identified several future research directions that can add to or enhance the proposed protocols in this thesis:

1. Transmission Power Control (TPC) techniques can be used to adjust the transmission power dynamically in WSNs and thus to significantly reduce the energy consumption [147] [9]. In the proposed protocols in this thesis, each node transmits packets at the same power level which is normally the maximum possible power level. However, when transmitting packets at high power level, it may generate significant interference in the network and consume more energy than necessary. In the case of two adjacent nodes with short distance from each other, low transmission power is effective to communicate. The power level should be high enough to guarantee the transmission and should be low enough to save energy. TPC techniques can be embedded into any existing Medium Access Control (MAC) protocol [148]. As a future research direction, a cross-layer clustering protocol can be proposed such that it takes into consideration finding the optimal CHs and finding the optimal transmission power for each SN.
2. The proposed routing protocols can be further improved by using sleeping techniques [149]. WSNs consist of a large number of SNs which may result in nodes share the same monitored regions and redundant information is collected, therefore some nodes can be turned off to preserve energy while the others still work to offer full coverage [150]. The Optimal Coverage Problem (OCP) in WSN is defined as finding the smallest set of nodes to monitor an area in order to save energy while meeting the full coverage and connectivity requirements [151]. On the other hand, sensor scheduling selects only a subset of SNs to be sensing active, in a way that the area covered by these active nodes can still be the same as the one covered by all nodes. Both network clustering and sensor scheduling can help to conserve energy. As a future research direction, an integrated solution for both problems can be proposed to enhance the network's energy efficiency.
3. Currently, the commercialization of wireless charging technology is growing. Hence, realization of such technology could provide better solution to the energy issues in WSN deployments. For example, WiTricity [152] [153] successfully demonstrated this idea and showed the possibilities of wirelessly charge gadgets such as mobile phones, TVs etc., without the need for a battery source. Similarly,

DELL [154] technology has successfully applied a similar technique to their range of laptops. Also, POWERMAT [155] have been working on similar projects for other personal appliances. WSNs can benefit from this charging technology by using mobile relay nodes as recharging hotspot, since the key constraint is battery-drainage of SNs as the network evolves. One way to accomplish this is to use a mobile sink or BS to periodically charge the SNs at close proximity. The mobility of the sink could be randomized or could be triggered by an event such as a dying SN, depending on the optimization strategy in place. New research directions can be driven in the field of WSN if properly used wireless charging technology, as wireless charging technology promises a long-term breakthrough for WSNs.

4. ARTC-WSN can be further enhanced by considering the evacuees age and physical movement. There can be two cases to represent the evacuees movement state, *case1* represents young and adults and *case2* represents children, elderly and disabled. By considering these factors, it will shed more light on the implication of tuning each parameter on a real-world scenario with evacuees have different movement speed and response speed.
5. Simulation is generally used to justify results of solutions that offer clustering techniques for WSNs. An interesting research direction would be to explore a real-world implementation of the proposed protocol designs through deployment of testbed for the cluster-based protocols on nodes equipped with energy harvesting capabilities which then can provide more insight on the operation of these networks within IoT.

Bibliography

- [1] D. Evans, “The Internet of Things: How the Next Evolution of the Internet Is Changing Everything,” *White Paper, Cisco IBSG*, pp. 2–4, 2011.
- [2] P. K. Verma, R. Verma, A. Prakash, A. Agrawal, K. Naik, R. Tripathi, M. Alsabaan, T. Khalifa, T. Abdelkader, and A. Abogharaf, “Machine-to-machine (m2m) communications: A survey,” *Journal of Network and Computer Applications*, vol. 66, pp. 83–105, 2016.
- [3] H. Ghayvat, J. Liu, S. Mukhopadhyay, and X. Gui, “Wellness Sensor Networks: A Proposal and Implementation for Smart Home for Assisted Living,” *Sensors Journal, IEEE*, vol. 15, no. 12, pp. 7341–7348, Dec 2015.
- [4] A. Alkandari, M. Alnasheet, and I. F. T. Alshaikhli, “Smart cities: a survey,” *Journal of Advanced Computer Science and Technology Research (JACSTR)*, vol. 2, no. 2, pp. 79–90, 2012.
- [5] M. R. Mundada, S. Kiran, S. Khobanna, R. N. Varsha, and S. A. George, “A Study on Energy Efficient Routing Protocols in Wireless Sensor Networks,” *International Journal of Distributed and Parallel Systems (IJDPS) Vol*, vol. 3, pp. 311–330, 2012.
- [6] F. J. Oppermann, C. A. Boano, and K. Römer, “A decade of wireless sensing applications: Survey and taxonomy,” in *The Art of Wireless Sensor Networks*. Springer, 2014, pp. 11–50.
- [7] A. M. Zungeru, L.-M. Ang, and K. P. Seng, “Classical and swarm intelligence based routing protocols for wireless sensor networks: A survey and comparison,” *Journal of Network and Computer Applications*, vol. 35, no. 5, pp. 1508–1536, 2012.
- [8] N. Pantazis, S. A. Nikolidakis, and D. D. Vergados, “Energy-efficient routing protocols in wireless sensor networks: A survey,” *Communications Surveys & Tutorials, IEEE*, vol. 15, no. 2, pp. 551–591, 2013.
- [9] T. Rault, A. Bouabdallah, and Y. Challal, “Energy efficiency in wireless sensor networks: A top-down survey,” *Computer Networks*, vol. 67, pp. 104–122, 2014.

- [10] A. Aziz, Y. Sekercioglu, P. Fitzpatrick, and M. Ivanovich, "A Survey on Distributed Topology Control Techniques for Extending the Lifetime of Battery Powered Wireless Sensor Networks," *Communications Surveys Tutorials, IEEE*, vol. 15, no. 1, pp. 121–144, First 2013.
- [11] S.-S. Wang and Z.-P. Chen, "LCM: A Link-Aware Clustering Mechanism for Energy-Efficient Routing in Wireless Sensor Networks," *Sensors Journal, IEEE*, vol. 13, no. 2, pp. 728–736, Feb 2013.
- [12] X. Liu, "Atypical Hierarchical Routing Protocols for Wireless Sensor Networks: A Review," *Sensors Journal, IEEE*, vol. 15, no. 10, pp. 5372–5383, Oct 2015.
- [13] L. M. Arboleda and N. Nasser, "Comparison of clustering algorithms and protocols for wireless sensor networks," in *2006 Canadian Conference on Electrical and Computer Engineering*. IEEE, 2006, pp. 1787–1792.
- [14] S. Tyagi and N. Kumar, "A systematic review on clustering and routing techniques based upon LEACH protocol for wireless sensor networks," *Journal of Network and Computer Applications*, vol. 36, no. 2, pp. 623–645, 2013.
- [15] H. Eren, *Wireless sensors and instruments: networks, design, and applications*. CRC Press, 2005.
- [16] D. Snoonian, "Smart buildings," *IEEE spectrum*, vol. 40, no. 8, pp. 18–23, 2003.
- [17] T. A. Nguyen and M. Aiello, "Energy intelligent buildings based on user activity: A survey," *Energy and buildings*, vol. 56, pp. 244–257, 2013.
- [18] S. Chren, B. Rossi, and T. Pitner, "Smart grids deployments within EU projects: The role of smart meters," in *Smart Cities Symposium Prague (SCSP), 2016*. IEEE, 2016, pp. 1–5.
- [19] M. Billinghamurst and T. Starner, "Wearable devices: new ways to manage information," *Computer*, vol. 32, no. 1, pp. 57–64, 1999.
- [20] J. W. Rettberg, *Seeing ourselves through technology: How we use selfies, blogs and wearable devices to see and shape ourselves*. Springer, 2016.
- [21] K. Karimi and G. Atkinson, "What the Internet of Things (IoT) needs to become a reality," *White Paper, FreeScale and ARM*, pp. 1–16, 2013.
- [22] Deloitte. [Online]. Available: <https://www2.deloitte.com/us/en/pages/financial-services/topics/center-for-financial-services.html>
- [23] G. Inc., "Forecast: Internet of things, endpoints and associated services, worldwide 2015," Oct 29, 2015.
- [24] T. S. Rappaport *et al.*, *Wireless communications: principles and practice*. Prentice Hall PTR New Jersey, 1996, vol. 2.
- [25] T. Prof. Murat. (2000) Lecture: Path Loss. [Online]. Available: <https://www.utdallas.edu/~torlak/courses/ee4367/lectures/lectureradio.pdf>

- [26] W. R. Heinzelman, A. Chandrakasan, and H. Balakrishnan, "Energy-efficient communication protocol for wireless microsensor networks," in *System sciences, 2000. Proceedings of the 33rd annual Hawaii international conference on*. IEEE, 2000, pp. 10–pp.
- [27] G. Smaragdakis, I. Matta, A. Bestavros *et al.*, "SEP: A stable election protocol for clustered heterogeneous wireless sensor networks," in *Second international workshop on sensor and actor network protocols and applications (SANPA 2004)*, 2004, pp. 1–11.
- [28] Q. Nadeem, M. B. Rasheed, N. Javaid, Z. Khan, Y. Maqsood, and A. Din, "M-GEAR: gateway-based energy-aware multi-hop routing protocol for WSNs," in *Broadband and Wireless Computing, Communication and Applications (BWCCA), 2013 Eighth International Conference on*. IEEE, 2013, pp. 164–169.
- [29] S. Sirsikar and S. Anavatti, "Issues of Data Aggregation Methods in Wireless Sensor Network: A Survey," *Procedia Computer Science*, vol. 49, pp. 194–201, 2015.
- [30] F. A. Aderohunmu, "Energy management techniques in wireless sensor networks: Protocol design and evaluation," Master Thesis, University of Otago, 2010.
- [31] T. J. Shepard, "A channel access scheme for large dense packet radio networks," *ACM SIGCOMM Computer Communication Review*, vol. 26, no. 4, pp. 219–230, 1996.
- [32] S. Yinbiao, P. Lanctot, and F. Jianbin, "Internet of things: wireless sensor networks," *White Paper, International Electrotechnical Commission*, <http://www.iec.ch>, 2014.
- [33] D. Parker, E. Mills, L. Rainer, N. Bourassa, and G. Homan, "Accuracy of the home energy saver energy calculation methodology," *Proceedings of the 2012 ACEEE Summer Study on Energy Efficiency in Buildings*, 2012.
- [34] T. Hong, S. C. Taylor-Lange, S. D'Oca, D. Yan, and S. P. Corgnati, "Advances in research and applications of energy-related occupant behavior in buildings," *Energy and Buildings*, vol. 116, pp. 694 – 702, 2016. [Online]. Available: "<http://www.sciencedirect.com/science/article/pii/S0378778815005307>"
- [35] S. Electric. (2008) Energy savings of up to 20% in the construction industry. [Online]. Available: http://www2.schneider-electric.com/sites/corporate/en/press/press-kit/press-kit-viewer.page?c_filepath=/templatedata/Content_Browser/Media/data/en/shared/2006/05/20060501_may_june_2006_schneider_electric_s_homes_project_selected_by_the_frenc.xml
- [36] N. K. Suryadevara, S. C. Mukhopadhyay, S. D. T. Kelly, and S. P. S. Gill, "WSN-based smart sensors and actuator for power management in intelligent buildings," *IEEE/ASME Transactions On Mechatronics*, vol. 20, no. 2, pp. 564–571, 2015.
- [37] G. Fortino, A. Guerrieri, G. M. O'Hare, and A. Ruzzelli, "A flexible building management framework based on wireless sensor and actuator networks," *Journal of Network and Computer Applications*, vol. 35, no. 6, pp. 1934–1952, 2012.

- [38] K. Jaafar and M. K. Watfa, "Sensor networks in future smart rotating buildings," in *2013 IEEE 10th Consumer Communications and Networking Conference (CCNC)*. IEEE, 2013, pp. 962–967.
- [39] A. Pantelopoulos and N. G. Bourbakis, "A Survey on Wearable Sensor-Based Systems for Health Monitoring and Prognosis," *IEEE Transactions on Systems, Man, and Cybernetics, Part C (Applications and Reviews)*, vol. 40, no. 1, pp. 1–12, Jan 2010.
- [40] F. Aiello, F. L. Bellifemine, G. Fortino, S. Galzarano, and R. Gravina, "An agent-based signal processing in-node environment for real-time human activity monitoring based on wireless body sensor networks," *Engineering Applications of Artificial Intelligence*, vol. 24, no. 7, pp. 1147–1161, 2011.
- [41] M. M. Baig and H. Gholamhosseini, "Smart health monitoring systems: an overview of design and modeling," *Journal of medical systems*, vol. 37, no. 2, pp. 1–14, 2013.
- [42] P. Castillejo, J.-F. Martinez, J. Rodriguez-Molina, and A. Cuerva, "Integration of wearable devices in a wireless sensor network for an E-health application," *IEEE Wireless Communications*, vol. 20, no. 4, pp. 38–49, 2013.
- [43] N. F. B. I. Gulcharan, H. Daud, N. M. Nor, T. Ibrahim, and M. Z. Shamsudin, "Investigation of Stability and Reliability of the Patient's Wireless Temperature Monitoring Device," *Procedia Computer Science*, vol. 40, pp. 151–159, 2014.
- [44] K. Baskaran, "A survey on futuristic health care system: Wbans," *Procedia Engineering*, vol. 30, pp. 889–896, 2012.
- [45] H. Yan, L. D. Xu, Z. Bi, Z. Pang, J. Zhang, and Y. Chen, "An emerging technology—wearable wireless sensor networks with applications in human health condition monitoring," *Journal of Management Analytics*, vol. 2, no. 2, pp. 121–137, 2015.
- [46] Y. Ren, R. Werner, N. Pazzi, and A. Boukerche, "Monitoring patients via a secure and mobile healthcare system," *IEEE Wireless Communications*, vol. 17, no. 1, pp. 59–65, February 2010.
- [47] M. Souil and A. Bouabdallah, "On QoS provisioning in context-aware wireless sensor networks for healthcare," in *Computer Communications and Networks (ICCCN), 2011 Proceedings of 20th International Conference on*. IEEE, 2011, pp. 1–6.
- [48] M. Díez-Minguito, A. Baquerizo, M. Ortega-Sánchez, G. Navarro, and M. Losada, "Tide transformation in the Guadalquivir estuary (SW Spain) and process-based zonation," *Journal of Geophysical Research: Oceans*, vol. 117, no. C3, 2012.
- [49] G. Navarro, I. E. Huertas, E. Costas, S. Flecha, M. Díez-Minguito, I. Caballero, V. López-Rodas, L. Prieto, and J. Ruiz, "Use of a real-time remote monitoring network (RTRM) to characterize the Guadalquivir estuary (Spain)," *Sensors*, vol. 12, no. 2, pp. 1398–1421, 2012.

- [50] F. Chiti, A. D. Cristofaro, R. Fantacci, D. Tarchi, G. Collodo, G. Giorgetti, and A. Manes, "Energy efficient routing algorithms for application to agro-food wireless sensor networks," in *IEEE International Conference on Communications, 2005. ICC 2005. 2005*, vol. 5, May 2005, pp. 3063–3067.
- [51] L. Kang, B. Qi, D. Janecek, and S. Banerjee, "Ecodrives: A mobile sensing and control system for fuel efficient driving," in *Proceedings of the 21st Annual International Conference on Mobile Computing and Networking*. ACM, 2015, pp. 358–371.
- [52] M. A. Rahman, S. Anwar, M. I. Pramanik, and M. F. Rahman, "A survey on energy efficient routing techniques in Wireless Sensor Network," in *2013 15th International Conference on Advanced Communications Technology (ICACT)*, Jan 2013, pp. 200–205.
- [53] D. Kumar, "Performance analysis of energy efficient clustering protocols for maximising lifetime of wireless sensor networks," *IET Wireless Sensor Systems*, vol. 4, no. 1, pp. 9–16, 2014.
- [54] TinyOS. [Online]. Available: <http://www.tinyos.net>
- [55] H. Abrach, S. Bhatti, J. Carlson, H. Dai, J. Rose, A. Sheth, B. Shucker, J. Deng, and R. Han, "MANTIS: System support for multimodal networks of in-situ sensors," in *Proceedings of the 2nd ACM international conference on Wireless sensor networks and applications*. ACM, 2003, pp. 50–59.
- [56] P. Zhang, C. M. Sadler, S. A. Lyon, and M. Martonosi, "Hardware design experiences in zebranet," in *Proceedings of the 2nd international conference on Embedded networked sensor systems*. ACM, 2004, pp. 227–238.
- [57] R. Sugihara and R. K. Gupta, "Programming models for sensor networks: A survey," *ACM Transactions on Sensor Networks (TOSN)*, vol. 4, no. 2, p. 8, 2008.
- [58] S. Sharma, R. K. Bansal, and S. Bansal, "Issues and Challenges in Wireless Sensor Networks," in *2013 International Conference on Machine Intelligence and Research Advancement*, Dec 2013, pp. 58–62.
- [59] A. Ahmed, J. Ali, A. Raza, and G. Abbas, "Wired vs wireless deployment support for wireless sensor networks," in *TENCON 2006-2006 IEEE Region 10 Conference*. IEEE, 2006, pp. 1–3.
- [60] J. Li, Y. Bai, H. Ji, J. Ma, Y. Tian, and D. Qian, "Power: Planning and deployment platform for wireless sensor networks," in *2006 Fifth International Conference on Grid and Cooperative Computing Workshops*. IEEE, 2006, pp. 432–436.
- [61] M. Brain, "How motes work," *Howstuffworks.com*, 2008.
- [62] R. Mulligan and H. M. Ammari, "Coverage in wireless sensor networks: a survey," *Network Protocols and Algorithms*, vol. 2, no. 2, pp. 27–53, 2010.

- [63] J. N. Al-Karaki and A. E. Kamal, "Routing techniques in wireless sensor networks: a survey," *IEEE Wireless Communications*, vol. 11, no. 6, pp. 6–28, Dec 2004.
- [64] J. Polastre, R. Szewczyk, and D. Culler, "Telos: enabling ultra-low power wireless research," in *IPSN 2005. Fourth International Symposium on Information Processing in Sensor Networks, 2005*. IEEE, 2005, pp. 364–369.
- [65] W. Dargie and C. Poellabauer, *Fundamentals of wireless sensor networks: theory and practice*. John Wiley & Sons, 2010.
- [66] D. Chen and P. K. Varshney, "QoS Support in Wireless Sensor Networks: A Survey." in *International conference on wireless networks*, vol. 233, 2004, pp. 1–7.
- [67] E. Troubleyn, I. Moerman, and P. Demeester, "QoS challenges in wireless sensor networked robotics," *Wireless personal communications*, vol. 70, no. 3, pp. 1059–1075, 2013.
- [68] A. Sharif, V. Potdar, and E. Chang, "Wireless multimedia sensor network technology: A survey," in *2009 7th IEEE International Conference on Industrial Informatics*, June 2009, pp. 606–613.
- [69] C. Li, H. Zhang, B. Hao, and J. Li, "A survey on routing protocols for large-scale wireless sensor networks," *Sensors*, vol. 11, no. 4, pp. 3498–3526, 2011.
- [70] F. Hu and X. Cao, *Wireless sensor networks: principles and practice*. CRC Press, 2010.
- [71] N. Al-Nabhan, M. Al-Rodhaan, A. Al-Dhelaan, and X. Cheng, "Connected dominating set algorithms for wireless sensor networks," *International Journal of Sensor Networks*, vol. 13, no. 2, pp. 121–134, 2013.
- [72] J. Pan, Y. T. Hou, L. Cai, Y. Shi, and S. X. Shen, "Topology control for wireless sensor networks," in *Proceedings of the 9th annual international conference on Mobile computing and networking*. ACM, 2003, pp. 286–299.
- [73] S. M. Zin, N. B. Anuar, M. L. M. Kiah, and A.-S. K. Pathan, "Routing protocol design for secure WSN: Review and open research issues," *Journal of Network and Computer Applications*, vol. 41, pp. 517–530, 2014.
- [74] M. A. Mahmood, W. K. Seah, and I. Welch, "Reliability in wireless sensor networks: A survey and challenges ahead," *Computer Networks*, vol. 79, pp. 166–187, 2015.
- [75] J. N. Al-Karaki and A. E. Kamal, "Routing techniques in wireless sensor networks: a survey," *IEEE wireless communications*, vol. 11, no. 6, pp. 6–28, 2004.
- [76] R. Rathna, R. Dhanalakshmi, and T. Sasipraba, "Centralised against distributed medium access control scheduling for environmental monitoring sensors," *IET Wireless Sensor Systems*, vol. 5, no. 6, pp. 271–276, 2015.
- [77] M. Ilyas and I. Mahgoub, *Handbook of sensor networks: compact wireless and wired sensing systems*. CRC press, 2004.

- [78] P. Uplap and P. Sharma, "Review of heterogeneous/homogeneous wireless sensor networks and intrusion detection system techniques," in *International Conference on Recent Trends in Information, Telecommunication and Computing, ITC*, 2014.
- [79] S. Tanwar, N. Kumar, and J. J. Rodrigues, "A systematic review on heterogeneous routing protocols for wireless sensor network," *Journal of network and computer applications*, vol. 53, pp. 39–56, 2015.
- [80] K. T. Kim, C. H. Lyu, S. S. Moon, and H. Y. Youn, "Tree-based clustering (TBC) for energy efficient wireless sensor networks," in *Advanced Information Networking and Applications Workshops (WAINA), 2010 IEEE 24th International Conference on*. IEEE, 2010, pp. 680–685.
- [81] W. B. Heinzelman, A. P. Chandrakasan, and H. Balakrishnan, "An application-specific protocol architecture for wireless microsensor networks," *Wireless Communications, IEEE Transactions on*, vol. 1, no. 4, pp. 660–670, 2002.
- [82] H. Furtado and R. Trobec, "Applications of wireless sensors in medicine," in *MIPRO, 2011 Proceedings of the 34th International Convention*, May 2011, pp. 257–261.
- [83] F. Mieyeville, M. Ichchou, G. Scorletti, D. Navarro, and W. Du, "Wireless sensor networks for active vibration control in automobile structures," *Smart Materials and Structures*, vol. 21, no. 7, p. 075009, 2012.
- [84] L. Mainetti, L. Patrono, and A. Vilei, "Evolution of wireless sensor networks towards the Internet of Things: A survey," in *Software, Telecommunications and Computer Networks (SoftCOM), 2011 19th International Conference on*, Sept 2011, pp. 1–6.
- [85] S. Tyagi and N. Kumar, "A systematic review on clustering and routing techniques based upon leach protocol for wireless sensor networks," *Journal of Network and Computer Applications*, vol. 36, no. 2, pp. 623–645, 2013.
- [86] O. Younis, M. Krunz, and S. Ramasubramanian, "Node clustering in wireless sensor networks: recent developments and deployment challenges," *IEEE network*, vol. 20, no. 3, pp. 20–25, 2006.
- [87] N. Kokash, "An introduction to heuristic algorithms," *Department of Informatics and Telecommunications*, pp. 1–8, 2005.
- [88] L. Qing, Q. Zhu, and M. Wang, "Design of a distributed energy-efficient clustering algorithm for heterogeneous wireless sensor networks," *Computer communications*, vol. 29, no. 12, pp. 2230–2237, 2006.
- [89] D. Kumar, T. C. Aseri, and R. Patel, "EEHC: Energy efficient heterogeneous clustered scheme for wireless sensor networks," *Computer Communications*, vol. 32, no. 4, pp. 662–667, 2009.

- [90] S. Tyagi, S. Gupta, S. Tanwar, and N. Kumar, "EHE-LEACH: Enhanced heterogeneous LEACH protocol for lifetime enhancement of wireless SNs," in *Advances in Computing, Communications and Informatics (ICACCI), 2013 International Conference on*, Aug 2013, pp. 1485–1490.
- [91] K. T. Kim, C. H. Lyu, S. S. Moon, and H. Y. Youn, "Tree-Based Clustering(TBC) for Energy Efficient Wireless Sensor Networks," in *2010 IEEE 24th International Conference on Advanced Information Networking and Applications Workshops*, April 2010, pp. 680–685.
- [92] X. Yang, "Metaheuristic Optimization," vol. 6, no. 8, p. 11472, 2011, revision 91488.
- [93] F. Glover, "Future paths for integer programming and links to artificial intelligence," *Computers & operations research*, vol. 13, no. 5, pp. 533–549, 1986.
- [94] F. W. Glover and G. A. Kochenberger, *Handbook of metaheuristics*. Springer Science & Business Media, 2006, vol. 57.
- [95] F. Glover and M. Laguna, *Tabu Search*. Springer, 2013.
- [96] A. Rahmanian, H. Omranpour, M. Akbari, and K. Raahemifar, "A novel genetic algorithm in LEACH-C routing protocol for sensor networks," in *Electrical and computer engineering (CCECE), 2011 24th Canadian conference on*. IEEE, 2011, pp. 001 096–001 100.
- [97] P. Kuila, S. K. Gupta, and P. K. Jana, "A novel evolutionary approach for load balanced clustering problem for wireless sensor networks," *Swarm and Evolutionary Computation*, vol. 12, pp. 48–56, 2013.
- [98] N. A. Latiff, C. C. Tsimenidis, and B. S. Sharif, "Energy-aware clustering for wireless sensor networks using particle swarm optimization," in *Personal, Indoor and Mobile Radio Communications, 2007. PIMRC 2007. IEEE 18th International Symposium on*. IEEE, 2007, pp. 1–5.
- [99] N. M. A. Latiff, C. C. Tsimenidis, and B. S. Sharif, "Performance comparison of optimization algorithms for clustering in wireless sensor networks," in *2007 IEEE International Conference on Mobile Adhoc and Sensor Systems*, Oct 2007, pp. 1–4.
- [100] E. A. Khalil and A. A. Bara'a, "Energy-aware evolutionary routing protocol for dynamic clustering of wireless sensor networks," *Swarm and Evolutionary Computation*, vol. 1, no. 4, pp. 195–203, 2011.
- [101] C.-J. Jiang, W.-R. Shi, X.-l. TANG *et al.*, "Energy-balanced unequal clustering protocol for wireless sensor networks," *The Journal of China Universities of Posts and Telecommunications*, vol. 17, no. 4, pp. 94–99, 2010.
- [102] E. Robey and B. Fowlkes, "Selective events in T cell development," *Annual review of immunology*, vol. 12, no. 1, pp. 675–705, 1994.

- [103] E. V. Rothenberg, "The development of functionally responsive T cells," *Advances in immunology*, vol. 51, pp. 85–214, 1992.
- [104] K. K. Baldwin, B. P. Trenchak, J. D. Altman, and M. M. Davis, "Negative selection of T cells occurs throughout thymic development," *The Journal of Immunology*, vol. 163, no. 2, pp. 689–698, 1999.
- [105] R. N. Germain, "T-cell development and the CD4–CD8 lineage decision," *Nature Reviews Immunology*, vol. 2, no. 5, pp. 309–322, 2002.
- [106] S. Tyagi, S. Tanwar, S. Gupta, N. Kumar, S. Misra, J. Rodrigues, and S. Ullah, "Bayesian Coalition Game-based optimized clustering in Wireless Sensor Networks," in *Communications (ICC), 2015 IEEE International Conference on*. IEEE, 2015, pp. 3540–3545.
- [107] F. Comeau, *Optimal clustering in wireless sensor networks employing different propagation models and data aggregation techniques*. Dalhousie University, 2008.
- [108] M. Aslam, E. Munir, M. Bilal, M. Asad, A. Ali, T. Shah, and S. Bilal, "HADCC: Hybrid Advanced Distributed and Centralized Clustering Path Planning Algorithm for WSNs," in *Advanced Information Networking and Applications (AINA), 2014 IEEE 28th International Conference on*, May 2014, pp. 657–664.
- [109] M. F. Othman and K. Shazali, "Wireless sensor network applications: A study in environment monitoring system," *Procedia Engineering*, vol. 41, pp. 1204–1210, 2012.
- [110] S. Okdem and D. Karaboga, "Routing in Wireless Sensor Networks Using Ant Colony Optimization," in *First NASA/ESA Conference on Adaptive Hardware and Systems (AHS'06)*, June 2006, pp. 401–404.
- [111] J. F. Yan, Y. Gao, and L. Yang, "Ant colony optimization for wireless sensor networks routing," in *Machine Learning and Cybernetics (ICMLC), 2011 International Conference on*, vol. 1, July 2011, pp. 400–403.
- [112] L. Luo and L. Li, "An Ant Colony System Based Routing Algorithm for Wireless Sensor Network," in *Computer Science and Electronics Engineering (ICCSEE), 2012 International Conference on*, vol. 2, March 2012, pp. 376–379.
- [113] R. V. Kulkarni and G. K. Venayagamoorthy, "Particle Swarm Optimization in Wireless-Sensor Networks: A Brief Survey," *IEEE Transactions on Systems, Man, and Cybernetics, Part C (Applications and Reviews)*, vol. 41, no. 2, pp. 262–267, March 2011.
- [114] M. Lin, Z. h. Wang, C. w. Zou, and M. Yu, "Double Cluster-Heads Routing Policy Based on the Weights of Energy-Efficient for Wireless Sensor Networks," in *Computational and Information Sciences (ICCIS), 2010 International Conference on*, Dec 2010, pp. 696–699.
- [115] D. Karaboga, S. Okdem, and C. Ozturk, "Cluster based wireless sensor network routing using artificial bee colony algorithm," *Wireless Networks*, vol. 18, no. 7, pp. 847–860, 2012.

- [116] S. Okdem, D. Karaboga, and C. Ozturk, "An application of wireless sensor network routing based on artificial bee colony algorithm," in *2011 IEEE Congress of Evolutionary Computation (CEC)*. IEEE, 2011, pp. 326–330.
- [117] G. Ran, H. Zhang, and S. Gong, "Improving on LEACH protocol of wireless sensor networks using fuzzy logic," *Journal of Information & Computational Science*, vol. 7, no. 3, pp. 767–775, 2010.
- [118] H. Bagci and A. Yazici, "An energy aware fuzzy unequal clustering algorithm for wireless sensor networks," in *Fuzzy systems (FUZZ), 2010 IEEE international conference on*. IEEE, 2010, pp. 1–8.
- [119] S. Mirjalili, S. M. Mirjalili, and A. Lewis, "Grey wolf optimizer," *Advances in Engineering Software*, vol. 69, pp. 46–61, 2014.
- [120] E. Emary, H. M. Zawbaa, C. Grosan, and A. E. Hassenian, "Feature subset selection approach by gray-wolf optimization," in *Afro-European Conference for Industrial Advancement*. Springer, 2015, pp. 1–13.
- [121] N. Muangkote, K. Sunat, and S. Chiewchanwattana, "An improved grey wolf optimizer for training q-Gaussian Radial Basis Functional-link nets," in *Computer Science and Engineering Conference (ICSEC), 2014 International*. IEEE, 2014, pp. 209–214.
- [122] W. Long and S. Xu, "A novel grey wolf optimizer for global optimization problems," in *2016 IEEE Advanced Information Management, Communicates, Electronic and Automation Control Conference (IMCEC)*, Oct 2016, pp. 1266–1270.
- [123] S. Bandyopadhyay and E. J. Coyle, "Minimizing communication costs in hierarchically clustered networks of wireless sensors," in *Wireless Communications and Networking, 2003. WCNC 2003. 2003 IEEE*, vol. 2. IEEE, 2003, pp. 1274–1279.
- [124] F. A. Aderohunmu, "Optimization of energy-efficient transmission protocol for wireless sensor networks," Ph.D. dissertation, University of Otago, 2013.
- [125] M. Handy, M. Haase, and D. Timmermann, "Low energy adaptive clustering hierarchy with deterministic cluster-head selection," in *Mobile and Wireless Communications Network, 2002. 4th International Workshop on*. IEEE, 2002, pp. 368–372.
- [126] R. W. Perry, M. K. Lindell, and M. R. Greene, *Evacuation planning in emergency management*. LexingtonBooks, 1981.
- [127] P. Arthur and R. Passini, *Wayfinding: people, signs, and architecture*, 1992.
- [128] O. J. Akinwande, H. Bi, and E. Gelenbe, "Managing Crowds in Hazards With Dynamic Grouping," *IEEE Access*, vol. 3, pp. 1060–1070, 2015.
- [129] G. Barrenetxea, F. Ingelrest, G. Schaefer, and M. Vetterli, "Wireless Sensor Networks for Environmental Monitoring: The SensorScope Experience," in *2008 IEEE International Zurich Seminar on Communications*, March 2008, pp. 98–101.

- [130] W. Wang, K. Lee, and D. Murray, "Integrating sensors with the cloud using dynamic proxies," in *2012 IEEE 23rd International Symposium on Personal, Indoor and Mobile Radio Communications-(PIMRC)*. IEEE, 2012, pp. 1466–1471.
- [131] B. Perumal, P. Rajasekaran, and H. Ramalingam, "WSN integrated Cloud for Automated Telemedicine (ATM) based e-healthcare applications," in *Proceedings of the 4th International Conference on Bioinformatics and Biomedical Technology (IPCBBE'12)*, vol. 29, 2012, pp. 166–170.
- [132] K. Ahmed and M. Gregory, "Integrating wireless sensor networks with cloud computing," in *Mobile Ad-hoc and Sensor Networks (MSN), 2011 Seventh International Conference on*. IEEE, 2011, pp. 364–366.
- [133] M. Qiu, Z. Ming, J. Wang, L. T. Yang, and Y. Xiang, "Enabling cloud computing in emergency management systems," *IEEE Cloud Computing*, vol. 1, no. 4, pp. 60–67, 2014.
- [134] "Benefits of Cloud computing To Wireless Sensor Networks," July 2013. [Online]. Available: <http://www.wsnmagazine.com/cloud-computing-wsn/>
- [135] E. Gelenbe, K. Hussain, and V. Kaptan, "Simulating autonomous agents in augmented reality," *Journal of Systems and Software*, vol. 74, no. 3, pp. 255–268, 2005.
- [136] E. Gelenbe and F.-J. Wu, "Large scale simulation for human evacuation and rescue," *Computers & Mathematics with Applications*, vol. 64, no. 12, pp. 3869–3880, 2012.
- [137] S. Belardo, K. R. Karwan, and W. Wallace, "An investigation of system design considerations for emergency management decision support," *IEEE Transactions on Systems, Man, and cybernetics*, no. 6, pp. 795–804, 1984.
- [138] L. Chalmet, R. Francis, and P. Saunders, "Network models for building evacuation," *Fire Technology*, vol. 18, no. 1, pp. 90–113, 1982.
- [139] H. Bi and E. Gelenbe, "Cloud enabled emergency navigation using faster-than-real-time simulation," in *Pervasive Computing and Communication Workshops (PerCom Workshops), 2015 IEEE International Conference on*. IEEE, 2015, pp. 475–480.
- [140] C. Kruger, G. Hancke, and D. Bhatt, "Wireless sensor network for building evacuation," in *Instrumentation and Measurement Technology Conference (I2MTC), 2012 IEEE International*. IEEE, 2012, pp. 2572–2577.
- [141] H. Bi and E. Gelenbe, "A cooperative emergency navigation framework using mobile cloud computing," in *Information Sciences and Systems 2014*. Springer, 2014, pp. 41–48.

- [142] A. Zhan, F. Wu, and G. Chen, "Sos: A safe, ordered, and speedy emergency navigation algorithm in wireless sensor networks," in *Computer Communications and Networks (ICCCN), 2011 Proceedings of 20th International Conference on*. IEEE, 2011, pp. 1–6.
- [143] S. Escolar, D. Villa, F. J. Villanueva, R. Cantarero, and J. C. López, "An adaptive emergency protocol for people evacuation in high-rise buildings," in *2016 IEEE Symposium on Computers and Communication (ISCC)*, June 2016, pp. 364–371.
- [144] Y. Chen, L. Sun, F. Wang, and X. Zhou, "Congestion-Aware Indoor Emergency Navigation Algorithm for Wireless Sensor Networks," in *2011 IEEE Global Telecommunications Conference - GLOBECOM 2011*, Dec 2011, pp. 1–5.
- [145] P.-Y. Chen, Z.-F. Kao, W.-T. Chen, and C.-H. Lin, "A distributed flow-based guiding protocol in wireless sensor networks," in *2011 International Conference on Parallel Processing*. IEEE, 2011, pp. 105–114.
- [146] E. Spartalis, I. G. Georgoudas, and G. C. Sirakoulis, "Ca crowd modeling for a retirement house evacuation with guidance," in *International Conference on Cellular Automata*. Springer, 2014, pp. 481–491.
- [147] L. H. Correia, D. F. Macedo, A. L. dos Santos, A. A. Loureiro, and J. M. S. Nogueira, "Transmission power control techniques for wireless sensor networks," *Computer Networks*, vol. 51, no. 17, pp. 4765–4779, 2007.
- [148] J. Vales-Alonso, E. Egea-López, A. Martínez-Sala, P. Pavón-Mariño, M. V. Bueno-Delgado, and J. García-Haro, "Performance evaluation of MAC transmission power control in wireless sensor networks," *Computer Networks*, vol. 51, no. 6, pp. 1483–1498, 2007.
- [149] W. Liu, Y. Shoji, and R. Shinkuma, "Logical correlation-based sleep scheduling for energy-efficient wsns in smart homes," in *Personal, Indoor, and Mobile Radio Communications (PIMRC), 2015 IEEE 26th Annual International Symposium on*. IEEE, 2015, pp. 2026–2031.
- [150] Z.-H. Zhan and J. Zhang, "Bio-inspired computation for solving the optimal coverage problem in wireless sensor networks: A binary particle swarm optimization approach," in *Bio-Inspired Computation in Telecommunications*, pp. 263–285, 2015.
- [151] X. Wang, F. Sun, and X. Kong, "Research on optimal coverage problem of wireless sensor networks," in *2009 WRI International Conference on Communications and Mobile Computing*, vol. 1, Jan 2009, pp. 548–551.
- [152] S. Ho, J. Wang, W. Fu, and M. Sun, "A comparative study between novel witrlicity and traditional inductive magnetic coupling in wireless charging," *IEEE Transactions on Magnetics*, vol. 47, no. 5, pp. 1522–1525, 2011.
- [153] WiTricity. [Online]. Available: Witracity.com/
- [154] DELL. [Online]. Available: <http://www.techradar.com/news/mobile-computing/laptops/dell-s-wireless-charging-laptop-breaks-cover-639135>

[155] POWERMAT. [Online]. Available: <http://powermat.com/>

